ABSTRACT

Title of Dissertation:	INVESTIGATION OF GLYCOENZYME SUBSTRATE SPECIFICITY FOR GLYCOENGINEERING OF THERAPEUTIC ANTIBODIES
	Darnell Markee Harris, Doctor of Philosophy, 2025
Dissertation directed by:	Professor, Lai-Xi Wang, Chemistry and Biochemistry

Immunoglobulin G (IgG) antibodies have been exploited as drug candidates due to their target specificity and ability to elicit host cell effector functions. These Y-shaped glycoproteins possess two antigen-binding (Fab) regions for selective binding to epitopes and one constant (Fc) region for mediating effector functions. As glycoproteins, these antibodies are also N-glycosylated at position N297, where the Fc glycans modulate the stability and effector functions of the antibodies. However, due to the non-template synthesis of these antibody glycans, the resulting oligosaccharide composition and structures are highly heterogeneous.

My work aims to leverage the substrate specificities of various glycosyltransferase enzymes to generate antibody preparations with homogenous glycan structures. For my first project, I performed a comparative study on three sialyltransferases, including two bacterial sialyltransferases from Helicobacter cetorum (HcST-22) and

from Photobacterium damselae (Pd2,6ST), respectively, and the human α-2,6-sialyltransferase (ST6Gal1), to determine which is more efficient at sialylating intact antibody Fc glycans. We found that HcST-22 was more efficient than Pd2,6ST and ST6Gal-1 at sialylating intact Fc glycans. For my second project, I contributed to a collaborative effort in generating intravenous immunoglobulin (IVIg) glycoforms. I incorporated two sialic acid derivatives, 2-keto-3-deoxy-D-glycero-D-galacto-nononic acid (KDN) and 9-azido-9-deoxy-Neu5Ac (9AzNeu5Ac), onto free glycan before transferring these glycans onto deglycosylated IVIg. The resulting azide-tagged IVIg was then further elaborated by the click addition of sialocomplex-type glycan asparagine with a DBCO tag (SCT-Asn-DBCO) to yield a final glycoform that extended the Fc glycan and increased the valency of the terminal native sialic acid. For my third research project, I designed a novel Fc-glycosylated site-specific antibody drug conjugate (ADC) design with a drug to antibody ratio (DAR) of 6. I achieved this by glycoengineering the Fc glycan of recombinant trastuzumab to generate a triantennary agalactosylated complex type glycan at the N297 position. Then, using a mutant N-acetylgalatosamine (GalNAc) transferase enzyme β1,4-GalT Y289L I transferred N-azidoacetylgalactosamine (GalNAz) to each glycan terminus of the triantenary Herceptin, then click-conjugated a cytotoxic payload onto each azide on the antibody Fc region, generating a trastuzumab ADC with a DAR of 6. Through a cell viability assay, we determined that this homogeneously glycosylated DAR-6 ADC showed potent anti-cancer activity.

INVESTIGATION OF GLYCOENZYME SUBSTRATE SPECIFICITY FOR GLYCOENGINEERING OF THERAPEUTIC ANTIBODIES

by

Darnell Markee Harris

Dissertation submitted to the Faculty of the Graduate School of the
University of Maryland, College Park, in partial fulfillment
of the requirements for the degree of
Doctor of Philosophy
2025

Advisory Committee:
Professor Lai-Xi Wang, Chair
Professor Kwaku Dayie
Professor David Fushman
Professor Myles Poulin
Professor Wenxia Song

Acknowledgements

This endeavor has truly been as worthwhile as it was challenging. Through trials and hardships, I not only became a better scientist, but a better problem solver in general. If I could offer any advice to the past version of myself first entering graduate school, I would tell him to keep moving forward despite overwhelming frustration and failures. I would also tell him to tap on his support more, as he would be going through a program filled with so many people willing to help him. I of course learned through this program how to think critically and creatively when presented with a problem, but I also gained a lot of insight into the spirit of collaboration that truly drives scientific discovery and innovation. I am honored to be a part of a community of brilliant and curious minds set to understand and change the world.

I would like to start off by thanking my mentor and chair of my committee, Distinguished University Professor Lai-Xi Wang. Through my PhD experience he has offered support and insight into new projects, as well as new problems that came up. His steadfast commitment to discovery and innovation has kept me goal oriented, and his leadership kept the vision for my various projects clear. I am eternally grateful to have been chosen to work in his lab and for the support I've received ever since.

I would also like to thank the members of my lab, past and present. Through no small effort, they helped me through my journey through the program by offering support, insight, and a willingness to collaborate when needed. In addition to the honor of calling these brilliant scientists colleagues, I am elated to also call them friends. In particular, I'd like to thank Drs. Chao Li, Guanghui Zong, and Grace Lunde for their mentorship and support, especially when I was first starting in the lab. I'd also like to thank Margaryta Gomozkova, Natasha Owitipana,

and Helena Yun for their emotional support, especially in the latter years of my journey. Lastly, I'd like to thank the other members of the Wang Lab: Dr. Qiang Yang, Dr. Yuanwei Dai, Dr. Roushu Zhang, Dr. Xiao Zhang, Dr. Kun Huang, Dr. Miao Liu, Dr. Sunaina Prabhu, Dr. Chong Ou, Dr. Thomas Connor Donahue, Dr. Xianyang Wang, Dr. Jinghua Han, Dr. Diksha Rai, Nikolai Tolstoy, Yuxin Wang, Zoe Katz, and Gabriel Pantusa. I would not have achieved all I have without your guidance and support. Thank you.

I'd like to thank my mother for her undying love, support, and dedication. At every stage of my life, she was a steadfast support and a key player on the journey to meeting my goals and accomplishing my dreams. When I doubted myself, she had enough confidence and reassurance for the both of us. There are no words strong enough to express my gratitude for everything she's done for me, but I'm still determined to try regardless. We did it, Ma!

I'd like to thank my partner Dr. Michael Lamontagne. I was able to overcome all my challenges within the program and without in no small part due to his love, diligence, support, and kindness. I could not be happier to have him by my side through this accomplishment. To the future we build together.

I would also like to thank my dissertation committee; Professors Theodore Kwaku Dayie, David Fushman, and Myles Poulin. Their advice help me see anything from progress to issues from a fresh perspective, and inspired me to think critically about any approach I explored. Their time and guidance wer invaluable to me as I proceeded through my PhD journey.

I'd like to thank my friends, particularly Kito Gilbert-Bass, Adam Rabayda, Megan Holman, Otto Euller, and Rebecca Falconer. Separated by distance, but united by the time and memories we share, you all will forever have a special place in my heart.

Finally, I'd like to thank the Chemistry and Biochemistry Department and the National Institute of Standards and Technology for their financial support thought the Dolphus E. Milligan Graduate Fellowship.

Table of Contents

List of Schemes

List of Tables

List of Figures

List of Abbreviations

AAL	*Aleuria aurantia* lectin
ADC	Antibody Drug Conjugate
ADCC	Antibody-Dependent Cellular Cytotoxicity
B4GalT	β-1,4-galactotransferase
BgaA	*Alkalophilic Bacillus* β1,4-galactosidase
BODIPY	4,4-difluoro-4-bora-3a-4a-diaza-s-indacene
BSII	*Bandeiraea simplicifolia* II
CAIA	Collagen Antibody Induced Arthritis
CAZy	Carbohydrate-Active Enzyme database
CDC	Complement Dependent Cytotoxicity
DAR	Drug to Antibody Ratios
DBCO-NHS	Dibenzylcyclooctyne - *N*-hydroxysuccinamide
DC	Dendridic Cell
DC-SIGN	DC-Specific ICAM-3 Grabbing Non-integrin
DMC	2-chlorodimethylimidazolium chloride
DMEM	Dulbecco's Modified Eagle Medium
DxD	Asparagine-X-Asparagine
E.coli	*Escherichia coli*
EC_{50}	Half-Maximal Effective Concentration
EndoA	*Arthrobacter protophormiae* Endo-β-N-acetylglucosaminadase
EndoF3	*Flavobacterium meningosepticum* Endo-β-N-acetylglucosaminadases 3
EndoS	*Streptococcus pyrogenes* Endo-β-N-acetylglucosaminadases
EndoS2	*Streptococcus pyrogenes* serotype M49 Endo-β-N-acetylglucosaminadases
ENGase	Endo-β-N-acetylglucosaminadases
Fab	Antigen Binding Fragment
Fc	Constant or Crystalizable Fragment
FPLC	Fast-Performance Liquid Chromatography

FUT8	α1,6-fucosyltransferase
GalNAc	*N*-acetylgalactosamine
GalNAz	*N*-azidoacetylgalactosamine
GH	Glycosylhydrolase
GlcNAc	*N*-acetylglucosamine
GMD	GDP-mannose 4,6-dehydratase
GnT-III	*N*-acetylglucosaminyltransferase III
GT	Glycosyltransferase
HPAEC-PAD	High-Performance Anion Exchange Chormatography with Pulsed Amperometric Detection
HPLC	High-Performance Liquid Chromatography
IC	Immune Complex
IdeS	*Streptococcus pyrogenes* Protease Enzyme
Ig	Immunoglobulin
IgA	Immunoglobulin A
IgD	Immunoglobulin D
IgE	Immunoglobulin E
IgG	Immunoglobulin G
IgM	Immunoglobulin M
IPTG	Isopropy-β-D-thiogalactopyranoside
ITAM	Immunoreceptor Tyrosine-Based Activation Motif
ITIM	Immunoreceptor Tyrosine-Based Inhibition Motif
ITP	Immunothrombocytopenia Purpura
IVIg	Intravenous Immunoglobulin
K/BxN	Rheumatoid Arthrits Mouse Model
KDN	2-keto-3-deoxy-D-glycero-D-galacto-nononic acid
LC-ESI-MS	Liquid Chomatography Electrospray Ionization Mass Spectrometry
MALDI-TOF	Matrix-Assisted Laser Desorption Ionization - Time of Flight
MMAE	Monomethyl Auristatin E
MWCO	Molecular Weight Cut-Off
Neu5Ac	*N*-acetylneuraminic Acid

Neu5Gc	*N*-glycolylneuraminic acid
NK	Natural Killer
NmCSS	*Neisseria Mengingitidis* CMP-Sialic Acid Synthetase
NMR	Nuclear Magnetic Resonance
OST	Oligosaccharyltransferase
PABC	*p*-aminocarbamate
PEG	Polyethylene Glycol
ppGalNAcT	Poly-peptide *N*-acetylgalactosamine transferase
RCA	*Ricinus communis* Agglutinin
SGP	Sialoglycopeptide
SIGN-R1	Specific Intercellular Adhesion Molecule-3-grabbing Non-integrin
SNA	*Sambucus nigra* Agglutinin
SPAAC	Strain-Promoted Azide -Attached Cycloaddition
ST	Sialyltransferase
ST6Gal-I	α-2,6-sialyltransferase
TLC	Thin Layer Chromatography

Chapter 1: Principles of Antibody Glycan Remodeling for Gain of Functions

1.1 Protein Glycosylation

Protein glycosylation is a post translational modification that involves the covalent attachment of saccharide residues on a protein. These attachments are common, particularly in extracellular and cell surface proteins[1]. Glycosylation contributes to the structural stability of the protein, modulation of protein-protein interactions, and signaling of protein quality. Like many cellular processes, glycosylation is an enzymatic process involving a myriad of different glycosyl hydrolases (GHs) and glycosyltransferase (GTs) enzymes for dynamic trimming and building of complex saccharide structures known as glycans. However, even among identical proteins, the structures of their glycans may vary due to the non-template nature of protein glycosylation.

There are two types of protein glycosylation: *N*-glycosylation and *O*-glycosylation (**Figure 1.1**)[2]. *O*-glycosylation describes the covalent linkage of either a serine or threonine hydroxyl residue to the reducing-end anomeric position of a glycan. A family of GalNAc transferases (ppGalNAcT) initiate the incorporation of an α-*N*-acetylgalactosamine (GalNAc) residue onto a serine or threonine on a protein in the Golgi apparatus after the protein has been expressed and folded[3, 4]. This GalNAc residue is then extended by a series of glycosyltransferase enzymes to generate the mature *O*-glycan prior to protein release from the Golgi. While generally heterogeneous in structure, *O*-glycans can be subcategorized into major "core" structures. Core 1 consists of a β1,3-galactose linkage to the initial GalNAc, while Core 2 builds

off this structure with the incorporation of a β1,6 linked *N*-acetylglucosamine (GlcNAc) residue. Core 3, however, is distinct from Cores 1 and 2 in that it begins with a β1,3-GlcNAc linkage to the initial GalNAc. Core 4 builds off of Core 3 with the incorporation of β1,6-GlcNAc. Further extensions to these Core structures give rise to highly complex *O*-glycans[5].

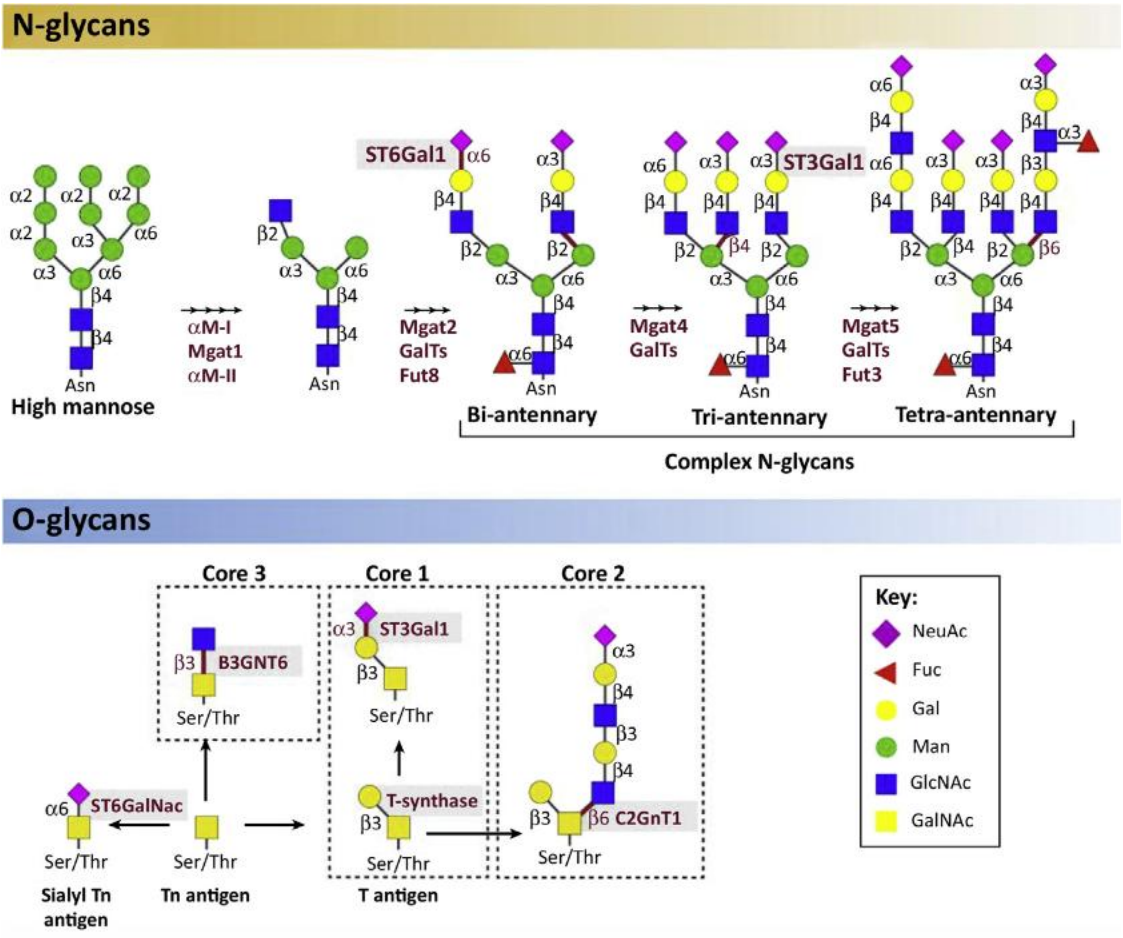

Figure 1.1. Depictions of the *N*-glycosylation and *O*-glycosylation with the most relevant enzymes responsible for glycan trimming and modification. Taken from a publication by Cerliani *et al.*[6]

N-glycosylation describes the covalent linkage of an asparagine amide residue to the reducing-end anomeric position of a glycan. The asparagine, however, can only be an acceptor for glycosylation if it is within the N-X-S/T consensus sequence, where X is any amino acid residue except proline. *N*-glycosylation is the most prominent type of glycosylation in

eukaryotes, with very complex yet somewhat conserved structures[7]. An *N*-glycan is assembled through stepwise incorporations of monosaccharides onto a lipid anchor on the endoplasmic reticulum (ER) membrane by various glycosyltransferases. Once the assembly is complete, an oligosaccharyltransferase (OST) enzyme transfers the *N*-glycan *en bloc* from the lipid anchor to the N-X-S/T glycosylation consensus sequence of the nascent protein. The *N*-glycan on the protein is trimmed to the Man9GlcNAc2 or Man8GlcNAc2 form in the ER and the glycoprotein is then trafficked to the Golgi apparatus, where the glycan can be further trimmed and modified into mature glycoforms before being released either into the extracellular space or onto the cell surface. Eukaryotic *N*-glycans on mature glycoproteins generally retain a conserved *N*-acetylchitobiose core consisting of two β1,4-linked GlcNAc residues followed by a β1,4-linkage to a branching α1,3- and α1,6-trimannose structure. From this conserved structure the glycan can be further modified via various glycosyl hydrolases and transferases to generate one of three canonical structures: high-mannose, hybrid-type, and complex-type[8]. This modification process is the main driver in *N*-glycan heterogeneity.

1.2 Antibody structure and function

Antibodies, also known as immunoglobulins, are a family of glycoproteins that are vital in humoral immune function. These proteins are produced by B cells, and they all are symmetrical "Y" shaped tetramers consisting of two identical sets of light chains and heavy chains assembled to form two antigen binding domains (Fab) and one constant or crystallizable domain (Fc)[9]. The Fab regions display high specificity and affinity for target antigens, and with two antigen binding site per antibody molecule, each antibody can bind multiple target antigens at once. This high valency allows for antibodies to chain antigens together, with some antigens being bound by multiple antibodies forming antibody antigen clusters known as Immune

Complexes (ICs). During this IC formation, the Fc domains of each antibody face outward in a multivalent display, which act as ligands for host immune cell receptors to induce immune effector functions of innate immune cells such as Dendritic Cells (DCs) and Natural Killer (NK) cells for antigen clearance. Through this functionality, antibodies essentially act as the bridge between the highly specific adaptive immune system with the prompt and abundant response of the innate immune system. This versatility and specificity make these antibodies vital not only in endogenous host immune function, but also as targeted biologic drugs for treatments of various illnesses such as cancers and infections.

There are 5 distinct classes of antibodies in humans: Immunoglobulin (Ig) Classes A, D, E, G, and M. Immunoglobulin Classes D (IgD) and M (IgM) are produced by B cells prior to T-cell stimulation and represent relatively low-affinity antibodies. However, they are important for initial immune mobilization, with IgM antibodies being able to initiate a process called Complement-Dependent Cytotoxicity (CDC), which describes the recruitment of circulating proteins to IgM ICs to induce local inflammation, recruit effector cells, tag the target antigenic cell for immune cell phagocytosis, and form pore complexes on target cells leading to lysis and cell death. IgA, IgE, and IgG antibodies are produced after T-cell stimulation and display higher affinities towards target antigens and more specialized effector functions. IgA is specialized for immunity and microbial regulation and mucosal barrier sites such as the mouth and gut, while IgE facilitates allergy responses. IgG antibodies, in contrast, are the most abundant antibody class in serum, providing the bulk of the humoral immunity in the body by facilitating both CDC and Antibody-Dependent Cellular Cytotoxicity (ADCC), the latter of which involves the recruitment and activation of effector cells such as NK cells through Fc binding with IgG ICs to cell surface receptors, prompting these cells to secrete cytotoxic proteins and kill the target cell

(**Figure 1.2**)[10]. This ability to mediate ADCC has made IgG antibodies attractive therapeutic tools for treating various diseases and illnesses. For this reason, the IgG antibody isoform will be the focus of this work.

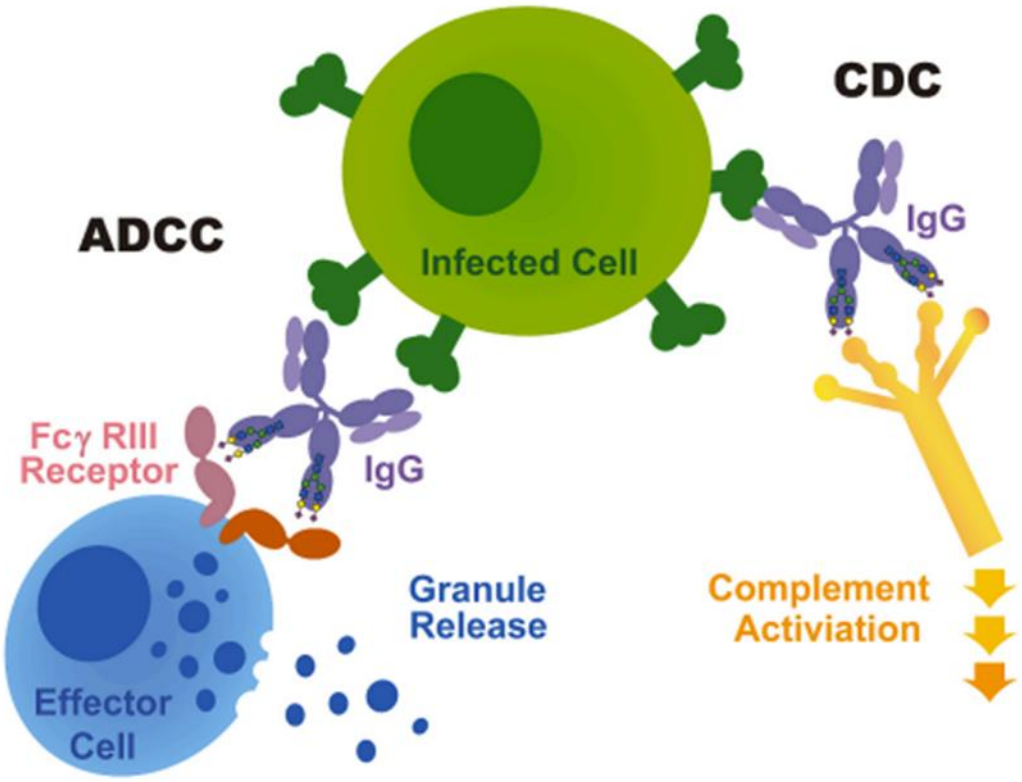

Figure 1.2. Schematic of ADCC and CDC effector functions. Adapted from publication by Wang *et al.*[11]

The cell surface receptors responsible for antibody mediated cell activation are a family of transmembrane receptors known as Fcγ Receptors (FcγRs). The six FcγRs expressed on human immune cells are FcγRI, FcγRIIa, FcγRIIb, FcγRIIc, FcγRIIIa, and FcγRIIIb (**Figure 1.3**). All of these receptors express cytosolic Immunoreceptor Tyrosine-Based Activation Motifs (ITAMs) that initiate cell activation upon ligand binding save FcγRIIb, which possesses an Immunoreceptor Tyrosine-Based Inhibition Motif (ITIM), initiating cell inhibition upon ligand binding.[12-14] The counterproductivity of FcγRIIb provides immune homeostasis to prevent an

overactive immune system and autoimmunity. In addition, immune homeostasis is also achieved due to the relatively low binding affinities exhibited by these receptors, with most having a 10^{-3}-10^{-5} M binding affinity except for the high affinity FcγRI receptor with a 10^{-6}-10^{-8} M affinity[12, 14, 15]. This low affinity requires high avidity interactions to induce the signaling cascade for cell activation, which is mainly achieved through interactions with IgG ICs. The combination of low affinity receptors and co-expression of activation and inhibition receptors are essential for maintaining a functional immune system while avoiding instances of autoimmunity.

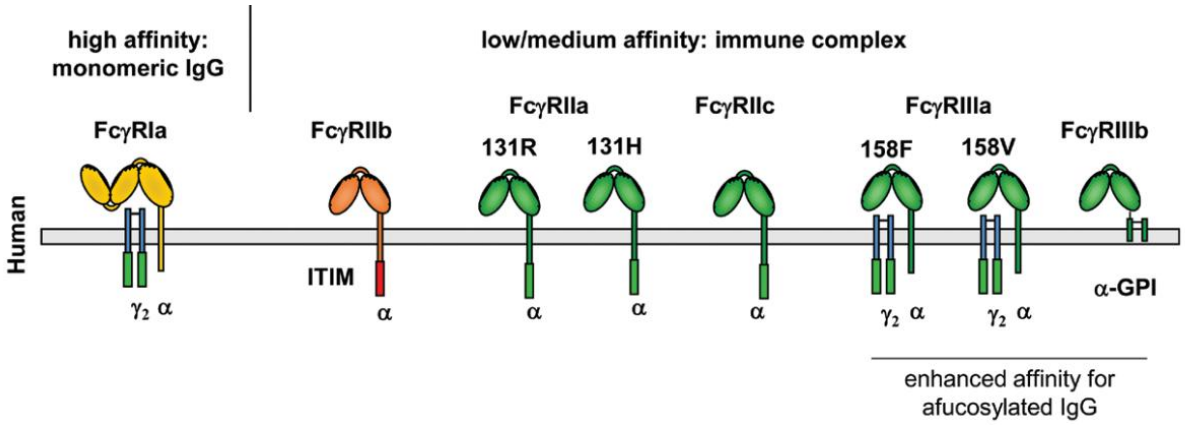

Figure 1.3. Fcγ receptors expressed on immune cells of humans. Figure adapted from publication by Brückner *et al.*[16].

While the primary sequence of certain regions of the IgG Fab domains differs in polyclonal antibody preparations attributing to their antigen specificity, the Fc domain is largely conserved, with slight sequence and structural differences between the four IgG isotypes (IgG1-4). This structural conservation is essential for antibody FcγR recognition and subsequent cell activation. However, another feature shared by all IgG antibodies is a conserved *N*-glycosylation site at position N297 of the Fc region (**Figure 1.4**). This glycan generally consists of a canonical complex-type structure with varying degrees of galactosylation, sialylation, fucosylation, and

bisecting GlcNAc. However, the presence of this glycan is crucial for antibody serum half-life, proteins stability, and more notably, FcγR binding[17-20]. In most instances, it is believed that the glycan doesn't directly contribute to the IgG Fc-FcγR binding interactions but instead restricts the Fc domain to the most desirable conformations for FcγR binding. However, the N297 glycan is essential for FcγRIIIa binding and facilitation of ADCC effector functions[21]. While the presence of the N297 glycan has been shown to be necessary for antibody functionality, the individual saccharide contributions remain more ambiguous.

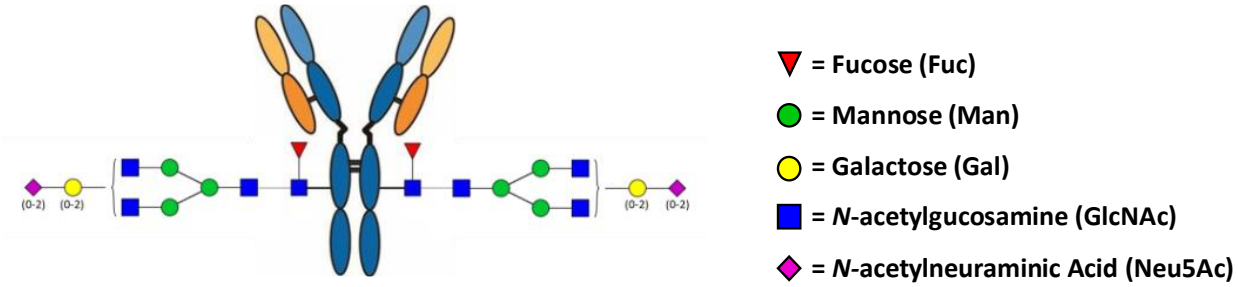

Figure 1.4. Structure of an IgG antibody. The conserved Fc N-glycans are heterogeneous with varied decoration of the outer sugar residues.

1.3 Antibody glycosylation and effector functions

All IgG antibodies share a conserved *N*-glycosylation site at position N297, occupied by complex type glycans with heterogeneous saccharide compositions. Many studies have shown that the presence or absence of certain saccharide moieties have certain effects on antibody functionality. For example, terminal galactosylation of IgG Fc glycans has been shown to enhance CDC activity by increasing Fc binding affinity with the C1q protein, which then initiates a downstream cascade that ultimately leads to increased local inflammation, effector cell recruitment, and target cell membrane perforation[22-24]. However, terminal sialylation of the N297

galactose residues reduced C1q binding, indicating that the galactose residues must be at the terminal position of the glycan to enhance C1q binding[25].

In contrast, lack of α1,6- "core" fucosylation enhances ADCC by increasing Fc binding affinity with the ADCC-activating FcγRIIIa receptor on NK cells. This is due to carbohydrate-carbohydrate interactions between the N162 *N*-glycan of FcγRIIIa and the N297 *N*-glycan on the IgG antibody, which are only favorable without the steric hinderance provided by core fucosylation[21, 26]. Among the FcγR family, FcγRIIIa is unique in this glycan-glycan interaction as a driving factor for Fc binding and subsequence ADCC initiation. Interestingly, neither galactosylation nor sialylation appears to have as profound an effect as the lack of core fucosylation for FcγRIIIa binding and ADCC activation.

The α2,6-sialylation of IgG Fc glycans with the *N*-acetylneuraminic acid (Neu5Ac), the only form of sialic acid expressed in humans, has been shown to convey anti-inflammatory activity in the context of autoimmune diseases. Professor Jeffrey Ravetch reported that human-derived Intravenous Immunoglobulin (IVIg) with enriched terminal α2,6-Neu5Ac content reduces both joint inflammation in arthritic mouse models and platelet depletion in immunothrombocytopenia (ITP) mouse models, while depletion of this sialylation disrupts the IVIg-dependent anti-inflammatory activity altogether[27-29]. However, the molecular mechanism behind sialylated IgG reducing autoimmune inflammation remains poorly understood.

These studies clearly show the effects of oligosaccharide composition of the N297 glycan on antibody function. Despite this, antibody glycan structures remain largely heterogeneous either from recombinant expressed or extracted from blood serum. For example, various studies have isolated IgG antibodies from human sera and found that on average fucose had the highest abundance on IgG Fc glycans at 94%, followed by galactose at 67%, bisecting GlcNAc at 10%,

monosialylation at 18%, and disialylation at 1% within human antibody preparations (**Figure 1.5**)[2, 30-33]. This diversity within the N297 glycan structure poses a significant obstacle in antibody glycan structure-function studies and thus highlights a need for methodologies for generation of homogenous antibody glycoforms.

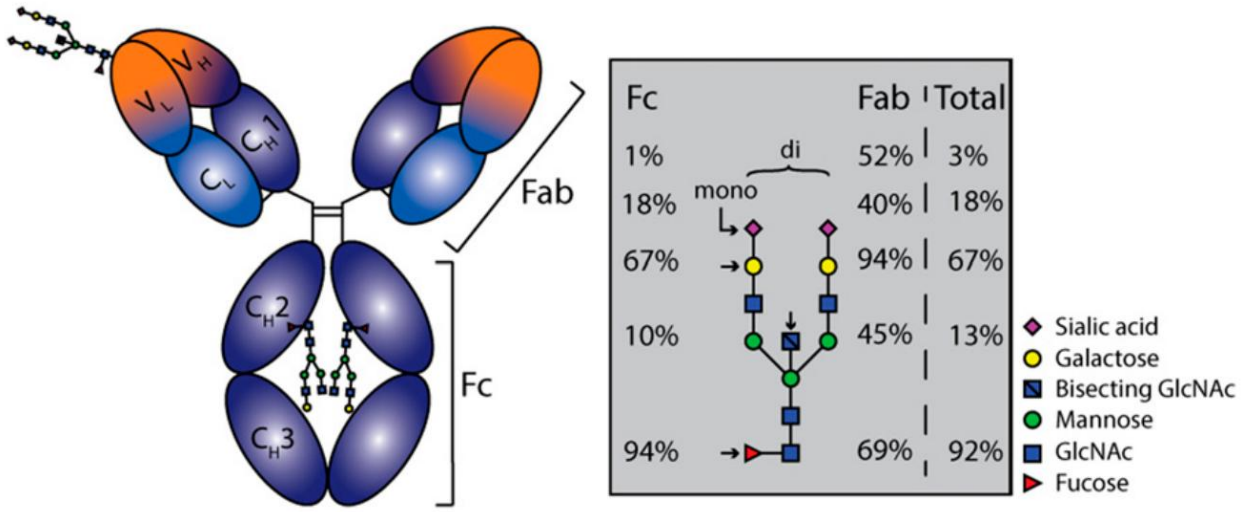

Figure 1.5. Average oligosaccharide content of glycans on either the conserved Fc glycosite or a non-conserved Fab glycosite from human serum IgG. Figure adapted from a publication by van de Bovenkamp *et al.*[33]

1.4 Antibody glycan engineering

The high heterogeneity of antibody glycoforms makes detailed glycan structure-function studies in antibodies difficult. Whether expressed in recombinant expression systems or extracted from animal serum, the resulting antibody glycan structures remain relatively varied. Due to this, many research groups have developed novel approaches for tackling this issue. I will highlight some of the major approaches in the following subsections.

1.4.1 Lectin affinity characterization and fractionation of IgG glycoforms

Many methodologies exist to characterize and even create homogeneous IgG glycoform preparations. One classic method is to use saccharide binding proteins called lectins to enrich for the presence of a given sugar. Leveraging a lectin's particular affinity for specific glycostructures has given rise to the detection technique known as lectin blotting. For example, a collaborative study between the Rademacher group in the UK and the Kobata group in Japan used *Ricinus communis* agglutinin (RCA) affinity to terminally galactosylated IgG glycoforms, in tandem with gel chromatography and enzymatic digestion assays, to investigate a potential association with changes in IgG galactosylation and rheumatoid arthritis and primary osteoarthris[34]. Similarly, Hay and colleages used lectins from RCA I and *Bandeiraea simplicifolia* II (BSII), which bound terminal galactose and terminal GlcNAc, respectively, to investigate disease-specific correlations in levels of galactose vs GlcNAc. They found that IgG preparations from patients with rheumatoid arthritis, juvenile onset chronic arthritis, and Crohn's disease have a reciprocal relationship in galactose:GlcNAc content. Conversely, they also found that IgG preparations from patients with Sjögren's syndrome and osteoarthritis have a parallel galactose:GlcNAc relationship[35]. Fucose-binding lectin, *Aleuria aurantia* lectin (AAL), has been used to detect and monitor enzymatic fucosidase activity on fucosylated IgG glycoforms[36, 37].

Furthermore, lectins have been used in HPLC affinity chromatographic analysis to determine the prevalence of a particular glycan motif in an antibody mixture. For example, a 2003 study by Shitara and colleagues used lectin fractionation to isolate IgG antibodies based on either core fucosylation, bisecting GlcNAc, or galactose content to determine the extent to which the presence of galactose or bisecting GlcNAc contribute to ADCC relative to the absence of fucose. They found that galactosylation and bisecting GlcNAc have a less significant impact to

ADCC than fucosylation[38]. Notable still is the use of lectin chromatography to fractionate IgG preparations, essentially enriching a particular glycoform within a preparation. This technique has been used extensively by groups such as the Ravetch Group using *Sambucus nigra* agglutinin (SNA) to enrich for sialylated IgG to study Fc-sialylation-dependent anti-inflammatory activity of Intravenous Immunoglobulins (IVIg), a human derived polyclonal antibody mixture[28, 29]. This discovery of the anti-inflammatory effects of IVIg somewhat contradicts the current understanding of the proinflammatory of IgGs, making the isolation of Fc sialylated IgGs critical for the investigation into the IVIg anti-inflammatory IgG mechanism of action. Unfortunately, SNA lectin fractionation has a major disadvantage in that it reportedly has a very low affinity for Fc sialylation relative to Fab sialylation. This means that most of the SNA-fractionated whole IgG from an IVIg preparation will have mostly Fab sialylation enrichment, which has been shown not to convey the anti-inflammatory activity[39, 40]. Obstacles such as this highlight the need for generating glycoforms of interest, not just detecting them.

1.4.2 Metabolic engineering of IgG expression systems

Metabolic engineering is another approach the biosynthetic pathways of the cell line expressing recombinant IgGs are altered to increase the prevalence of certain glycoforms. For example, many groups have engineered their IgG expressing mammalian cell lines to also overexpress the *N*-acetylglucosaminyltransferase III (GnT-III) enzyme, which will incorporate bisecting GlcNAc to the Fc glycans and decrease core fucosylation[21, 41-44]. Other groups have achieved a reduction of fucosylation by generating knockouts (KOs) of the α1,6-fucosyltransferase (FUT8) enzyme that produces core fucosylated glycoforms, either alone[45], or with the additional knockdown of GDP-mannose 4,6-dehydratase (GMD), an enzyme required

for the biosynthesis of GDP-L-Fucose[46]. In addition to co-expression and knockout techniques, Jefferis and colleages reported the development of IgG3 Fc mutations in 1996 to increase the degree of digalactosylation and sialylation on the N297 glycan. They made point mutations to residues known to interact with the oligosaccharide resides and found that particularly the IgG3 F243A mutant had the highest degree of galactosylation and sialylation while also retaining its effector functions, albeit at a somewhat reduced capacity[47]. Since then, other groups have used the mutants developed by the Jefferis group, due to the increased Fc conformational flexibility that allows for the increased access to the N297 glycosite and thus, more processed glycan species[48, 49].

1.4.3 *in vitro* chemoenzymatic glycan remodeling of IgG

A common approach to generating fully sialylated IgG Fc glycoforms by using *in vitro* chemoenzymatic methods. Some groups have used recombinant bovine B4GalT to fully galactosylate the IgG glycans, then used recombinant human ST6Gal-I to incorporate the α2,6-sialic acid at each terminal position of the IgG glycans[25, 50, 51]. However, these enzymes are not specific for a particular glycosite, so if an antibody is Fab glycosylated, then that could present additional competing sites for enzymatic modification. In addition, these reactions, particularly in the case of the ST6Gal-I enzyme, can be very slow, often taking many days and need to be pushed vigorously to completion. Recently, Ye and colleagues reported a mutant bacterial sialyltransferase that showed enhanced activity in sialylation of antibody Fc glycans, using trastuzumab (Herceptin) as a model monoclonal antibody. They expressed a truncated variant of the Psp2,6ST sialyltransferase, referred to as Psp2,6ST(111-511)-His_6 with two point mutations at A366G and A235M. This truncation, along with the double point mutations, increased the sialylation efficiency on IgG Fc while also increasing donor substrate promiscutity[52]. Further

development of these chemoenzymatic methods for generating disialylated IgG antibodies will greatly aid in studies regarding the IVIg anti-inflammatory activity and its powerful approach for antibody glycoengineering.

A powerful chemoenzymatic approach developed by our group leverages a category of GH enzymes known as endo-β-*N*-acetylglucosaminadases (ENGases) to chemoenzymatically remodel antibodies. These enzymes bind to carbohydrate motifs of *N*-glycans via lectin domains before cleaving the glycosidic bond between the two initial GlcNAc residues on *N*-glycans using a retaining GH cleavage mechanism (**Figure 1.6A**)[53]. These enzymes fall into one of two families according to the Carbohydrate-Active Enzymes database (CAZy): GH18 and GH85. While these enzymes recognize *N*-glycans, their capacity to recognize the three canonical *N*-glycan structures (complex-type, oligomannose-type, or hybrid-type) varies significantly between individual ENGase. These ENGases are remarkable in their capacity not only to cleave *N*-glycans from glycoproteins and peptides *en bloc*, but to catalyze the *en bloc* transglycosylation on truncated acceptor substrates (**Figure 1.6B**)[54-60].

A)

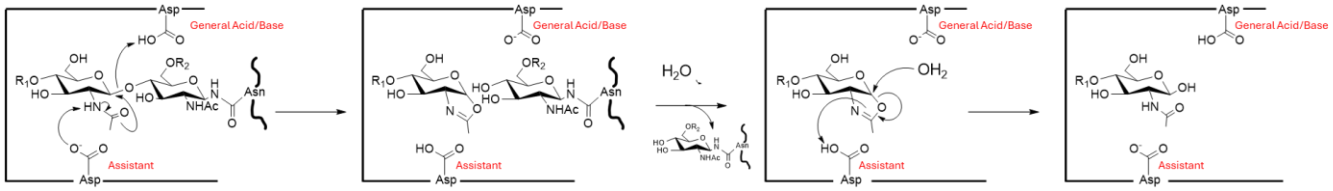

B)

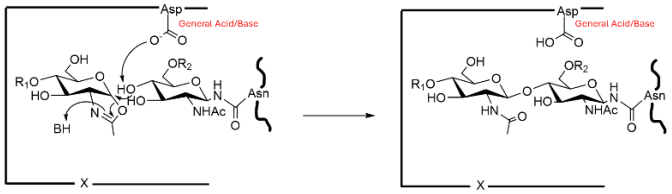

Figure 1.6. Enzymatic mechanism of action for A) wild-type GH18 glycosyl-hydrolase enzymes and B) GH18 mutant glycosynthase enzymes.

In 2008, our group remodeled intact recombinant IgG Fc using yeast cell expression to generate afucosylated high-mannose IgG Fc, then transferring sugar oxazolines onto the truncated Fc glycosite using EndoA, a GH85 ENGase from *Arthrobacter protophormiae*, to generate homogenous preparations of both natural and non-natural IgG Fc glycoforms. These glycoforms were then used to test FcγRIIIa binding[61]. One significant limitation to the work, however, was that while IgG Fc glycans naturally core fucosylated and complex-type glycans, EndoA can only recognize afucosylated oligomannose structures. This necessitated the IgG Fc expression in yeast, and the glycoforms were generally truncated versions of natural IgG Fc glycans. In 2012, shortly after this study, Davis and co-workers characterized the substrate specificity of the previously reported EndoS, a GH18 ENGase from *Streptococcus pyrogenes*[62], which can cleave both fucosylated and afucosylated complex type glycans from the IgG Fc glycosite[63], our group reported the first novel EndoS D233A and D233Q glycosynthase mutants

that could act on intact antibodies for enzymatic Fc glycan remodeling with natural full-size *N*-glycans[64].

In 2016, our group reported another class of new glycosynthase mutants derived from two GH18 ENGases, EndoF3 from *Flavobacterium meningosepticum* and EndoS2 from *Streptococcus pyrogenes*. The EndoF3 D165A and D165Q glycosynthase mutants could catalyze the transglycosylation of triantennary complex type glycan oxazoline onto fucosylated IgG[65], while the EndoS2 D184M and D184Q glycosynthase mutants showed higher transglycosylation efficiency for IgG Fc with a more relaxed substrate specificity than the EndoS mutants[66]. The EndoS2 glycan remodeling system was later used in 2017 by our group to test FcγRIIIa binding efficiency as a function of sialylation, galactosylation, and core fucosylation[67], elaborating on our 2008 study. Finally, in 2018, our group combined the EndoS2 selectivity for IgG Fc and the EndoF3 selectivity for fucosylated glycans to site-selectively remodel both Fab and Fc glycans on the commercial monoclonal theurapeutic IgG, Cetuximab, effectively highlighting the versatility of this glycan remodeling technique[68]. These ENGases provide robust methods in IgG glycan remodeling and have been powerful tools for antibody and glycoprotein glycan

remodeling (**Figure 1.7**).

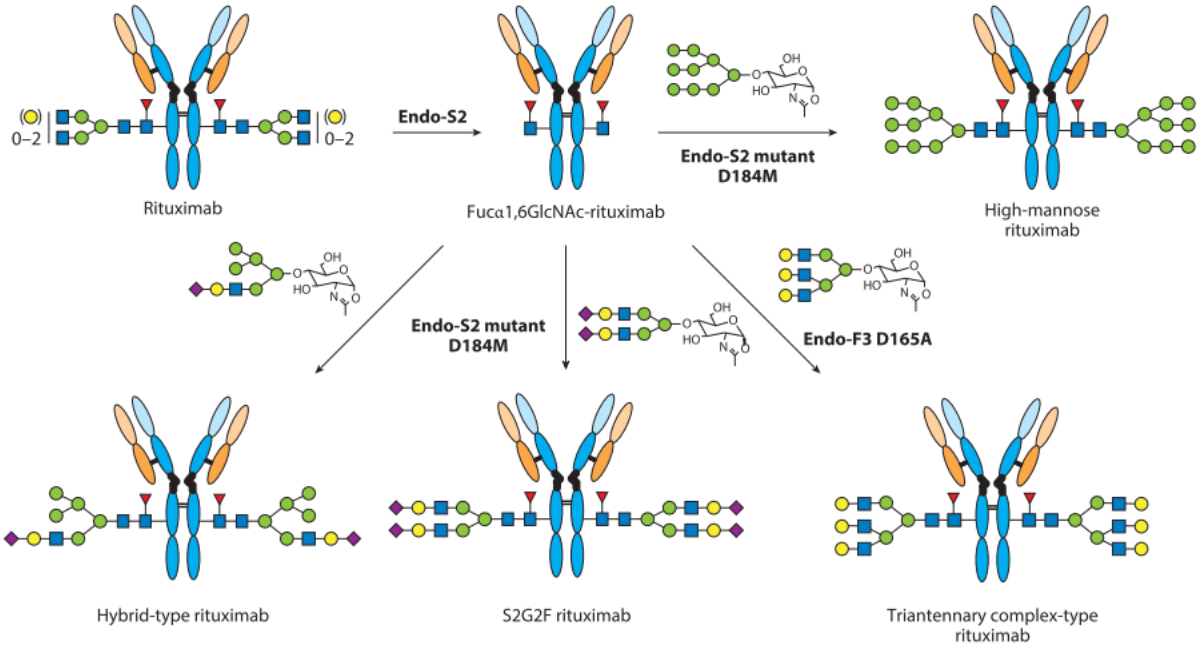

Figure 1.7. Schematic of ENGase-catalyzed deglycosylation and transglycosylation to produce homogenous antibody glycoforms. Figure adapted from publication by Wang *et al.*[69]

Building on these developments, my research projects aim to further investigate several GTs for chemoenzymatic synthesis of novel antibody glycoforms for exploring their therapeutic applications. My project highlighted in chapter 2 compares three sialyltransferase enzyme activity on free and IgG Fc-bound complex-type glycans to identify the optimal enzyme for the chemoenzymatic synthesis of fully sialylated IgG glycoforms. Chapter 3 will highlight the work in my second project to generate two novel IVIg glycoforms, each with a sialic acid analog terminating the Fc glycans. The goal of synthesizing these analogs is to probe the structural significance of key features of Neu5Ac that may play a role in facilitating IVIg-dependent anti-inflammatory activity. Finally, my third project highlighted in chapter 4 will detail the chemosynthetic approach to generate an Antibody Drug Conjugate (ADC) with cytotoxic

payload conjugated site-specifically to the IgG Fc glycans, while maintaining the core chitobiose-tri-mannose structure characteristic of *N*-glycans. By generating an ADC with a relatively high Drug to Antibody Ratio (DAR) with the core glycan structure intact, we can assess the efficacy of this novel construct relative to other glycan-conjugated ADCs without the intact core structures.

Chapter 2: Comparison of the enzymatic activity of three Sialyltransferases on Free N-glycans and Intact Antibody

2.1 Introduction

Human IgG antibodies are sialylated in the Golgi Apparatus by the ST6Gal-I sialyltransferase (EC 2.4.99.1). This enzyme belongs to the GT29 family of GTs in the CAZy database, along with all other eukarylotic and viral sialyltransferases. The folded structure of ST6Gal-I follows the type II architecture typical among Golgi-resident GTs, consisting of a short N-terminal cytosolic tail, a single transmembrane domain, a flexible stem region, and a large catalytic C-terminal domain[70-72]. ST6Gal-I also adopts what's known as a GT-A fold structure in its catalytic domain, characterized by an α/β/α sandwich resembling a Rossmann fold[73]. Interestingly, while most GT-A fold enzymes possess an Asp-X-Asp (DxD) motif to coordinate a required divalent metal cation (either Mn^{2+} or Mg^{2+}), ST6Gal-I does not possess this motif, indicating it does not need the metal cofactor for its ST activity. Interestingly, while ST6Gal-I does not share very much sequence homology with other human STs, all GT29 STs form 4 distinct motifs: Sialylmotifs L (large), S (small), motif III, and VS (very small)[74].

The mechanism of action for the ST6Gal-I sialylation of Galβ1-4GlcNAc acceptor substrates follows the S_N2-like reaction of an inverting enzyme. Sialylmotifs L and III bind to the sugar nucleotide donor substrate, while S binds to the donor and acceptor substrates. Sialylmotif VS contains the catalytic H270 residue, which partially deprotonates the 6'-OH of the terminal galatose residue for the nucleophilic substitution at the C2 position of the Neu5Ac donor, yielding the final sialylated product and releasing CMP[72]. An additional mechanistic proposal suggests that the anomeric position is primed for the reaction via tension in the Neu5Ac C2-CMP

bond, generating an oxocarbenium intermediate. This proposal is strongly supported by the development of effective ST inhibitors based on this oxocarbenium transition state[75, 76], but more detailed studies are needed to fully understand the mechanism of action of this sialyltransferases.

Recombinant ST6Gal-I has previously been used for the α2,6-sialylation of antibodies[50, 77, 78]. Unfortunately, the ST6Gal-I is slow in disialylating IgG Fc glycans and requires pushing with donor substrate over multiple days. For this reason, other α-2,6-sialyltransferases need to be tested for efficient sialylation activity on IgG Fc glycans. Potential candidates for efficient Fc sialylation include bacterial STs in the GT38, GT42, GT52, and GT80 CAZy families. The first bacterial α2,6-ST ever cloned was from *Photobacterium damselae* (Pd2,6ST). It is a GT80 enzyme that's used extensively for sialylation of free glycans and boasts ease of expression relatively to mammalian STs as well as relaxed substrate specificity[79-81]. This enzyme is noted for having a GT-B fold structure in its catalytic domain, characterized by two domain structures called Rossmann folds, domains that consist of an α-helical region flanked by two β-sheets (α/β/α), as well as a catalytic aspartate residue for the deprotonation of the acceptor substrate hydroxyl group[82]. Chen and colleagues have made extensive progress characterizing the donor substrate specificities and utilizing the enzyme to generate both natural and non-natural sialoglycans[80, 81, 83-85]. Recently, an α2,6ST from *Photobacterium* sp. *JT-ISH-224* (Psp2,6ST) was engineered to disialylate IgG Fc more efficiently. Despite limited structural information on this enzyme, in 2020, Ye and colleagues engineered a truncated double mutant Psp2,6ST (111-511) A2235M/A366G capable of producing a majority of the disialylated glycoform within a few hours and pushing steps[52].

Aside from the GT80 ST family, the Wakarchuk group has discovered two α2,6ST from the GT42 family. Like the GT29 family of STs, this family is believed to have a GT-A fold,

complete with the four sialylmotifs[71, 86-88]. The GT42 family of STs had previously only consisted of α2,3-STs, with the most famous of them being from *Campylobacter jejuni* (CST I and CST II). However, Wakarchuk and colleagues recently characterized two α2,6-ST: one from *Helicobacter acinonychis* (HAC1268) and another form *Helicobacter cetorum* (HcST)[89, 90]. The latter displayed relatively high activity for glycoprotein substrates, which the Wakarchuk group further enhanced by making a 42 amino acid truncation (HcST-22)[90]. However, the IgG Fc di-sialylation efficiency of these bacterial ST enzymes has yet to be explored.

The following work aimed to compare the efficiency of the recently reported ST from *Helicobacter cetorum* (HcST-22), as well as the ST from *Photobacterium damselae* (Pd2,6ST) to fully sialylate free and IgG Fc bound complex-type *N*-glycans relative to the notably low-efficiency ST activity of the commonly used human ST6Gal-I. These studies revealed HcST-22 to be much more efficient at sialylating IgG Fc than ST6Gal-I and Pd2,6ST, the latter of which had very little activity on IgG antibodies.

2.2 Results and Discussion

2.2.1 ST arm preference for free biantennary complex type substrate. One of our goals for this study was to observe any preference for the α1,6Man (upper) or α1,3Man (lower) arm substrates of the biantennary free complex type glycan exhibited by the three sialyltransferase enzymes. In a fully galactosylated biantennary complex-type glycan, both arms should be ideal substrates for an α2,6-sialyltransferase. However, it's been previously reported that the human ST6Gal-I (hST6Gal-I) used in this study has as much as a 13-fold preference for the α1,3-Man arm substrate relative to the α1,6Man arm substrate through NMR studies[91, 92]. Arm preference, however, has not been reported for either of the two bacterial enzymes used in this study.

To monitor the enzymatic preference for sialylating the α1,6Man or the α1,3Man arm of a biantennary glycan, we set up the reaction shown in **Scheme 2.1** using a biantennary glycan obtained through treating sialoglycopeptide (SGP) with PNGase F to generate the free disialylated complex type glycan with the intact chitobiose core at the reducing end, then further treating this product with neuraminidase to yield the asialo-digalactosyl product (G2-GN_2)(**1**). We then used **1** as the acceptor substrate for Sialyltransferase reactions using either HcST-22, Pd2,6ST, or hST6Gal-I and the sialic acid sugar nucleotide donor substrate (CMP-Neu5Ac). The reaction will first yield two monosialylated intermediate products, one having terminal sialylation on the α1,3-arm of the glycan (S1bG2-GN_2)(**2a**), and one having sialylation on the α1,6-arm of the glycan (S1aG2-GN_2)(**2b**). As the reaction continues, the intermediates will be sialylated again to yield the di-sialylated glycan product (S2G2-GN_2)(**3**).

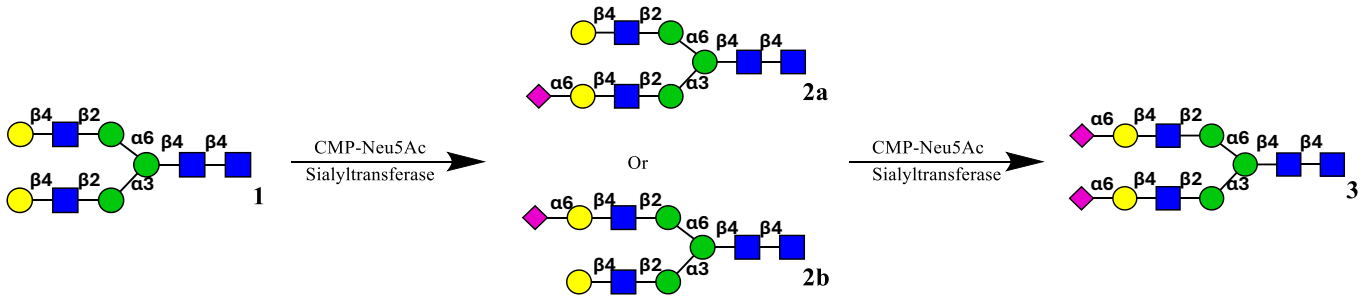

Scheme 2.1. Sialyltransferase reaction on free biantennary asialocomplex-type glycan

We monitored the accumulation of these products by High-Performance Anion Exchange Chromatography with Pulsed Amperometric Detection (HPAEC-PAD), paying close attention to the abundance of the intermediate **2a** and **2b** products in the earlier timepoints of the reaction to determine whether the STs were exhibiting an arm preference (**Figure 2.1**). Isoform ratios were determined by integrating the peak area at intermediate time points in triplicate for each ST using

the Chromeleon 8.1 chromatogram processing software, then averaging each isoform peak area before generating the **2a**:**2b** ratio. HcST-22 exhibited a 1.6-fold preference for the α1,6-arm substrate of the biantennary glycan. Conversely, the Pd2,6ST enzyme displays a higher production of **2a**, suggesting a 2-fold preference for the α1,3 arm. This selectivity of Pd2,6ST for α1,3Man arm is similar to that of the hST6Gal-I, which was previously reported to show a virtually exclusive preference for the α1,3-arm prior to being converted to **3** (**Table 2.1**)[91].

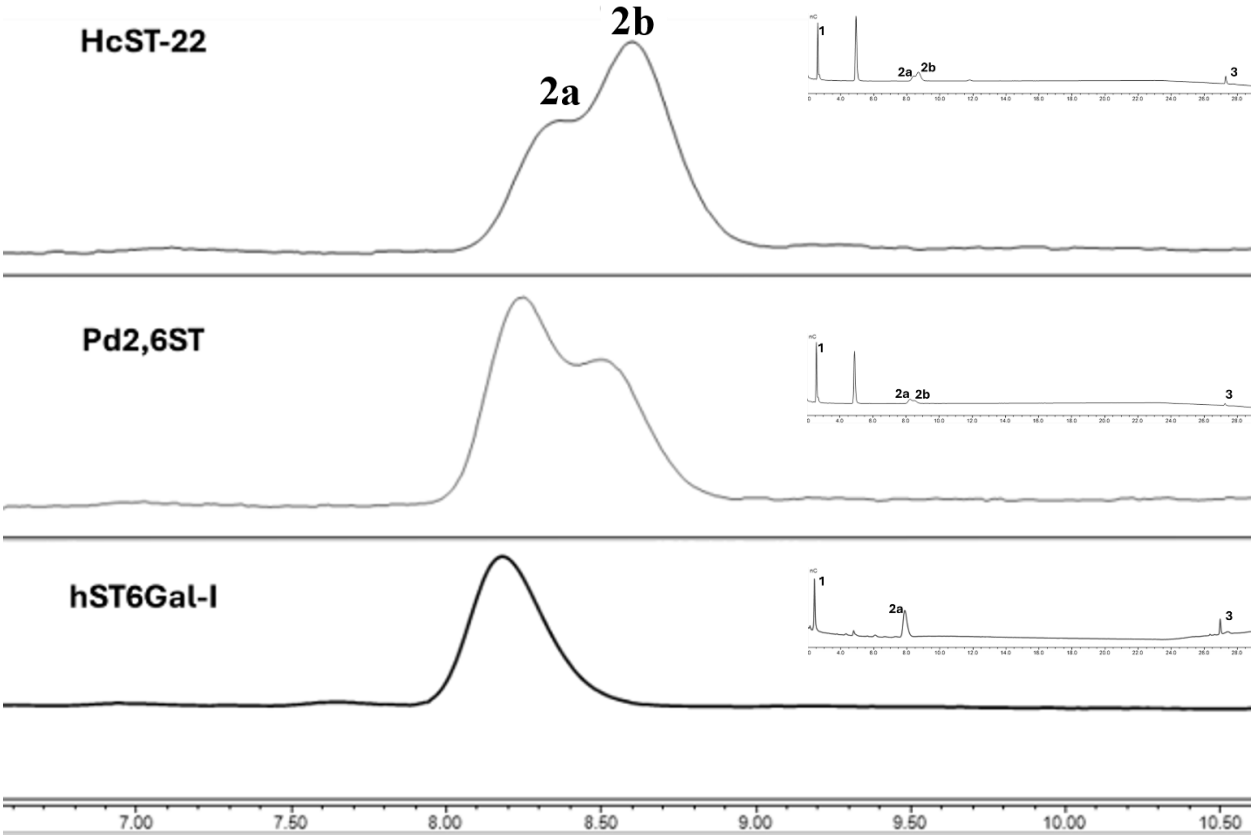

Figure 2.1 HPAEC-PAD analysis of monosialylated isoforms. HPAEC-PAD chromatogram of the monosialylated **2a** and **2b** intermediates during initial timepoints in ST reactions.

Table 2.1 Arm preference exhibited by STs.

Enzyme	**HcST-22**	**Pd2,6ST**	**hST6Gal-I**
2a:2b	5:8	2:1	NA*

*Only the **2b** product was observed, even as **3** was being accumulated. The **2a** product was not detectable

2.2.2 ST efficiency comparison free glycan. Next, we set out to assess the efficiency of each ST enzyme on free biantennary substrate to yield a fully sialylated product. The reaction follows the same scheme outlined in **Scheme 2.1**. We monitored enzyme efficiency and total yield using HPAEC-PAD. Compounds **1** and **3** were quantified using a standard curve of peak area vs molar amount and formation of **3** was monitored over time to generate a quantitative comparison of the yield of each enzyme displayed in **Figure 2.2**. These data indicate that HcST-22 is more efficient than Pd2,6ST, reaching product saturation after two hours while Pd2,6ST took more than four hours to reach the same point (**Figure 2.2A**). The commercial human ST6Gal-I was run using the number of enzyme units needed for the reaction to finish after 24 hours to serve as a standard for reaction efficiency (**Figure 2.2B**).

A)

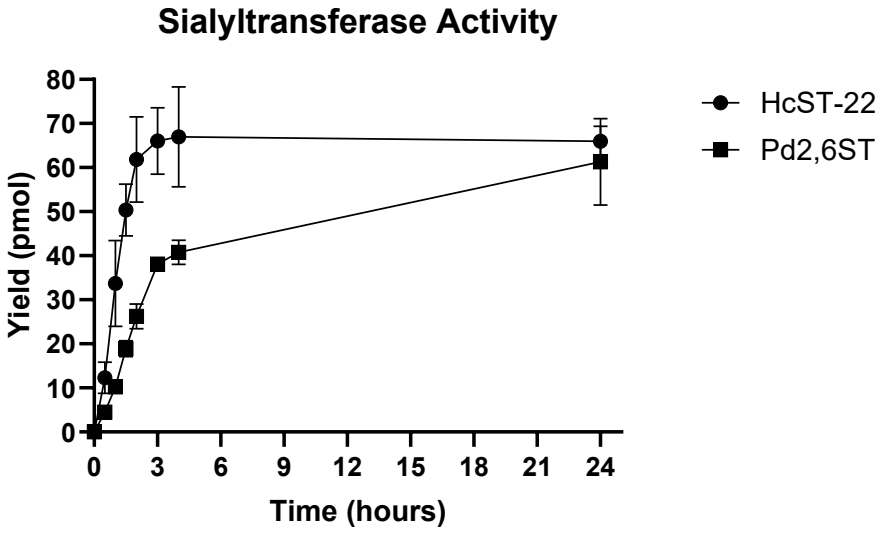

B)

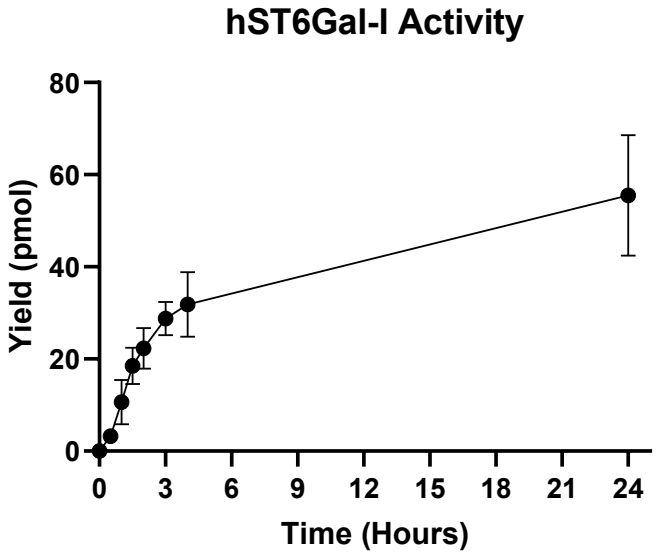

Figure 2.2 Comparison of bacterial sialyltransfer activity on free *N*-glycan substrate. Sialyltransferase reaction conducted with 10mM **1** starting material and 5 equivalents of donor substrate and monitored by HPAEC-PAD to determine conversion efficiency and yield. A) represents the enzymatic activity of 0.1 mg/mL HcST-22 (Blue)and 0.1 mg/mL Pd2,6ST (Orange). B) Represents the enzymatic activity of 1.39 mU/nmol substrate hST6Gal-I.

2.2.3 Direct Sialylation of Intact IgG by HcST-22. After assessing the activity of the STs on free glycan, we moved onto whole IgG as the substrate. For this study we used commercially obtained trastuzumab IgG antibody, possessing only one glycosylation site at the conserved N297 on the Fc domain. The glycosylation natively found at this site is a mixture of complex type glycoforms with variable degrees of galactosylation and sialylation. To reduce glycoform variation, we used ENGase-catalyzed chemoenzymatic glycan remodeling to generate homogenous fully galactosylated asialo-trastuzumab.

The trastuzumab starting material was generated by treating commercial trastuzumab with wildtype EndoS2 to cleave the β1,4-linkage between the first two *N*-acetylglucosamine (GlcNAc) residues, leaving only a single GlcNAc residue and the α1,6-Fucose if initially present (GNF-Trastuzumab). The deglycosylated antibody was purified via protein A column, and transglycosylation was performed by adding G2-oxazoline to the GNF-Trastuzumab in the presence of EndoS2 D184M glycosynthase mutant to generate the fully galactosylated G2F-Trastuzumab (**4**) (**Figure 2.3A**). Some monogalactosylated antibody was present due to the small population of G1-oxa in the oxazoline donor substrate, shown in **Figure 2.3A**. We then incubated **4** with an ST enzyme and the sugar nucleotide donor to assess whether the enzymes could recognize whole IgG glycans as acceptor substrates (**Scheme 2.2**).

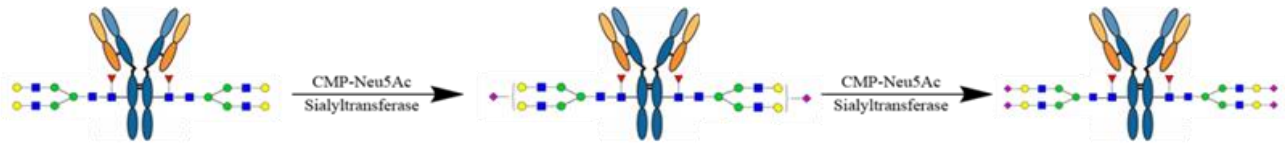

Scheme 2.2. Direct Antibody Sialyltransferase Reactions

Through monitoring the reaction using Liquid Chromatography coupled with Electrospray Ionization Mass Spectrometry (LC-ESI-MS), we observed the conversion of the **4** by the sialyltransferase enzymes into the monosialylated IgG intermediate (**5**), followed by the disialylated IgG final product (**6**). We show that HcST-22 is the most efficient enzyme at sialylating whole IgG Fc, producing a near quantitative yield of **6** after only 4 hours (Figure 3B). The Pd2,6ST, however, was only able to produce less than 5% of **5**, with no **6** product formed after approximately 24 hours (**Figure 2.3C**). The human ST6Gal-I performed somewhat better, with a 15% conversion to **5**, but no conversion to **6** after approximately 36 hours (**Figure 2.3D**). From these data, we conclude that the HcST-22 is the best enzyme for terminal sialylation of the conserved IgG Fc glycans compared to the other Pd2,6ST and human ST6Gal-I.

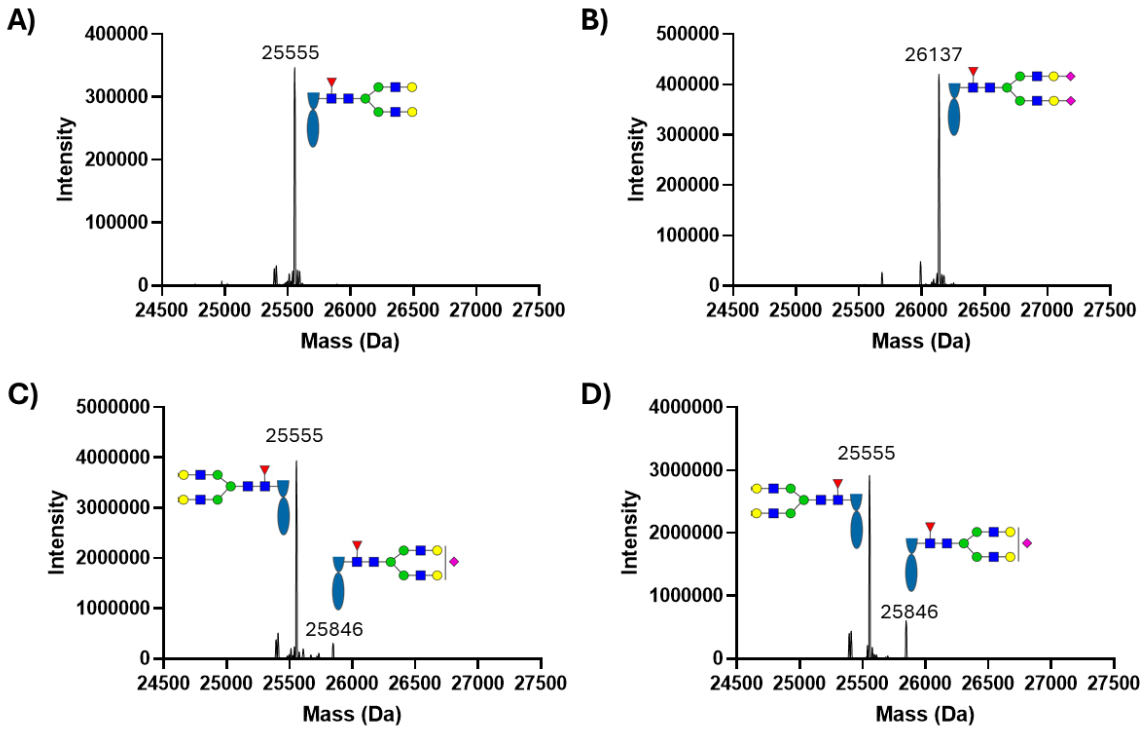

Figure 2.3 LC-ESI-MS analysis of ST reactions on intact IgG substrate. Sialylation reactions of G2F-Trastuzumab. Mass data shows IdeS digestion to Fc monomers of A) asialo-IgG-Fc starting material, B) 4 hour HcST-22 reaction, C) 24 hour Pd,2,6ST reaction, and D) 36 hour ST6Gal-I reaction. LC-ESI-MS analysis: G2F-Trastuzumab Fc monomer M = 25,554 Da, observed m/z 25,555 (deconvoluted); S1G2F-Trastuzumab M = 25,845 Da, observed m/z 25,846 (deconvoluted); S2G2F-Trastuzumab M = 26,136 Da, observed m/z 26,137 (deconvoluted).

2.3 Conclusion

These data indicate that HcST-22 is the most efficient ST at both the sialylation of free glycan as well as intact IgG Fc. We also demonstrated that the enzyme works well in a two-enzyme one-pot reaction with NmCSS generating CMP-Neu5Ac *in situ*. In addition to observing the enzymatic efficiency and IgG acceptor capabilities, we also observed differences in substrate arm preference of when using free biantennary *N*-glycan as an acceptor substrate. This work will

lay the foundation for characterizing ST substrate specificity, as well as comparing IgG Fc sialylation activity among various STs.

2.4 Materials and Methods

Materials: All chemicals, reagents, and solvents purchased from Sigma Aldrich, Carbosynth, and TCI and used as received unless otherwise specified. Humanized Herceptin monoclonal antibody, *Neisseria meningitidis* CMP-Sialic Acid Synthetase (NmCSS), and *Staphylococcus aureus* β-*N*-acetyl-endoglucosaminidase and its glycosynthase mutant (EndoS2 WT and D184M) were expressed recombinantly in house by other members of the lab for this project. Solid human ST6Gal-I was purchased commercially (Sigma Aldrich). Plasmids for the expressions of the 42aa trucated *Helicobacter cetorum* and *Photobacterium damselae* sialyltransferases (HcST-22 and Pd2,6ST) were generated by previous members of the lab.

2.4.1 Expression of HcST-22 and Pd2,6ST

Enzymes were expressed in *E.coli* as previously described. Plasmids of the respective enzymes were transformed into BL21(DE3) cells and incubated in LB broth with carbenicillin antibiotic at 37°C and shaking at 225rpm until OD_{600} reached 0.6-0.8. IPTG was then added and the temperature was reduced to 18°C and left to grow overnight. Cells were then harvested by centrifugation, lysed by sonication, and purified by Nickel chromatography on an AKTA pure 25L (Cytiva Life Sciences) FPLC system using a HisTrap column (5 mL). Proteins were buffer exchanged into 150 mM PBS pH 7.4. Purity and quality of the proteins confirmed by SDS-PAGE and concentration was measured by absorbance via Nanodrop (2000c) (Thermofisher).

2.4.2 Free Glycan sialyltransferase reaction

A solution of G2-GN_2 (821 µg, 0.5 µmol) was incubated with NmCSS (12.5 µg) and either HcST-22 or Pd2,6ST (5 µg) in a two-enzyme one-pot reaction with both Neu5Ac and CTP (50 mM, 5 eq per IgG molecule) at 37 °C in 50 µL of in 20 mM $MgCl_2$ in 100 mM Tris-Cl buffer (pH = 7.5). For the ST6Gal-I transfer reaction, a solution of G2-GN_2 (328 µg, 0.2 µmol) was incubated with commercial hST6Gal-I (1.39 mU/nmol G2-GN_2) with CMP-Neu5Ac (50 mM, 5 eq per G2-GN_2) at 37 °C in 20 µL of 20 mM $MgCl_2$ in 50 mM MES buffer (pH = 6.0). Reaction timepoints were taken over a 24-hour period and monitored by HPAEC-PAD.

2.4.3 Reaction analysis by High Performance Anion Exchange Chromatography with Pulse Amperometric Detection (HPAEC-PAD)

Free glycan reaction progress was monitored by HPAEC-PAD on a ThermoFisher Scientific Dionex™ ICS-6000 system with a electrochemical detector (ED50). The column was an anion exchange column (CarboPAC PA200 4 × 250 mm) for efficient separation of oligosaccharide isomers. Solvent lines consisted of line A (18.5 MΩ MilliQ water), line B (10 mM NaOH), line C (100 mM NaOH), and line D (1 M NaOAc in 100 mM NaOH). The method for analysis started with a 20 minute isocratic run (0-20 minutes, 50% line A, 47% line C, and 3% line D), followed by linear gradient for 5 minutes (20-25 minutes, 50% line A, 30% line C, and 20% line D).

2.4.4 Antibody Fc deglycosylation

The commercial trastuzumab (5 mg) was incubated with immobilized wild-type Endo-S2 (Endo-S2 WT)(200µg) in a total volume of 1.0 ml (150 mM PBS, pH 7.4). The mixture was incubated overnight at room temperature when LC-ESI-MS indicated the completion of deglycosylation. Then the reaction mixture was centrifuged at 8,000 rpm and purified by protein A column to

afford the deglycosylated trastuzumab (4.5 mg, 90% yield). ESI-MS: calculated for the Fc monomer after IdeS digestion, M = 24,134 Da; found (m/z) 24,135 (deconvolution data)

2.4.5 Semi-synthesis of G2F-Trastuzumab glycoform

A solution of commercial Trastuzumab (4.5 mg) and G2-oxazoline (1.3 mg, 15 eq per reaction site), generated as previously described[93], was incubated with Endo-S2 D184M (100 μg) at 30 °C in 1 mL of 150 mM PBS buffer (pH = 7.4), and the reaction was monitored by LC–MS of aliquots. Within 30 min, LC–MS analysis indicated the completion of the transglycosylation with conversion yield >95%; the product was purified using protein A chromatography and concentrated to a final yield of 3.6 mg (41.9 mg/mL as measured using Nanodrop, 80% yield). LC–MS: after IdeS digestion, LC–MS calculated for the Fc part, M = 25,554 Da; found (m/z), 25,555 (deconvolution data)

2.4.6 G2F-Trastuzumab Sialylation reaction conditions

A solution of G2F-Trastuzumab (600 μg, 30 mg/mL) was incubated with NmCSS (5 μg) and either HcST-22 or Pd2,6ST (4 μg) in a two-enzyme one-pot reaction with both Neu5Ac and CTP (30 mM, 150 eq per IgG molecule) at 37 °C in 20 μL of 20 mM $MgCl_2$ in 100 mM Tris-Cl buffer (pH = 7.5). For the ST6Gal-I transfer reaction, a solution of G2F-Trastuzumab (600 μg, 30 mg/mL) was incubated with commercial hST6Gal-I (18.5 mU/mg IgG) with CMP-Neu5Ac (30 mM, 150 eq per IgG molecule) at 37 °C in 20 μL of 20 mM $MgCl_2$ in 50 mM MES buffer (pH = 6.0). All reactions were monitored by LC–MS of aliquots. After IdeS digestion, LC–MS calculated for the fully sialylated Fc part, *M* = 26,136 Da.

2.4.7 Scale up and purification of HcST-22 treated fully sialylated Herceptin

A solution of G2F-Trastuzumab (1 mg), Neu5Ac (0.32 mg, 150 eq per IgG), and Na_2CTP (0.54 mg, 150 eq per IgG) was incubated in the presence of NmCSS (8.5 μg) and HcST-22 (6.8 μg) at

37 °C in 34 µL of 100mM Tris-Cl pH 7.5 and 20 mM $MgCl_2$ for 4 hours, monitored IdeS digestion and LC-MS. Upon completion, reaction mixture filtered and purified by protein G column for a final yield of 0.6 mg (60% yield). LC-MS: calculated for the whole antibody *M* = 149,871 Da; found (m/z), 149,872 (deconvolution data); after IdeS digestion, LC–MS calculated for the Fc part, M = 26,136 Da; found (m/z), 26,137 (deconvolution data).

2.4.8 Protein A purification of monoclonal antibodies and their conjugates

Antibody reaction mixtures were diluted to 1 mL in PBS buffer pH 7.4 and loaded on to a preequilibrated HiTrap Protein A HP 1 mL column (GE Healthcare) by syringe pump. The flowthrough was collected and re-loaded through the column. The column was washed thoroughly with 20 mL PBS pH 7.4 at 1 mL/min flow rate using an AKTA Pure FPLC system (Cytiva) and then eluted with 30 mM sodium citrate pH 2.6 buffer in one step for 10 minutes. Samples were collected as 1 mL fractions in tubes containing 100 µL 1 M Tris pH 8.5, and antibody containing fractions were identified by in-line UV detection at 280nm before being immediately buffer-exchanged to the appropriate buffer using Amicon Ultra 10 kDa MWCO centrifugal filters (Millipore). Antibody samples were collected, and final concentrations were determined by Nanodrop 2000c (Thermo Scientific).

2.4.9 LC-ESI-MS analysis of intact antibodies

Performed with an Exactive Plus Orbitrap Mass Spectrometer (Thermo Scientific) equipped with a Waters XBridge BEH300 C4 column (3.5 µm, 2.1 Å~ 50 mm) with solvent lines consisting of water (line A) and acetonitrile (line B) in a background of 0.1% formic acid. Mass spectra was deconvoluted using MagTran (ver 1.03 b2)

2.4.10 LC-ESI-MS of IdeS released IgG Fc monomers

Performed with an Exactive Plus Orbitrap Mass Spectrometer (Thermo Scientific) equipped with an Agilent Poroshell 300SB C8 column (5 µm, 1.0 Å~ 75 mm) with solvent lines consisting of water (line A) and acetonitrile (line B) in a background of 0.1% formic acid. Mass spectra was deconvoluted using MagTran (ver 1.03 b2)

2.5 Supplementary Data

A)

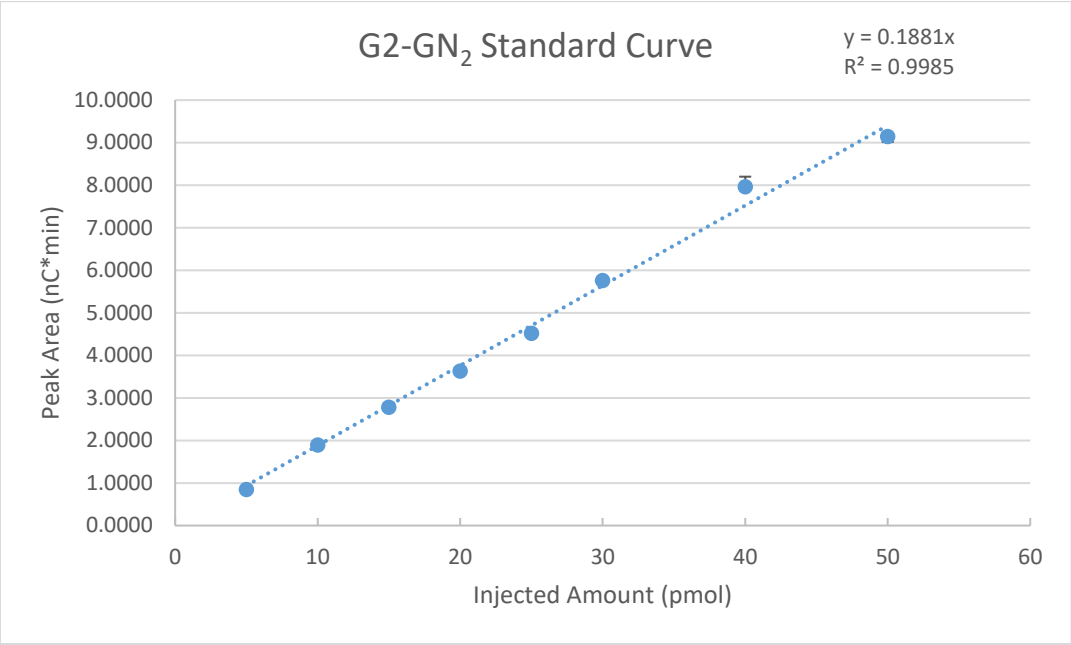

B)

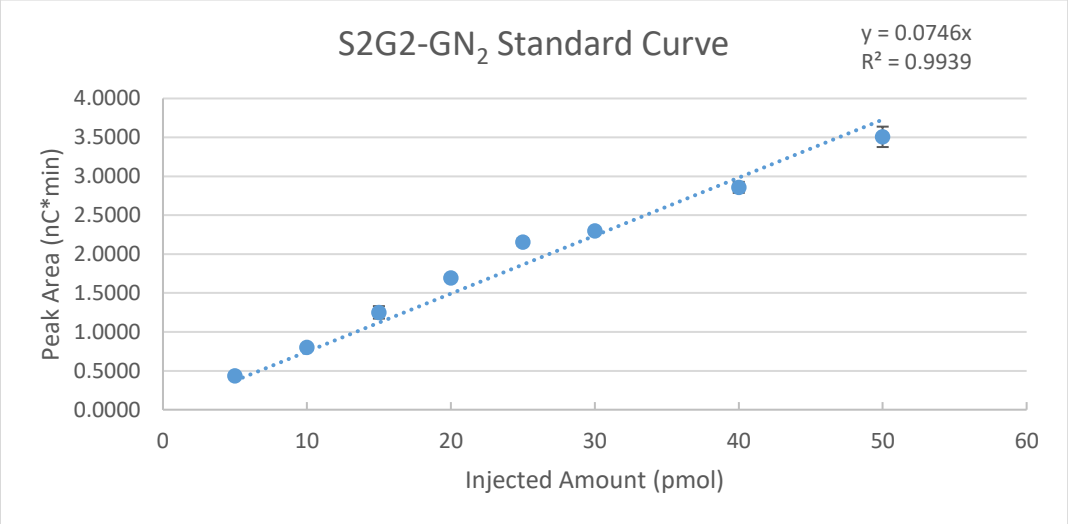

Figure 2.4. HPAEC-PAD-derived plot of peak area vs quantity of injected glycan for A) the G2-GN_2 starting material and B) the S2G2-GN_2 product.

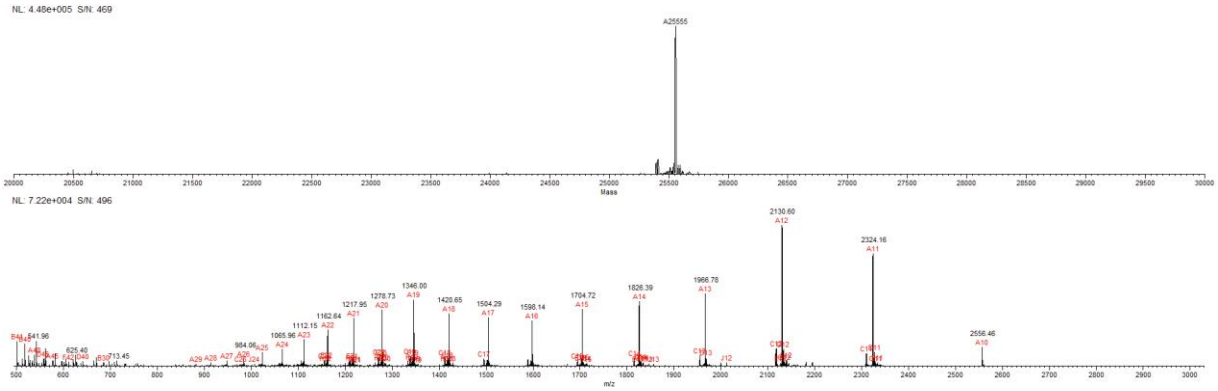

Figure 2.5. LC-ESI-MS spectrum of IdeS treated G2F-Trastuzumab Fc monomer.

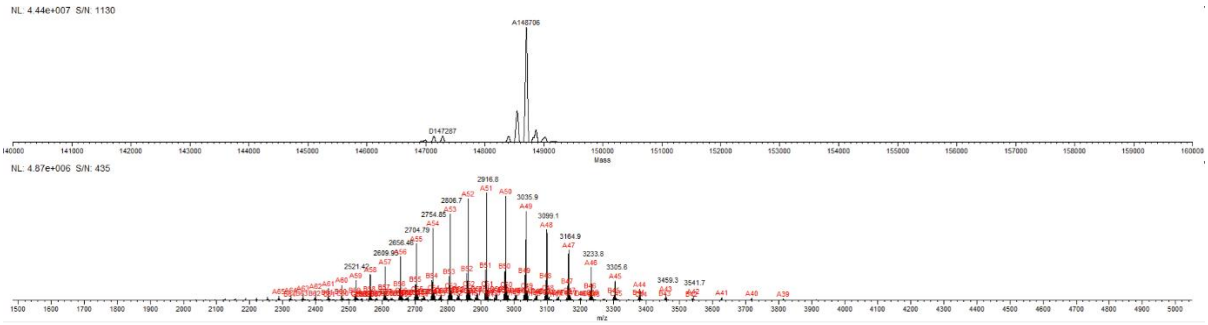

Figure 2.6. LC-ESI-MS spectrum of intact G2F-Trastuzumab antibody.

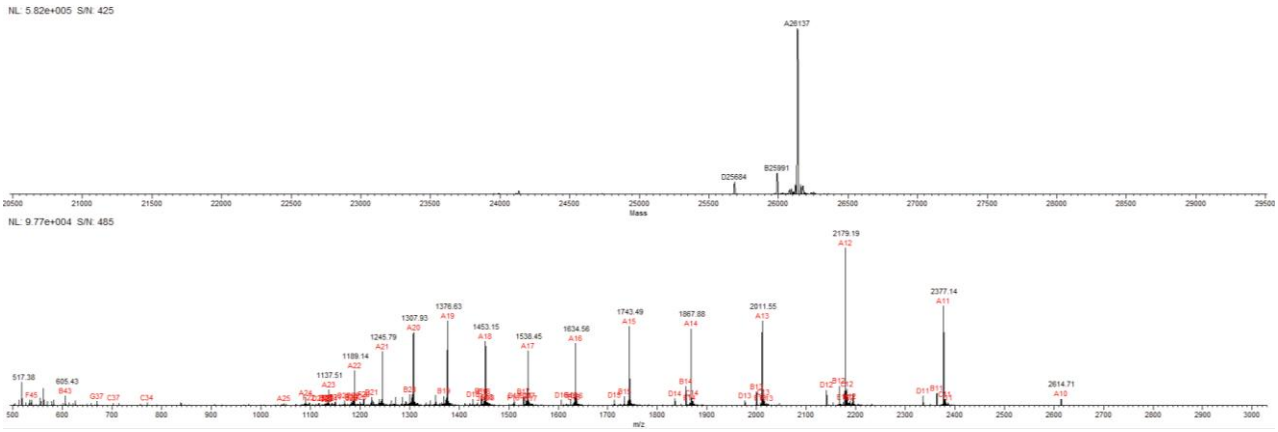

Figure 2.7. LC-ESI-MS spectrum of IdeS-treated HcST-22 reaction mixture with G2F-Trastuzumab starting material after 4 hours.

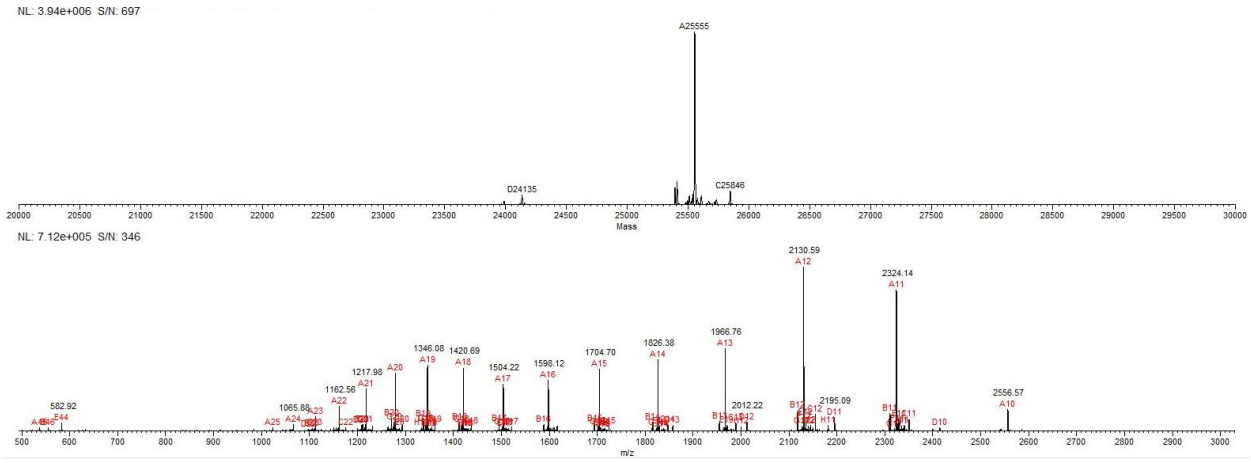

Figure 2.8. LC-ESI-MS spectrum of IdeS-treated Pd2,6ST reaction mixture with G2F-Trastuzumab starting material after 48 hours.

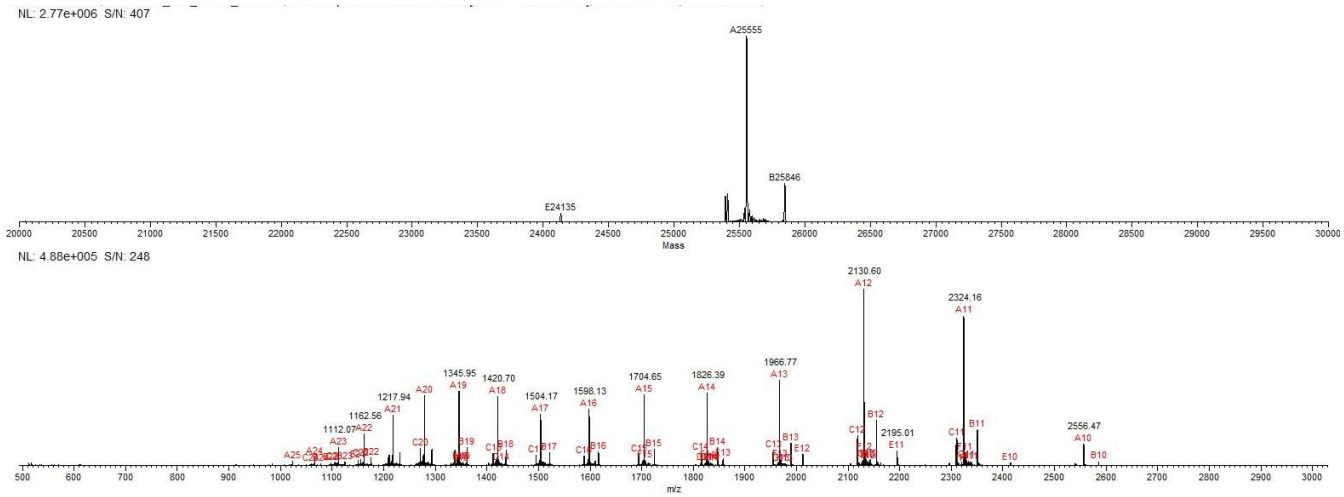

Figure 2.9. LC-ESI-MS spectrum of IdeS-treated hST6Gal-I reaction mixture with G2F-Trastuzumab starting material after 36 hours.

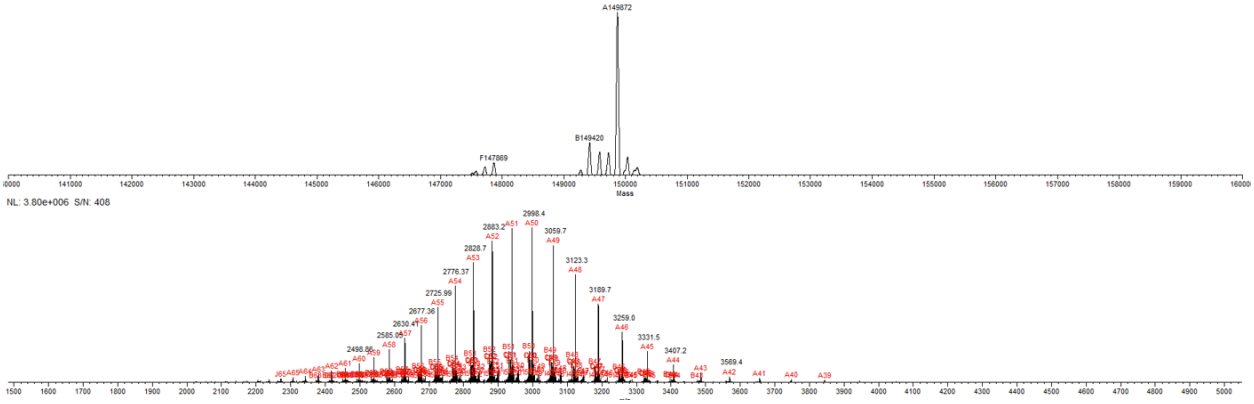

Figure 2.10. LC-ESI-MS spectrum of purified intact HcST-22-sialylated S2G2F-Trastuzumab antibody.

Chapter 3: Generation of IVIg Glycoforms for Probing the Structural Significance of Terminal Sialylation

3.1 Introduction

Intravenous Immunoglobulin (IVIg) is a therapeutic preparation consisting of antibodies extracted and concentrated from the serum tens of thousands of human donors. Preparations of IVIg are traditionally used to treat patients with recurring infections due to immunological deficiencies, as the vast donor pool confers humoral immunity representative of the collect community of the donor population[94]. However, in addition to treating infections in patients with immune deficiencies, IVIg has been shown to have anti-inflammatory activity in patients suffering from certain autoimmune conditions, such as Immunothrombocytopenia Purpura (ITP), Kawasaki disease, and Guillain-Barre syndrome[28, 29, 95].

Despite numerous reports of the anti-inflammatory effects of IVIg, the mechanism of action is poorly understood, largely due to the varying responses of different autoimmune disorders to IVIg. Numerous non-exclusive mechanistic proposals have been investigated over the decades since the discovery of the anti-inflammatory effect of IVIg, such as a concentration-dependent IgG clearance mechanism to essentially "flush" pathogenic IgG out of circulation, and an inhibitory effect on T cell and B cell cytokine production[96, 97]. One particularly compelling proposal was made by Professor Jeffrey Ravetch and colleagues, which attributes the anti-inflammatory effect of IVIg to terminal sialylation of the IgG Fc glycans[28, 29] resulting in the upregulation of the inhibitory FcγRIIB receptor on Macrophages[16, 98-100].

Ravetch and colleagues were able to show that mouse models treated with IVIG showed increased expression of the inhibitory FcγIIB receptor, an inhibitory cell surface receptor which

raises the threshold of effector cell activation.[27, 98] They further identified α2,6-sialylation on specifically the Fc region of the antibody granted IVIg its protective effects.[29] This finding was particularly notable given that FcγR binding interactions don't generally display such a profound functional dependence on the sialic acid linkage of the Fc glycan. The specific requirement of α2,6-sialylation suggests that FcγRs are not the direct effector targets of IVIg for conferring its anti-inflammatory activity given report that sialylation has very little impact on FcγR binding[67] and thus there must be an upstream receptor that initiated that modulates the expression of effector cell FcγRIIB .

Ravetch and colleagues probed for potential IVIg interaction partners until they identified mouse SIGN-R1, a calcium-dependent C-type lectin receptor, as indispensable to the anti-inflammatory effect of IVIg, as mice with deletions in SIGN-R1 expression get not protection from IVIg treatments.[101] In addition, they were able to show that SIGN-R1 knockout mice that expressed the human analog, DC-SIGN, rescued the anti-inflammatory function of IVIg treatment, validating this lectin an upstream competent of IVIg-dependent anti-inflammatory activity.[95] This finding is particularly strange because the canonical binding substrates for both SIGN-R1 and DC-SIGN are high mannose glycans and dextran, with little evidence for interactions with sialylated complex-type glycans.[101]

Notably, there are conflicting findings regarding the necessity of proposed components of the anti-inflammatory mechanism leading to a high degree of uncertainty for the mechanism as a whole. For example, Käsermann and colleages concluded in a 2014 publication that Fc sialylation, as well as basophils were dispensable to the anti-inflammatory activity of IVIg. They determined this by treating two arthritic mouse models (CAIA and K/BxN) SNA lectin-enriched sialylated IgG or sialylated Fc fragments. Prior to treating the mice, the researchers either

depleted the sialic acid content of the lectin-fractionated antibodies by incubating with neuraminidase, or they depleted basophils by treatment with anti-FcεR antibody. While they clearly illustrated the anti-inflammatory activity of the Fc portion of the IVIg, they saw no loss in activity with sialic acid or basophil depletion, suggesting they are not essential to the mechanism of action.[102] In addition to conflicting evidence for components within Ravetch's proposed mechanism of action, other groups have been finding evidence of other mechanisms of action with other autoimmune disease models.[100] The uncertainty surrounding details of the mechanism of action highlights the need for approaches aimed at determine direct interactions between sialylated IVIg and effector receptors.

While humans only have one sialic acid, Neu5Ac, the term "sialic acid" describes a family of 9-carbon negatively charged sugars. In other mammals, the sialic acid *N*-glycolylneuraminic acid (Neu5Gc) exists in addition to Neu5Ac. In certain species of fish and other invertebrates, 2-keto-3-deoxy-D-glycero-D-galacto-nononic acid (KDN) is a prevailing sialic acid on their glycoproteins.[103] Within bacteria, the structural diversity expands even more. While these sugars share similarities in structure, they are differentially recognized by receptors. Even in mammals such as mice that have both Neu5Ac and Neu5Gc, certain receptors will only interact with one or the other, and among those receptors, they will only bind to sialic acid linked to a specific position of a galactose. For example, sialic acid immunoglobulin-like lectin receptors (Siglecs) are lectin receptors characterized by their affinity to sialic acid, but their binding profiles differ greatly by linkage to a given sugar[104-106]. Siglec-2 will only bind to Neu5Ac linked at the carbon 6 (C6) position of a galactose on a glycan (Neu5Acα2,6Gal), but will not bind to Neu5Ac linked at the C3 of a similar glycan (Neu5Acα2,3Gal). In mice, a common animal model for human pathologies, Siglec-2 behaves similarly while showing

differential affinity for Neu5Ac vs Neu5Gc. Because Mice have very similar lectin and FcγR receptors, they were the preferred model for studying the mechanism of the IVIg anti-inflammatory mechanism. While much scrutiny has been cast on the use of mice for this purpose due to major differences in receptor expression and function relative to humans, it provided needed foundations for the study of IVIg activity[107]. Understanding how sialylated glycans structurally plays into the mechanism behind the therapeutic effects of IVIG may help to make informed proposals of the target of sialylated IVIG *in vivo*, and thus, gain some understanding of the mechanism behind IVIG protection and treatment.

3.2 Results and Discussion

To begin studying the structural characteristics Neu5Ac on antibodies required to confer anti-inflammatory activity, a collaborative effort was made to generate IVIg antibody glycoforms with specific modifications relative to fully sialylated IVIg with native sialic acid. We hypothesized that any structural deviations relative to the natural glycan structure in IVIg that disrupted autoimmune inhibitory activity would indicate that the modified feature of sialic acid was essential for IVIg anti-inflammatory function. To test this, I developed two sialylated IVIg glycoforms using chemoenzymatic remodeling. One IVIG glycoform is incorporated with sialic acid derivative KDN residues at each terminal site of the N297 glycosite, and the other consists additional sialocomplex-type glycans click-conjugated to the terminal positions of the fully sialylated IVIg N297 glycosite (**Figure 3.1**). We intend to perform *in vivo* mouse studies in collaboration with the Anthony group at the Harvard Medical School to determine anti-inflammatory activity of each glycoform.

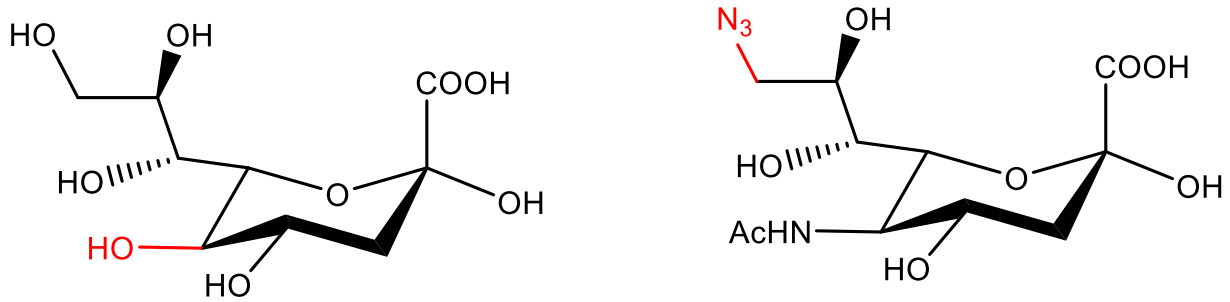

Figure 3.1. Structures of KDN and 9-azido-Neu5Ac sialic acid analog targets. Structural deviations from canonical Neu5Ac are shown in red.

3.2.1 Chemoenzymatic synthesis of terminal di-KDN complex-type glycan. Of the forms of sialic acids that exist in nature, the three predominantly expressed in vertebrate animals (Neu5Ac, Neu5Gc, and KDN) vary at the C5 position. While this C5 position has been known to be important for receptor binding to proteins such as siglecs, it is unknown how such variation would affect IVIg anti-inflammatory activity. To this end, we wanted to generate a glycoform that incorporated KDN into the terminal position of the IVIg glycan to see whether its anti-inflammatory activity would remain preserved. KDN was of particular interest also because unlike Neu5Ac and Neu5Gc, mice do not typically express this sialic acid on their glycans, meaning that none of their sialic acid binding proteins will be adapted for KDN binding.

To begin, we adapted a chemoenzymatic approach developed previously to synthesize the KDN monosaccharide[80, 81, 83, 108]. Mannose (**7**) was incubated with five molar equivalents of sodium pyruvate in the presence of *Pasteurella multocida* sialic acid aldolase to yield (KDN) (**8**) (**Scheme 3.1**).

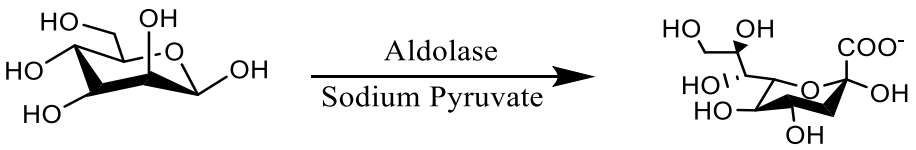

7 8

Scheme 3.1. Aldolase-catalyzed synthesis of KDN

Next, a one-pot two enzyme approach was employed to first convert **8** into the nucleoside donor substrate using *Nesseria meningitidis* CMP-sialic acid synthetase (NmCSS), then to transfer this activated donor substrate onto a free asialocomplex-type glycan acceptor (**9**) using *Photobacterium damselae* α-2,6-sialyltransferase (Pd2,6ST) to generate free di-KDN complex-type glycan (**10**) (**Scheme 3.2**). Reaction was monitored by LC-MS and MALDI-TOF, requiring frequent pushing over the course of several days with **8** and CTP to maximize production of **10**. After reaction progress had stalled, the product was purified by gel filtration and anion exchange chromatography (**Figure 3.2**).

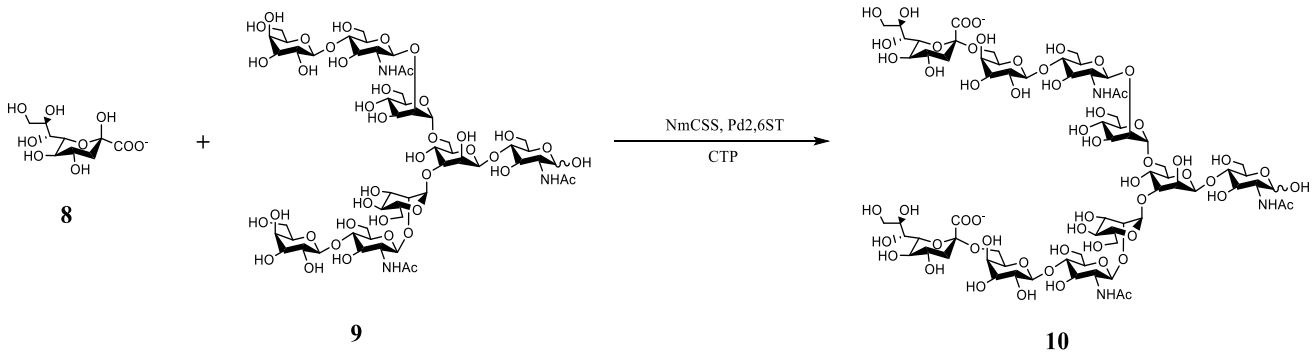

8 **9** **10**

Scheme 3.2. Synthesis of K2G2 Glycan

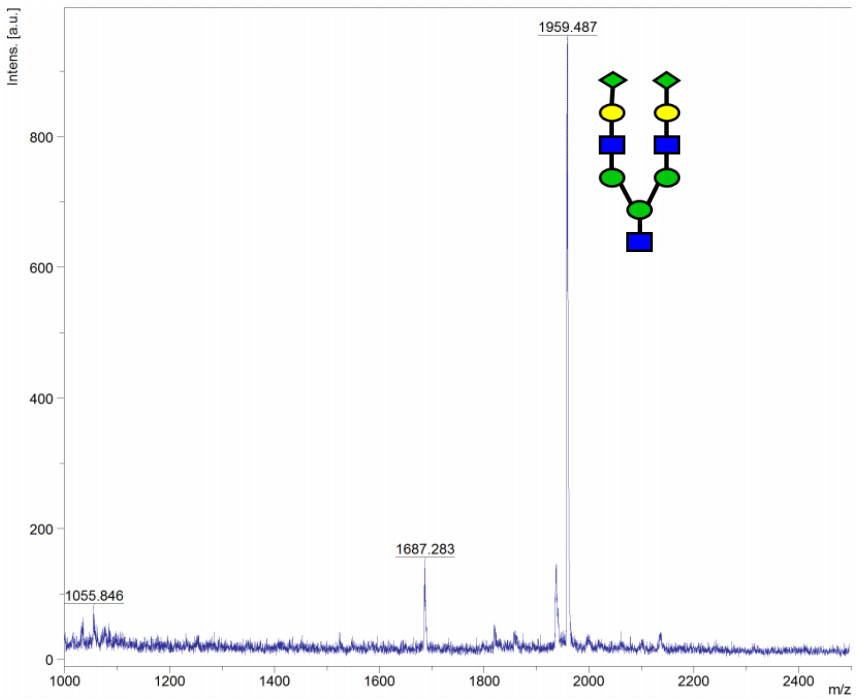

Figure 3.2 Mass analysis of the synthesized K2G2 product. MALDI-TOF MS spectrum of purified **4** glycan after anion exchange chromatography. Exact mass of **10**: 1937.65 Da; Mass found: m/z 1959.49 $[M + Na]^-$. Note, partial desialylation will spontaneously occur due to ionization energy from the MALDI-TOF laser, leading to monosialylation peaks that are not truly present in the product (m/z 1697).

3.2.2 Chemoenzymatic synthesis of terminal 9-azido sialocomplex-type glycan. In addition to studying the structural features of Neu5Ac that confers IVIg's anti-inflammatory activity, we also wanted to investigate whether recruitment of other surface proteins such as immune-inhibitory siglecs to FcγR-bound IVIg Fc plays a role in the anti-inflammatory mechanism of action. Such recruitment of these inhibitory factors could play a critical role by increasing the activation threshold for initiating cell-mediated inflammatory responses. To investigate this idea, we first want to generate an azide-tagged sialic acid (**Figure 3.3**) to incorporate onto the IVIg N297 glycosite. This sialic acid analog possessing the azido-bioorthogonal tag would then allow us to conjugate additional sialocomplex-type glycans, thereby extending the glycans.

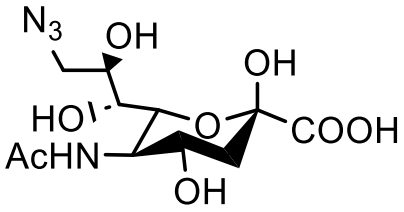

Figure 3.3. Structure of 9-azido-5-N-aceytneuraminic acid ($9N_3$Neu5Ac)

We synthetically modified the C9 position of commercial Neu5Ac to generate the 9-azido-Neu5Ac analog (**Scheme 3.3**). We began the chemical synthesis of this sialic acid compound by first protecting the C1 carboxylic acid position of commercial Neu5Ac via methyl esterification reaction to yield the 1MeNeu5Ac product (**11**). Addition of one equivalent of Tosylsulfonyl-chloride to **11** generated the C9-tosylated MeNeu5Ac (**12**) compound, priming the C9 position the subsequent substitution reaction and simultaneous C1 deprotection through the addition of sodium azide to generate the 9-azido-Neu5Ac (**13**) product. Purity and quality were assessed by LC-ESI-MS (**Figure 3.4A**). This sialoside was then transferred onto asialo free glycan (**3**) via the two-enzyme one-pot method (**Scheme 3.4**). A solution of **9** and **13** were incubated with NmCSS, Pd2,6ST, and CTP and monitored by LC-ESI-MS and MALDI-TOF. This reaction required less time and pushing to generate the majority disialylated product. The mixture was then desalted and separated by anion exchange chromatography to yield the final $9N_3$S2G2 glycan (**14**) (**Figure 3.4B**).

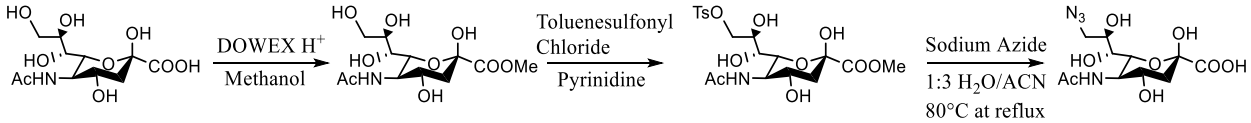

Scheme 3.3. Synthesis of 9-azido-Neu5Ac

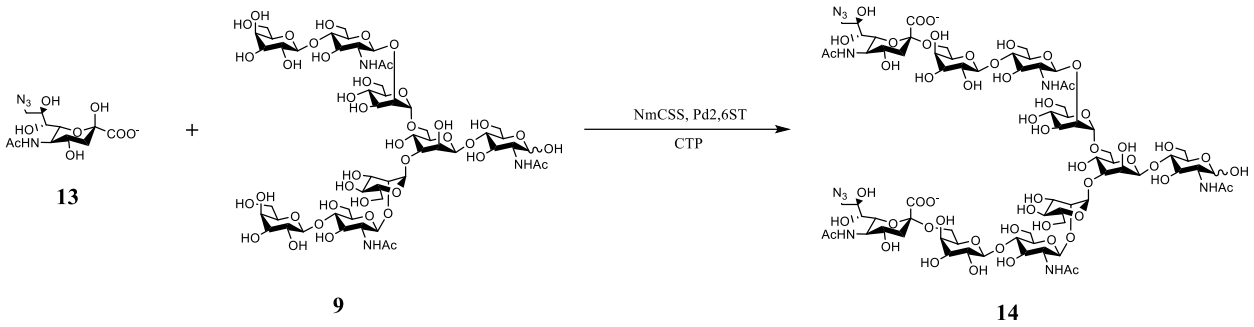

13 9 14

Scheme 3.4. Synthesis of $9N_3S2G2$ Glycan

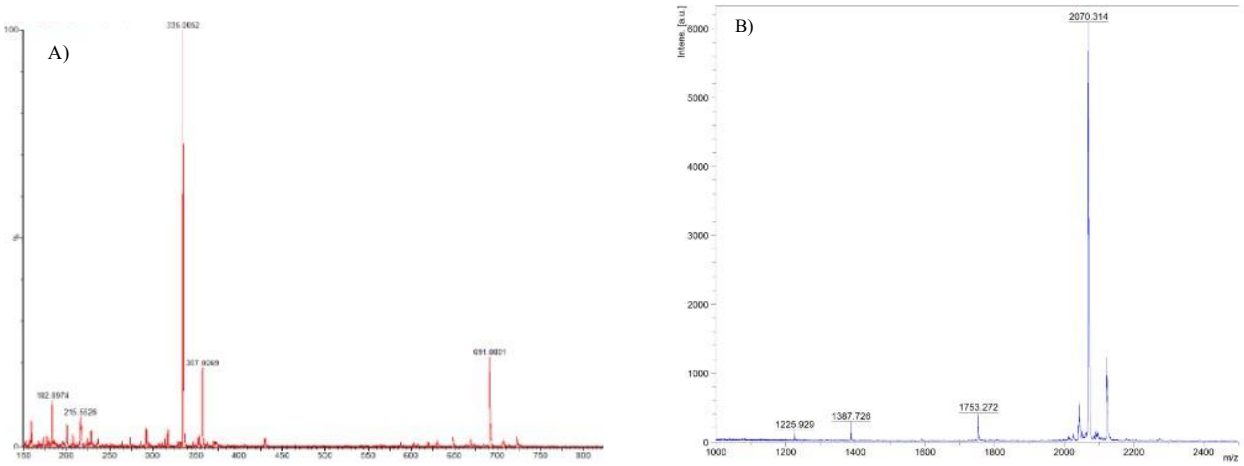

Figure 3.4 Mass analysis of the 9-azido-Neu5Ac and the $9N_3S2G2$ glycan. Mass data of A) the 9-azido-Neu5Ac (**7**) by LC-ESI-MS. Expected mass of **7**: 334.11 Da, Observed: m/z 335.01 $[M + H]^+$, m/z 357.01 $[M + Na]^+$, m/z 691.08 $[2M + Na]^+$. B) purified $9N_3S2G2$ glycan (**14**) glycan after anion exchange chromatography by MALDI-TOF. Exact mass of **14**: 2069.72 Da; Mass found: m/z 2070.31 $[M + H]^+$.

3.2.3 Chemoenzymatic Synthesis of IVIg Glycoforms. The desired IVIg glycoforms were generated by ENGase-mediated glycan remodeling (**Figure 3.5A**). The deglycosylated IVIg acceptor substrate was generated by incubating a commercial IVIg preparation (**15**) by incubating with immobilized EndoS2 WT, leaving only the terminal GlcNAc and terminal fucose at the N297 glycosite of IVIg (**16**) (**Figure 3.5B**). We then prepared the sialoglycan donor

substrates by incubating either **10** or **14** with 2-chlorodimethylimidazolium chloride (DMC) under basic conditions to the glycan oxazoline (**17** or **18**, respectively) (**Scheme 3.5**). We then incubated **16** and either **17** or **18** with the EndoS2 D184M glycosynthase mutant to generate the K2G2F-IVIg (**19**) and 9N_3S2G2F-IVIg (**20**). Reaction was monitored and confirmed by LC-ESI-MS before being purified by protein A chromatography (**Figure 3.5C and D**).

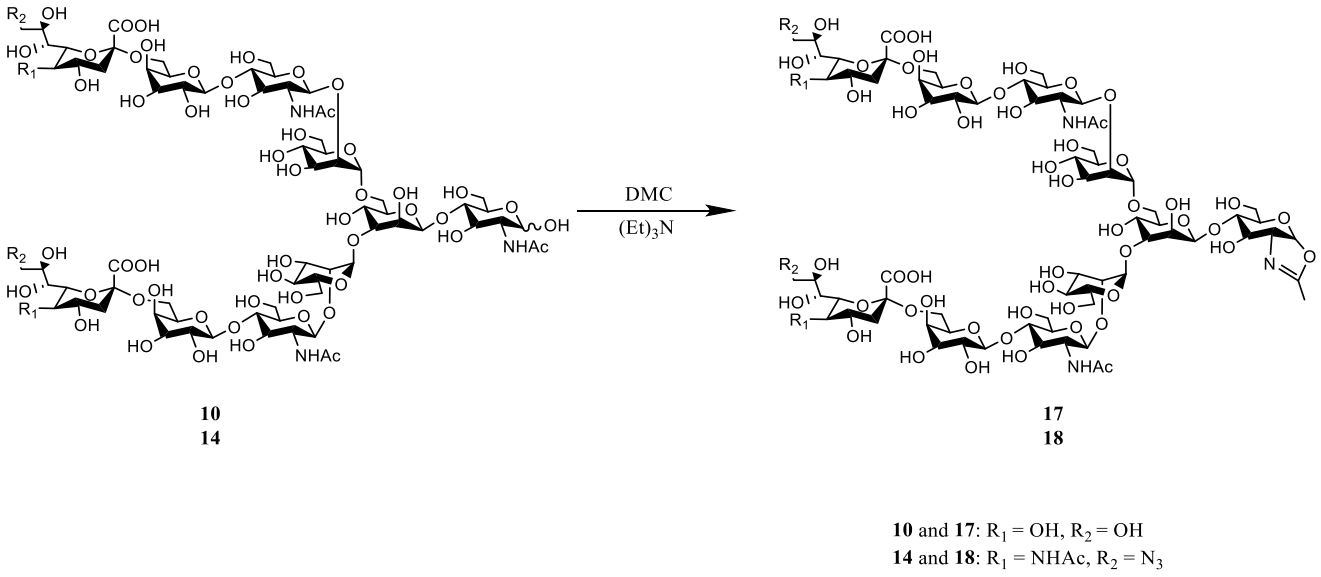

Scheme 3.5. Synthesis of glycan oxazolines

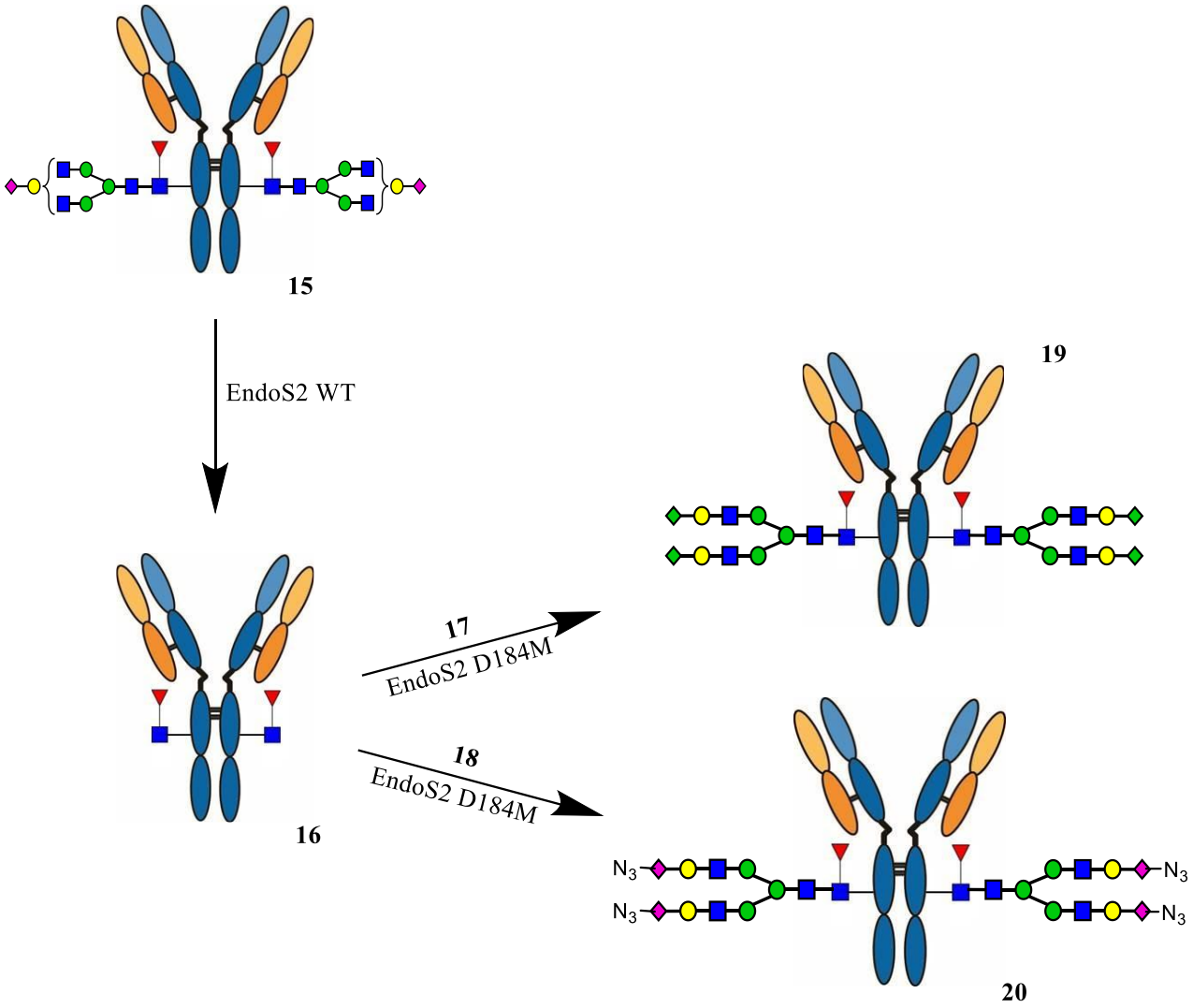

Scheme 3.6. Semi-synthesis of IVIg Glycoforms

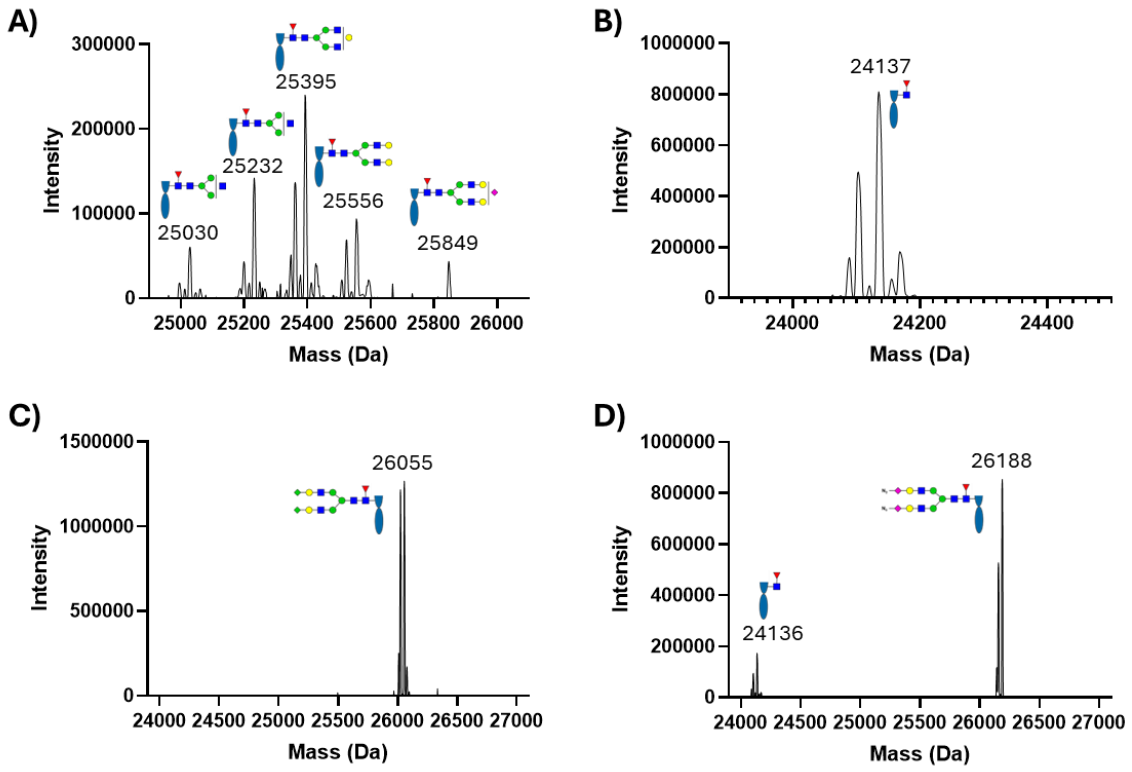

Figure 3.5 Synthesis of the sialylated IVIg glycoform derivatives. LC-ESI-MS data of Fc portions of IVIg Glycforms. A) Commercial IVIg preparations **15**. B) Deglycosylated IVIg **16**. C) K2G2F-IVIg **19**. D) $9N_3$S2G2F-IVIg **20**.

3.2.4 Semi-Synthesis and Conjugation of DBCO-Tag Sialoglycan Asparagine to Azido-Sialo-IVIg Glycoform. With the generation of the azide-tagged $9N_3$S2G2F-IVIg glycoform, we sought to conjugate additional glycans to the construct via azide-attached click conjugation. To do this, synthesized the DBCO-modified glycan (**Scheme 3.7**) by isolating sialoglycan-asparagine from sialoglycopeptide (SGP) by proteolytic digestion to leave only the disialylated asparagine-linked S2G2-Asn *N*-glycan (**21**) as previously described[109] (**Figure 3.6A**), then performing an amine-coupling reaction of the primary amine of **21** asparagine with commercial DBCO-C4-NHS, yielding S2G2-Asn-DBCO (**22**) (**Figure 3.6B**).

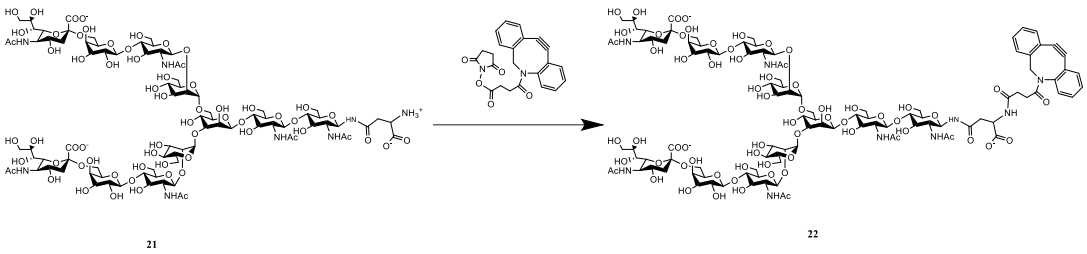

Scheme 3.7. Synthesis of DBCO-modified S2G2-Asparagine

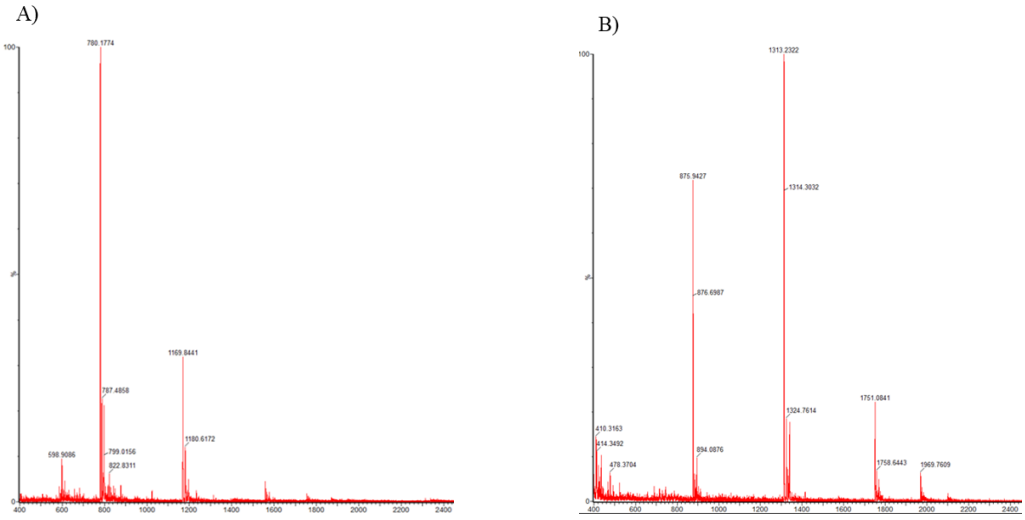

Figure 3.6 Synthesis of DBCO-tagged sialocomplex-type glycan-asparagine. LC-ESI-MS data of DBCO-glycan reaction. A) Mass data of **21**. Expected mass: 2336.83 Da, Observed: m/z 1169.84 $[M + 2H]^{2+}$, m/z 780.18 $[M + 3H]^{3+}$. B) Mass data of **22**. Expected mass: 2623.92 Da, Observed: m/z 1313.23 $[M + 2H]^{2+}$, m/z 875.94 $[M + 3H]^{3+}$.

The product was separated from the DBCO-NHS by gel filtration before being reacted with **20** via Strain-Promoted Azide-Attached Cycloaddition (SPAAC) click conjugation chemistry to generate the $(S2G2)_2S2G2F$-IVIg glycoform (**23**) (**Scheme 3.7**). This **23** product was confirmed by LC-ESI-MS before being purified by protein A column Chromatography (**Figure 3.7**)

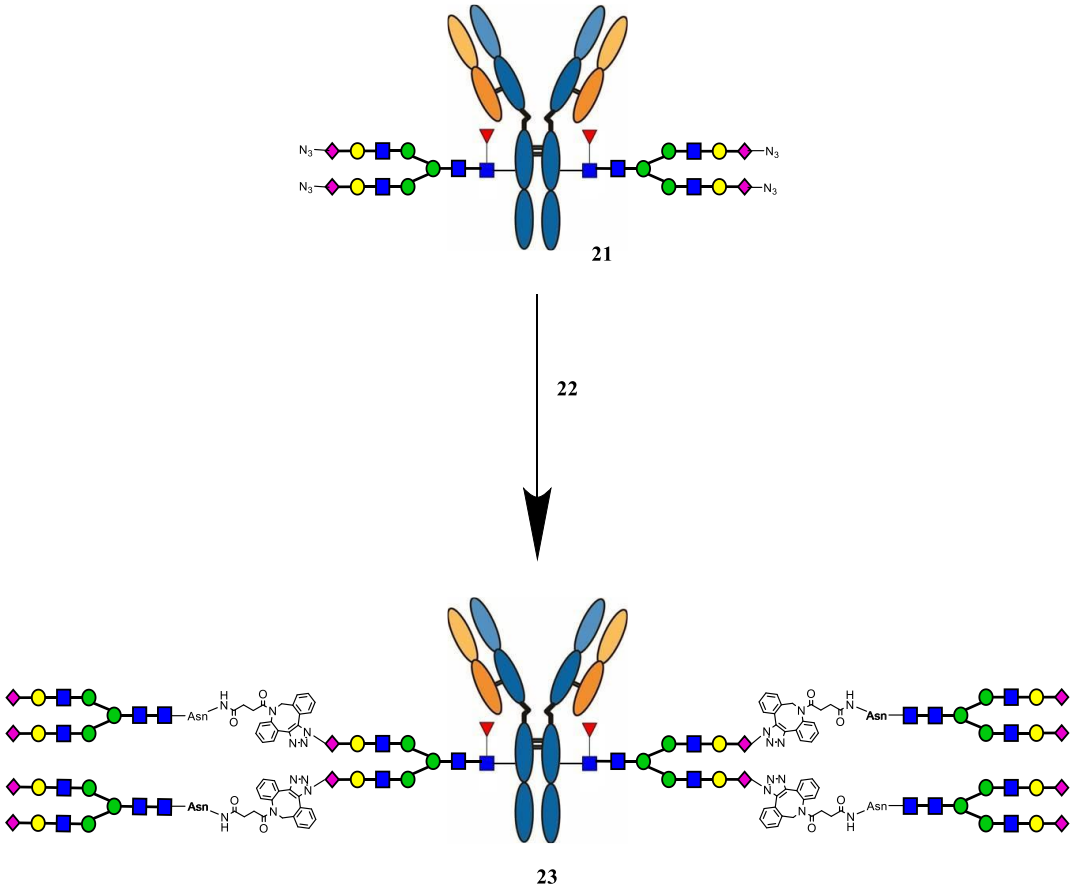

Scheme 3.8. SPAAC Click Conjugation Reaction

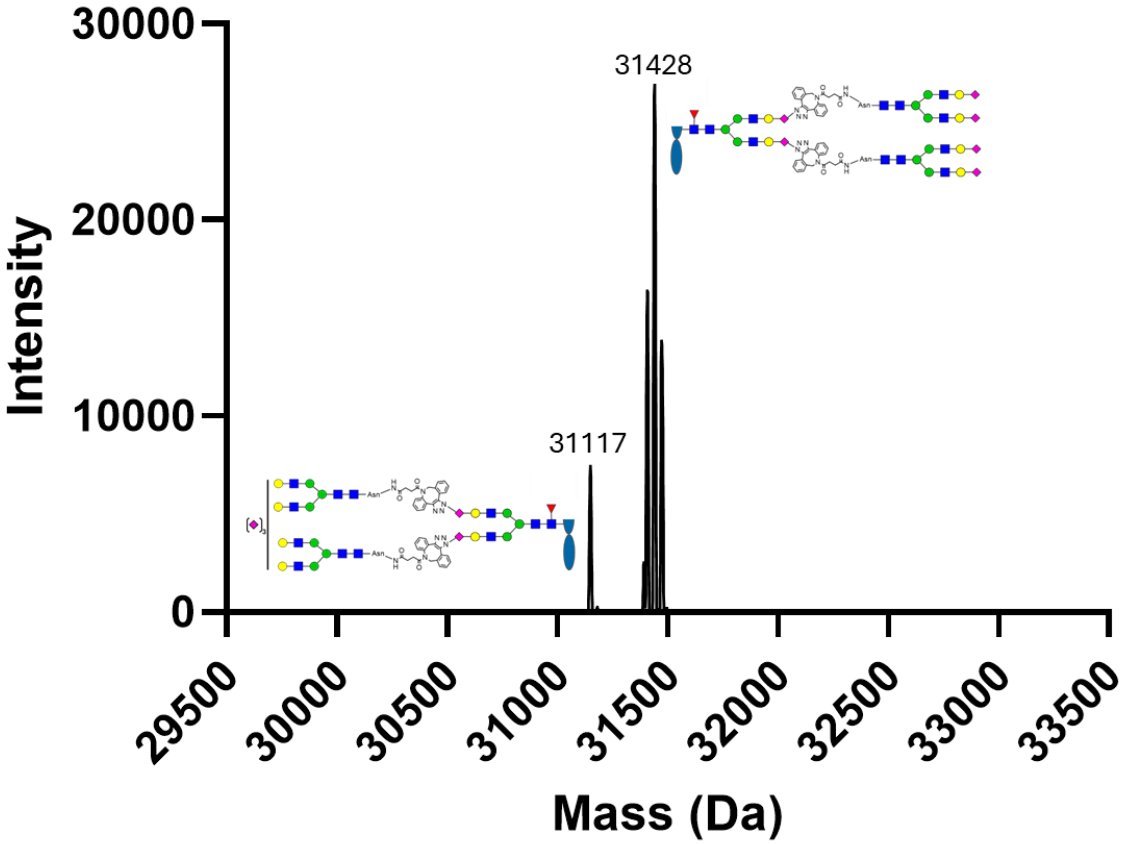

Figure 3.7 Conjugation of DBCO-S2G2-Asn to the 9N$_3$S2G2F-IVIg glycoform. LC-ESI-MS data of (S2G2)$_2$S2G2F-IVIg **23**

3.3 Conclusion

Through chemoenzymatic and semisynthetic methods, we contributed two novel IVIG, K2G2F-IVIG and (S2G2)$_2$S2G2F-IVIG, to the study of the structural impact of sialic acid to IVIG anti-inflammatory activity. We confirmed the generation of the final product by LC-MS, and our collaborators further confirmed the glycoform by HPLC analysis. After synthesis, both of these glycoforms remained relatively stable in solution, indicating that these glycoforms will

likely be suitable for *in vivo* anti-inflammatory studies. These glycoforms will be used by our collaborator, Dr. Robert Anthony, for *in vivo* mouse studies to determine whether these glycoforms will be able to elicit anti-inflammatory functions, and to what degree.

3.4 Materials and Methods

Materials: All chemicals, reagents, and solvents purchased from Sigma Aldrich, Carbosynth, and TCI and used as received unless otherwise specified. IVIG antibodies purchased from GlycoT, and lyophilized sialic acid aldolase enzyme was purchased from Carbosynth. *Neisseria meningitidis* CMP-Sialic Acid Synthetase (NmCSS) and *Photobacterium damselae* α-2,6-sialyltransferase (Pd2,6ST) enzymes were expressed recombinantly in house by other members of the lab for this project.

3.4.1 Chemoenzymatic synthesis of 2-keto-3-deoxy-D-glycero-D-galacto-nononic acid (8)

The Following reaction was performed as previously described[80, 108]. A solution of D-Mannose (0.5 g) was incubated with sodium pyruvate (1.5 g, 5 molar eq) in the presence of sialic acid aldolase (4.4 mg) at 37°C in 150 mM PBS pH 7.4 shaking at 150 rpm overnight. Formation of the KDN product was confirmed by TLC (7:3 ethanol to water) before being quenched with one volume of ice cold 95% ethanol and extracted by P-2 gel filtration to yield product as a white powder. LC-MS: calculated mass M = 268.1 Da, found (m/z) 291.1 $[M + Na]^+$

3.4.2 Synthesis of 9N$_3$Neu5Ac

A solution of Neu5Ac (500 mg, 1.63 mmol) was incubated with DOWEX H^+ resin (500 mg) in 10 mL of methanol overnight stirring at room temperature. Reaction completion was confirmed by TLC, and the mixture was purified by flash chromatography and dried *in vacuo* to yield the 1MeNeu5Ac. A solution of 1MeNeu5Ac redissolved in 10 mL of pyridine and chilled on ice and

stirring. Once ice cold, toluenesulfonyl-choride (310.5 mg, 1.63 mmol) was added slowly, then was warmed to room temperature and incubated while stirring overnight to yield the 1Me-9OTs-Neu5Ac product. Reaction completion was confirmed by TLC, and mixture was purified by flash chromatography and dried *in vacuo*. Finally, the compound was redissolved in 10 mL 1:3 acetone in water and incubated with sodium azide (317.6 mg, 4.89 mmol) in an oil bath at 80 °C at reflux overnight to yield the $9N_3$Neu5Ac final product. Reaction progress was confirmed by TLC before the reaction mixture was purified by flash chromatography (128.1 mg, 24% yield over three steps). LC-MS: calculated mass 334.11 Da, Observed: m/z 335.01 $[M + H]^+$, m/z 357.01 $[M + Na]^+$, m/z 691.08 $[2M + Na]^+$.

3.4.2 Isolation of asialocomplex-type free *N*-glycan

The *N*-glycan precursor, sialoglycoprotein (SGP), was isolated from egg yolk powder obtained commercially (BulkFoods) by step-wise ethanol extractions and C18 cartridge purification. A solution of SGP (60 mg) was then incubated overnight with wild-type EndoS2 and MvNA at 37°C in 150 mM PBS pH 7.4. Product was confirmed by LC-MS and desalted via G-10 gel filtration chromatography and anion exchange chromatography before being lyophilized to yield a white powder (28.3 mg, 94.1%). LC-MS: calculated mass 1437.5 Da, Observed: m/z 719.9 $[M + 2H]^{2+}$, m/z 1460.7 $[M + Na]^+$.

3.4.3 Sialyltransfer of KDN to free complex-type asialoglycan

KDN transfer was adapted from a method previously described[80, 81, 108]. A solution of asialoglycan (20 mg), KDN (18.7 mg, 5 molar eq.), and Na_2CTP (36.7 mg, 5 molar eq) was incubated in the presence of NmCSS (800 µg) and Pd2,6ST (800 µg) at 37°C in 2 mL of 20 mM $MgCl_2$ and 100 mM Tris pH 7.5 and was monitored by LC-MS. Once reaction progression ceased, the mixture was heat denatured and centrifuged at 13,000 rpm for 1 minute, and the

supernatant was desalted by G-15 gel filtration, purified by anion exchange chromatography (Capto Q XL, 5 mL) and desalted a final time via G-15 gel filtration. Filtrate was lyophilized to yield white powder (4.1 mg, 15.2%). LC-MS: calculated mass *M* = 1938.8 Da, found (m/z) 1959.5 $[M + Na - 2H]^-$.

3.4.4 Sialyltransfer of $9N_3$Neu5Ac to free complex-type asialoglycan

A solution of asialoglycan (30 mg), $9N_3$Neu5Ac (17.4 mg, 2.5 molar eq.), and Na_2CTP (27.5 mg, 2.5 molar eq) was incubated in the presence of NmCSS (800 µg) and Pd2,6ST (800 µg) at 37 °C in 3 mL of 20 mM $MgCl_2$ and 100 mM Tris pH 7.5 and was monitored by LC-MS. Once reaction progression ceased, the mixture was heat denatured and centrifuged at 13,000 rpm for 1 minute, and the supernatant was desalted by G-15 gel filtration, purified by anion exchange chromatography (Capto Q XL, 5 mL) and desalted a final time via G-15 gel filtration. Filtrate was lyophilized to yield white powder (1.1 mg, 2.5%). LC-MS: calculated mass *M* = 2069.7 Da, found (m/z) 2070.3 $[M + H]^-$. Reaction repeated multiple times to accumulate product.

3.4.5 Generating sialoglycan derivative oxazolines

Oxazoline reaction adapted from a previously described method[93]. A solution of either K2G2 (9.0) or $9N_3$Neu5Ac (10.7 mg) was reacted with 2-chlorodimethylimidazolium choride (DMC)(5 mg, excess) on ice in 150 µL 40% TEA in MilliQ water (v/v) for 30 minutes. Reaction then desalted by G-15 gel filtration and lyophilized (8.6 mg K2G2-oxa, 96.5%; 10.0 mg $9N_3$S2G2, 94.3%)

3.4.6 Glycan engineering of commercial IVIG to generate homogenous sialic acid derivative glycoforms

Commercial IVIG was enzymatically deglycosylated as previously described. A solution of deglycosylated IVIG (12.5 mg) incubated with Endo-S2 D184M (100µg) and either K2G2-Oxa

(5.8 mg, 30 eq) or $9N_3S2G2$-Oxa (2.5 mg, 15 eq) at 30 °C in 1 mL of 150 mM PBS pH 7.4 and monitored by LC-MS. Deglycosylation was confirmed by LC-ESI-MS before being purified by protein G column chromatography to afford the deglycosylated IVIG (37.5 mg, 93.8% yield). ESI-MS: calculated for the K2G2F-IVIG Fc monomer after IdeS digestion, M = 26,055 Da; found (m/z) 26,055 (deconvolution data); calculated for the $9N_3S2G2F$-IVIG Fc monomer after IdeS digestion, M = 26,187 Da; found (m/z) 26,188.

3.4.7 Generation of asparagine-linked S2G2 glycan

A solution of SGP (50 mg) was incubated with commercial Pronase (23.5 mg) at 37 °C in 1 mL of 5 mM $CaCl_2$ in 100 mM Tris-Cl pH 8.0 and 0.01% NaN_3 shaking at 150 rpm and monitored by LC-MS for 1 week. Reaction was confirmed by LC-MS and desalted by G-10 gel filtration before being lyophilized to yield a white solid (39.8 mg, 97.7%). LC-MS; calculated mass of SCT-Asn, M = 2,336.1 Da; found (m/z) 1,169.8 $[M + H]^{2+}$, 780.1 $[M + 2H]^{3+}$.

3.4.8 DBCO tagging of SCT-Asn

A solution of SCT-Asn (10 mg) was incubated with DBCO-C4-NHS (5.2 mg, 1.5 eq) at room temperature in 200 µL of 30% DMSO (v/v) in MilliQ water and monitored by LC-MS for 2 overnights. Reaction was confirmed by LC-MS and desalted by G-15 gel filtration before being lyophilized to yield a white solid (3.4 mg, 30%). LC-MS; calculated mass of SCT-Asn-DBCO, M = 2,623.9 Da; found (m/z) 1,313.2 $[M + H]^{2+}$, 875.9 $[M + 2H]^{3+}$.

3.4.9 Azide conjugation of SCT-Asn-DBCO to $9N_3S2G2F$-IVIG

A solution of $9N_3S2G2F$-IVIG (11 mg) was incubated with SCT-Asn-DBCO (1.9 mg, 2.5 eq per azide conjugation site) at room temperature in the dark in 1 mL of 30% DMSO (v/v) in MilliQ water and monitored by LC-MS for 2 overnights. Reaction was confirmed by LC-MS and

purified by protein G column chromatography (10.2 mg, 91.5%). LC-MS; calculated mass of $(S2G2)_2S2G2F$-IVIG after IdeS digestion, M = 31,436 Da; found (m/z) 31,438 (deconvoluted)

3.4.10 Mass analysis of free glycans and monosaccharides

LC-ESI-MS analysis of glycans was conducted on a Waters HPLC-SQD2 system equipped with a Waters XBridge C18 column (3.5 μm, 2.1× 50 mm). RP-HPLC separation utilized a gradient of water (line A) and acetonitrile (line B) with 0.1 % formic acid as the background. Peaks were detected by ESI-MS Waters SQD2 instrument.

3.5 Supplementary Data

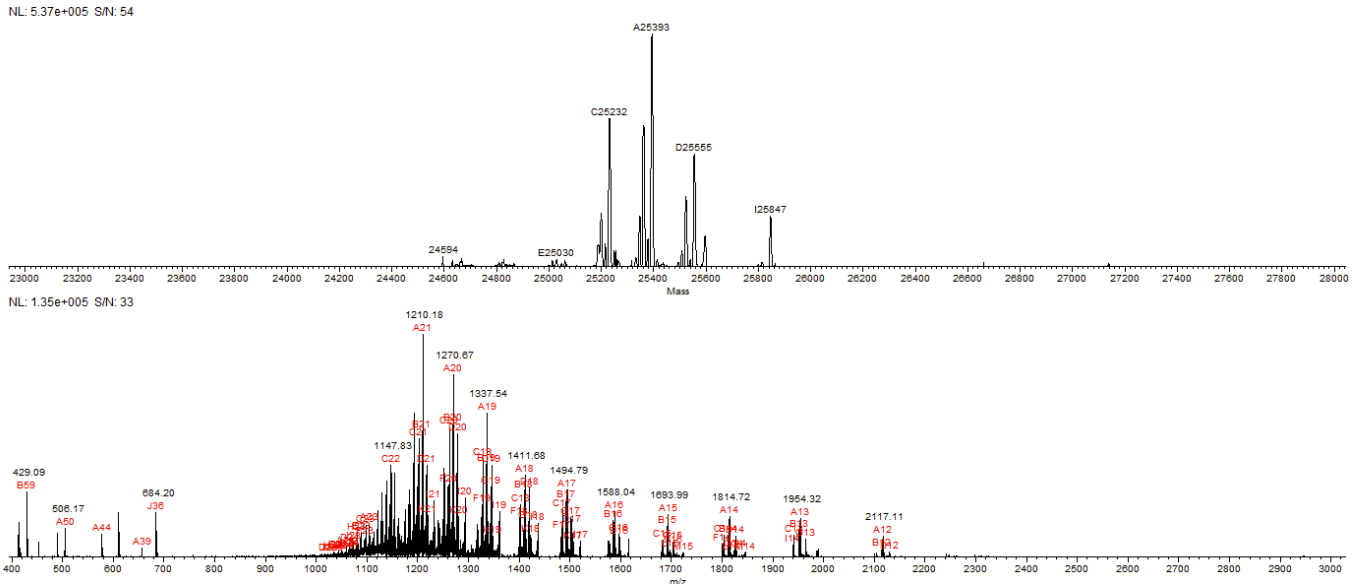

Figure 3.8. LC-ESI-MS spectrum of IdeS-treated IVIg Fc monomer.

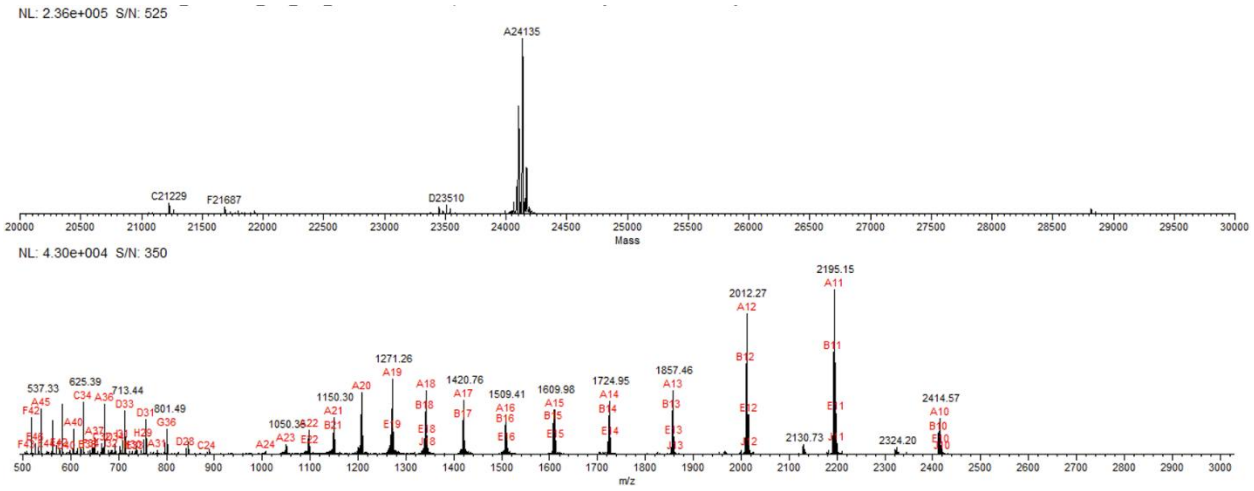

Figure 3.9. LC-ESI-MS spectrum of IdeS-treated GNF-IVIg Fc monomer.

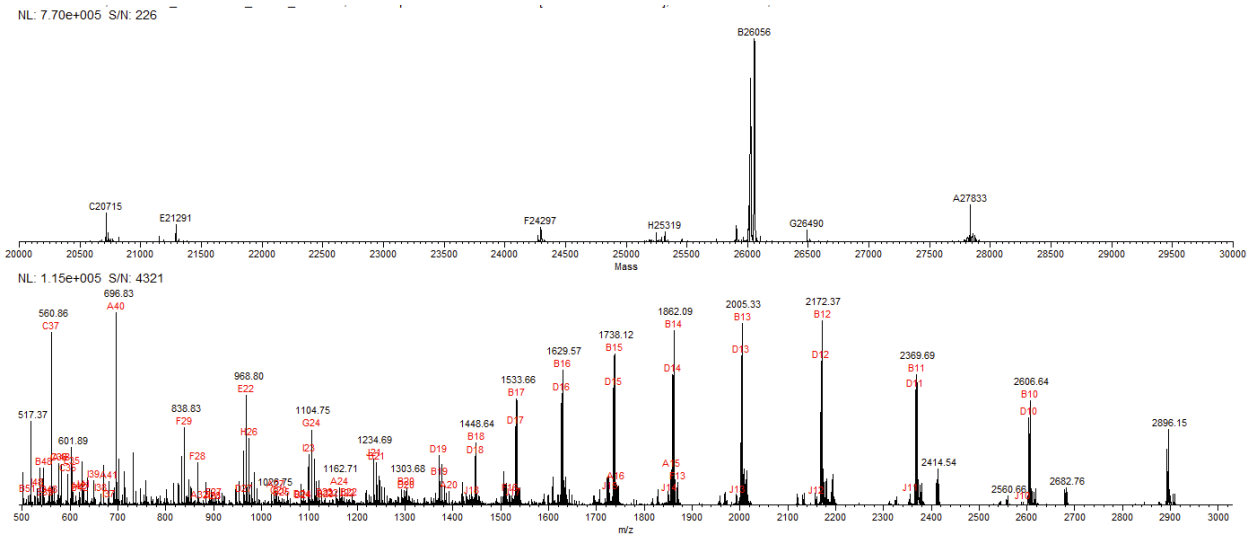

Figure 3.10. LC-ESI-MS spectrum of IdeS-treated K2G2F-IVIg Fc monomer.

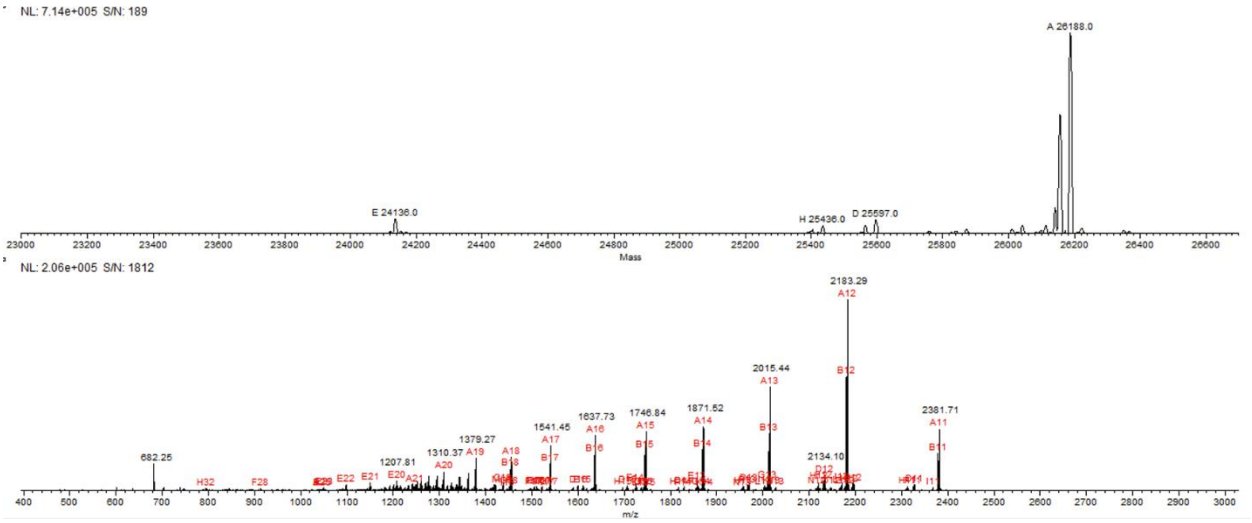

Figure 3.11. LC-ESI-MS spectrum of IdeS-treated $9N_3S2G2F$-IVIg Fc monomer.

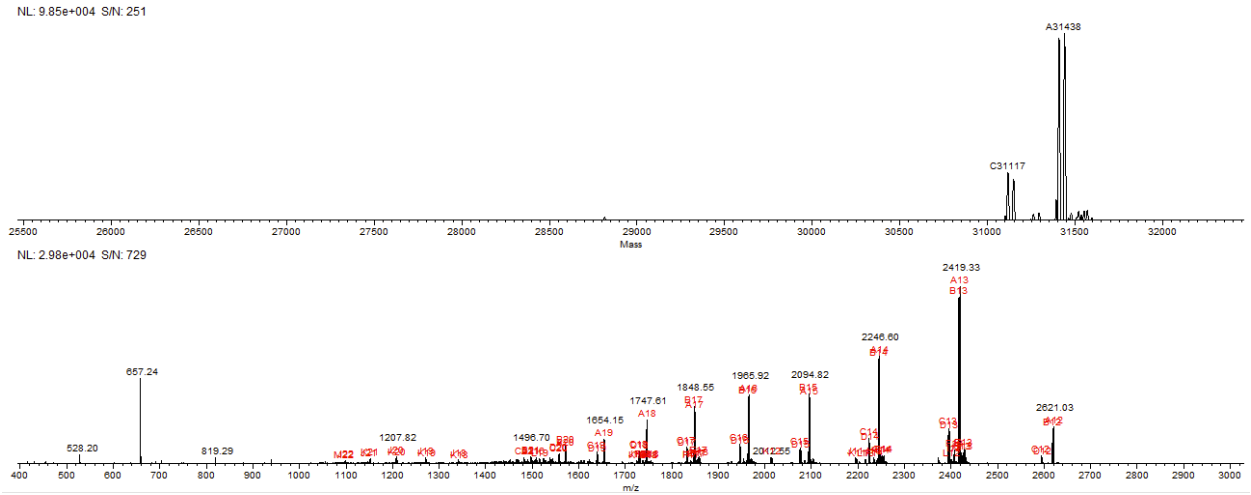

Figure 3.12. LC-ESI-MS spectrum of IdeS-treated $(S2G2)_2S2G2F$-IVIg Fc monomer.

Chapter 4: Chemoenzymatic synthesis of novel site-specific antibody-drug conjugates using a galactosyl transferase mutant

4.1 Introduction

Antibody Drug Conjugates (ADCs) are a growing class of drug renowned for their versatility, selectivity, and potency modulation. The guiding principle of their function, conceived by Paul Ehrlich's "Magic Bullet" concept, relies on the high antigen specificity of the antibody Fab region for the localization and internalization of the cytotoxic drugs into a target cell for selective cell killing[110, 111]. The design for this magic bullet concept relies on four key factors: the chosen antibody, the cytotoxic drug, and the linker, and conjugation strategy. An ideal antibody will target an epitope most prominently expressed uniformly on the surface of a cancer cell with minimal shedding to maximize internalization into the target cell. The epitope will also have low expression on non-cancerous cells to reduce off-target effects. The cytotoxic drug, also known as a payload, will ideally have high cytotoxicity and high bioaccumulation in the target cell upon internalization. Most current payloads typically used in ADC are either DNA synthesis or tubulin inhibitors targeting and disabling essential components to cell homeostasis and proliferation[112]. The linkers that hold the payload onto the antibody can be divided into two categories: cleavable and non-cleavable linkers. Cleavable linkers possess a specific cleavage site to readily detach a payload from its antibody, making it bioactive. The cleavage of this linkage type is typically tailored to cleave after internalization into a cell lysosome, and cleavage is typically very rapid. However, the readily cleavable site on this linker may cause early dissociation from the antibody while in circulation, reducing its half-life and increasing the risk for off target effects. Conversely, non-cleavable linkers do not possess readily cleavable sites.

Drugs linked to antibody with this linkage type are only released and become bioactive after the full degradation of the antibody component in the lysosome of the target cell. This linkage type generally boasts improved serum stability and reduced off-target effects, but the dissociation of the bioactive drug is slower than that of the cleavable linker[113]. Conjugation strategies are the technique by which drugs are added to the antibody. The strategies employed determine the number of drug units attached to the antibody. Common strategies include lysine conjugation, amino acid substitutions to generate more reactive conjugation sites, and reduction and conjugation of intermolecular disulfide bonds[114]. I will highlight these conjugation strategies in more detail below.

Various strategies have been employed to produce ADCs. Initial production of ADCs involved non-specific covalent conjugation reactions of the drug to solvent exposed amine or thiol functional groups of lysine or cysteine residues, respectively[115, 116]. While this conjugation strategy was effective in generating monoclonal antibodies loaded with cytotoxic drugs, the constructs suffered from highly heterogeneous drug to antibody ratio (DAR) values, poor solvent stability, and drugs conjugated to the fab region of the antibody interfered with antigen binding stability[117]. These limitations highlighted the need for site-specific conjugation strategies to control the DAR values while keeping the drugs away from the antigen binding region. Soft reduction of the intermolecular disulfide bonds of an antibody followed by reassembly with the payload incorporated has yielded a site-specifically conjugated ADC with controlled DAR values[118]. Another strategy is to introduce amino acid substitutions with either cysteines for thiol conjugation, or a non-natural amino acid such as *para*-acetyl- or *para*-azido-phenylalanine at specific sites for alkyloxime or alkyne-azide conjugation, respectively[119-122]. These targeted conjugation strategies helped to reduce fluctuations in DAR values within an ADC preparation,

and paired with improvements in linker hydrophilicity stability these ADCs had less off-target effects and more efficient pharmacokinetics.

Chemoenzymatic glycoengineering has a unique advantage as an ADC production strategy due to the conserved nature of IgG glycosylation. All IgG antibodies are *N*-glycosylated at the N297 site with very few therapeutic monoclonal antibodies having other *N*-glycosylation sites. This creates a very selective modification site between virtual all therapeutic Mabs to incorporate bio-orthogonal tags without the modification of peptide backbone residues. However, the heterogeneity the glycan necessitates the trimming, extension, cleavage, or replacement of the existing glycans to generate homogeneous glycoform preparations prior to conjugation. Fortunately, much progress has been made in terms of antibody glycan remodeling to make such modification not only possible, but highly efficient.

Sialic acid has been leveraged for the incorporation of bio-orthogonal tags. For example, in 1980, a group reported leveraging the IgG *N*-glycan sialylation for site-specific conjugation by oxidizing the glycerol tail of the sialic acid residues followed by oxime conjugation to yield an ADC product[123]. In 2014, Zhou and colleagues improved upon this strategy by chemoenzymatically galactosylating and sialylating the IgG Fc before the sialic acid oxidation and oxime ligation. However, this strategy carried the limitation of potentially oxidizing off-target amino acid residues such as methionine, which can reduce the stability and half-life of the antibody[124]. Li and colleagues used a similar technique of chemoenzymatically sialylating the IgG Fc glycans, but they used a C9-azido derivative. They then used Strain-Promoted Azide-Attached Cycloaddition (SPAAC) to conjugate a cyclooctyne-tagged drug site specifically to the antibody[77]. In addition to azide-tagged sialic acids, the Lewis group used a mutant β-1,4-galactotransferase (GalT Y289L) developed by Qasba and colleagues.[125] to transfer an azide-

bearing *N*-acetylgalactosamine (UDP-GalNAz) to an antibody for radiolabelling via SPAAC[126]. SynAffix later adopted this methodology to trim the IgG Fc glycan and incorporate GalNAz via GalT Y289L transfer, followed by copper-free SPAAC conjugation to generate DAR-2 ADCs[127]. Our lab has also made strides in glycosite functionalization for ADC development. We've isolated a ENGase truncated disialylated complex type *N*-glycan and functionalized the sialic acids by amine coupling at the C1 carboxylic position to introduce bio-orthogonal tags. We then incorporated this functionalized glycan to the IgG Fc glycosite by ENGase glycosynthase remodeling, then conjugated a drug-linker payload to the functionalized glycan to generate largely homogenous site-specific ADCs[128]. We also developed a methodology for trimming the IgG Fc glycan and incorporating disaccharide constructs with various azide-functionalized sites. By reacting these constructs with DBCO-tagged linker-drug payloads, we were able to efficiently produce homogenous ADCs of various DAR values[129]. Such methodologies give rise to largely homogenous antibody preparations with consistent average DAR ratios.

Glycosite modification offers customizability in terms of the intended DAR values of ADCs as well as site-selectivity in modification techniques. However, some of these methodologies require some form of glycoform truncation in the final ADC to generate DAR values other than 4. To date, it is unclear to what extent intact *N*-glycans contribute to the efficacy of ADC activity, so methodologies to preserve glycan structures in the development of ADCs would be valuable in evaluating the relationship between glycan structure and ADC efficacy. In this work, we expanded upon the SynAffix GlycoConnect technology to develope a DAR-6 trastuzamab ADC by chemoezymatically engineering a IgG Fc glycan to a triantennary glycan, incorporating terminal GalNAz residues via hGalT Y289L transfer of UDP-GalNAz, and click conjugating a dibenzylcyclooctyne (DBCO)-tagged linker-drug payload. This construct is

unique in having a relatively high DAR value while keeping the core *N*-glycan chitobiose structure intact.

4.2 Results and Discussion

4.2.1 Chemoenzymatic synthesis of tri-GalNAz tri-antennary free glycans. Prior to attempting to make the GalNAz ADC construct, we first needed to test whether a tri-antennary glycan acceptor would be an acceptable substrate for the human GalT Y289L mutant enzyme expressed by Natasha Owitipana in the Wang Lab. We first isolated the triantennary sialo-*N*-glycans via PNGase F treatment of commercial fetal bovine serum fetuin (Sigma Aldrich). The released glycans were subsequently isolated by anion exchange and gel filtration chromatography before being digested using sialidase and galactosidase enzymes to generate the asialo-agalacto-*N*-glycan (TG0-GN_2) starting material. From this product, the azido-bearing GalNAz was transferred onto the TG0 glycan acceptor substrate via incubation with human GalT Y289L β-1,4galactotransferase (hGalT Y289L) and the UDP-GalNAz donor substrate to generate the tri-GalNAz *N*-glycan (TGalNAz3-GN_2) (**Scheme 4.1**). Reaction completion was assessed by MALDI-TOF analysis (**Figure 4.1**).

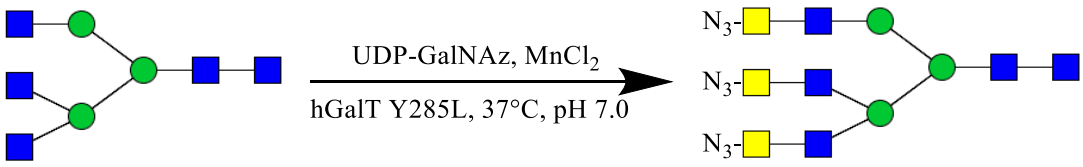

Scheme 4.1. GalNAz transfer reaction to free tri-antennary glycan

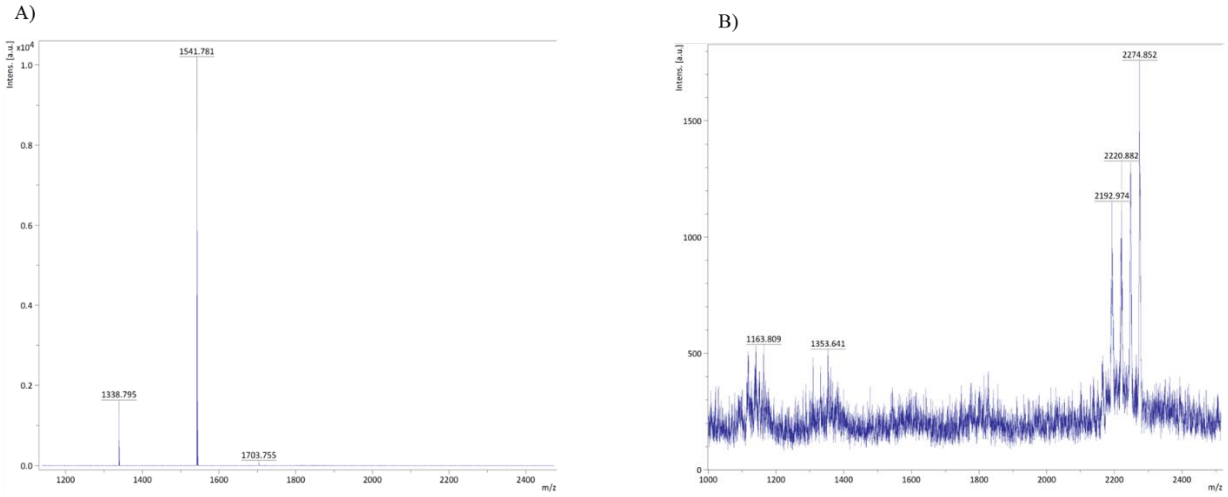

Figure 4.1 MALDI-TOF analysis of the UDP-GalNAz transfer on free triantennary *N*-glycan. Reaction monitoring of GalNAz to tri-antennary free glycan by MALDI-TOF analysis at A) time 0 and B) overnight. Expected mass of the starting material: 1519.57 Da, Observed: m/z 1541.78 $[M + Na]^+$. Expected mass of the reaction product: 2251.81 Da, Observed: m/z 2274.85 $[M + Na]^+$, m/z 2220.88 $[M + Na + 2H - 2N_2]^+$, m/z 2192.97 $[M + Na + 2H - 3N_2]^+$

4.2.2 GalNAz transfer reaction and SPAAC click conjugation reaction to generate DAR-6 Trastuzumab ADC. Having confirmed that tri-antennary free glycans are a viable substrate for the trans-GalNAz reaction, we then aimed to synthesize a DAR-6 trastuzumab ADC construct by chemoenzymatically generating a triantennary trastuzumab Fc glycoform, transferring GalNAz onto the Fc glycans, and click-conjugating a cytotoxic payload via SPAAC (**Scheme 4.2**).

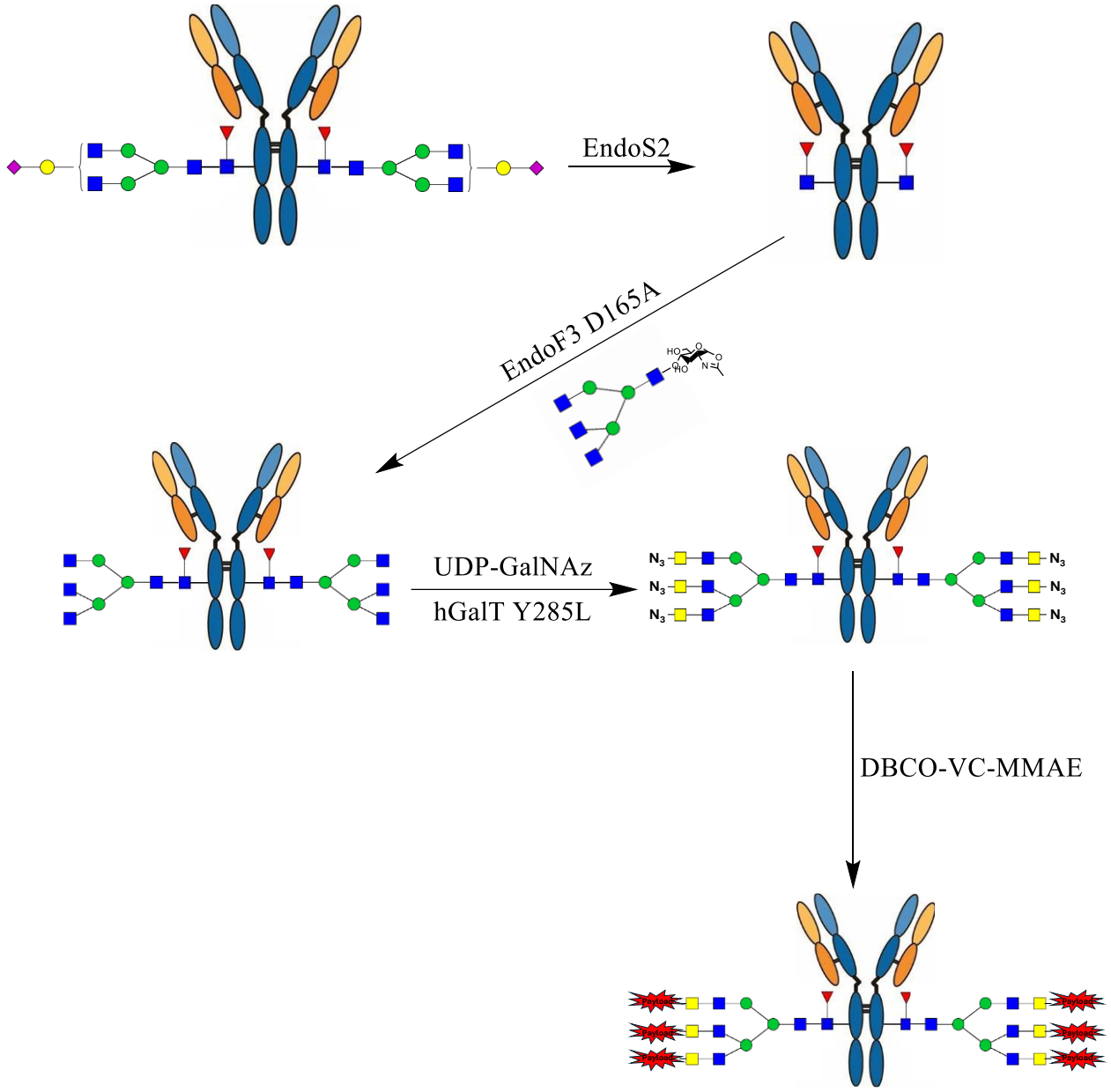

Scheme 4.2. Chemoenzymatic synthesis of DAR-6 ADC construct

We first generated the asialo-agalacto-triantennary trastuzumab glycoform (TG0F-Trastuzumab) by ENGase-catalyzed remodeling of the trastuzumab IgG antibody. We first cleaved the native glycans from the trastuzumab preparation using EndoS2, leaving only the core GlcNAc residue with α1,6-fucosylation (GNF-Herceptin). The resulting GNF-Herceptin was

used as an acceptor in a following transglycosylation reaction to conjugate the agalactosylated triantennary *N*-glycan oxazoline via EndoF3 D165Q glycosynthase transglycosylation to yield the TG0F-Trastuzumab glycoform, monitored and confirmed by LC-ESI-MS (**Figure 4.2**). After purification, a peak consistent with a monogalacosylated trastuzumab glycoform was observed, likely due to contamination with some monogalactosylated TG0-oxazoline.

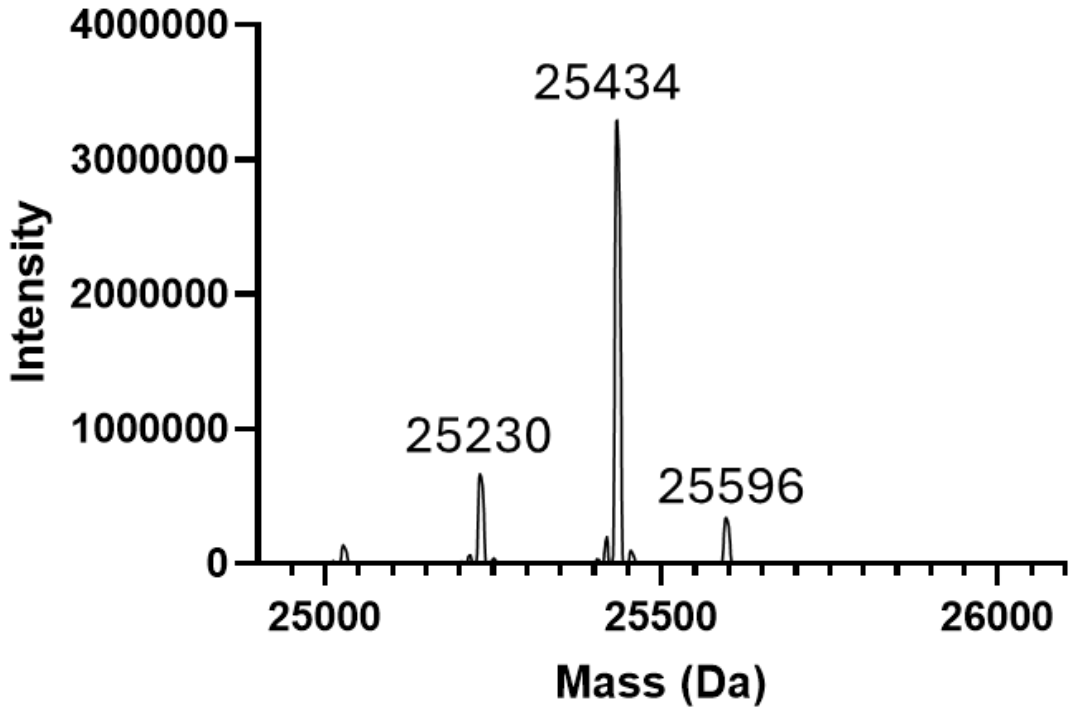

Figure 4.2 Semisynthesis of the triantenary trastuzumab glycoform. Deconvoluted LC-MS analysis of TG0F-Trastuzumab glycoform Fc region after IdeS proteolytic cleavage. Expected Mass: 25,433 Da; Observed Mass (Deconvoluted): 25,434 Da.

After generating this TG0F glycoform, the trans-GalNAz reaction was performed directly onto the Fc glycan of this Herceptin construct directly using a commercial UDP-GalNAz donor substrate and the hGalT mutant enzyme. The reaction was co-incubated with β1,4-galactosidase (BgaA) to remove the galactose residues from the contaminating monogalactosylated IgG

glycoforms. Due to the lack of activity of BgaA for GalNaz substrates, the UDP-GalNAz transfer was unaffected by this co-incubation, and the tri-GalNAz trastuzumab glycoform (TGalNAz3F-Trastuzumab) was formed after an overnight incubation, confirmed by LC-ESI-MS (**Figure 4.3A**).

Using this TGalNAz3F-Trastuzumab construct, we aimed to conjugate a cytotoxic payload to each site to obtain a DAR-6 construct. To do this, we employed a copper-free SPAAC strategy to attach the payload to the antibody without contaminating it with toxic copper ions. The clickable drug consisted of the cytotoxic drug, monomethyl auristatin E (MMAE), a PEG-valine-citrulline-PABC cathepsin cleavable linker, and a DBCO click handle, synthesized by others in the lab. This drug construct was reacted with the TGalNAz3F-Trastuzumab azide tags to generate the final TMMAE3F-Trastuzumab construct, purified by protein A column and confirmed by LC-ESI-MS analysis (**Figure 4.3B**).

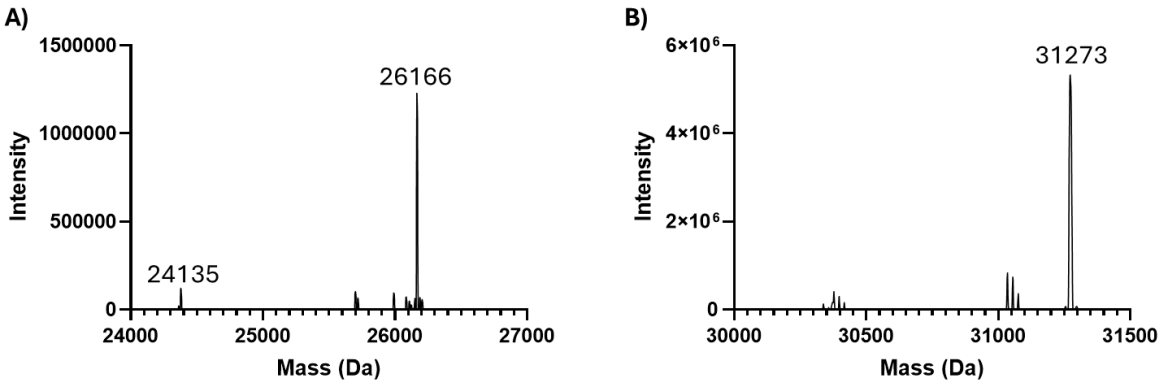

Figure 4.3 Semisynthesis of the DAR-6 ADC. Deconvoluted LC-MS analysis of a) terminal GalNAz-ylated TGalNAz3F-Trastuzumab Glycoform Fc after IdeS proteolytic cleavage and b) click conjugated TMMAE3F-Trastuzumab ADC construct Fc after IdeS proteolytic cleavage. Expected Mass of TGalNAz3F-Trastuzumab: 26,165 Da: Observed Mass (Deconvoluted): 26,166 Da. Expected Mass of TMMAEF-Trastuzumab: 31,271 Da: Observed Mass (Deconvoluted): 31,273 Da.

4.2.3 Cell Based Assay of DAR-6 ADC. After synthesis and characterization of this DAR-6 ADC, we used a cell viability assay using $HER2^+$ SK-BR-3 breast cancer cells to test the cytotoxicity of this novel construct. As a control, we generated a DAR-4 ADC using a similar technique as previously reported[126]. We were able to determine that the DAR-6 ADC (EC_{50} = 7.6 ng/mL) and the DAR-4 ADC (EC_{50} = 12.3 ng/mL) were consistent with the values from our previous publications[128, 129].

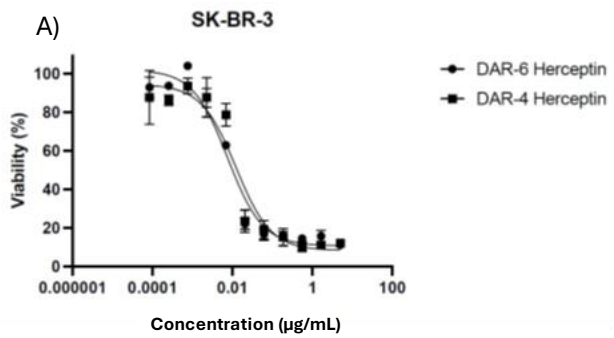

ADC	DAR-6	DAR-4
EC_{50} (ng/mL)	7.59 ± 2.31	12.3 ± 5.26

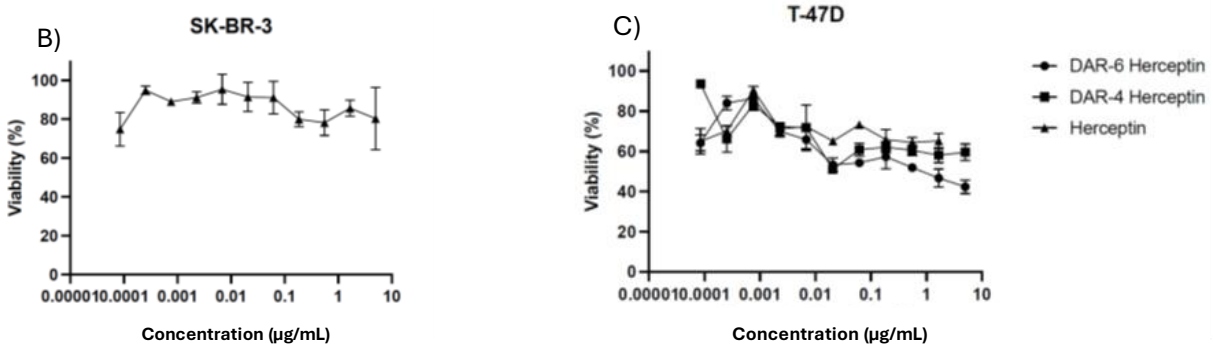

Figure 4.4 ADC cytotoxicity assay with HER2 expressing cancer cells. Cell-based cytotoxicity assay with a) high-expressing HER2 SK-BR-3 cells with their respective EC_{50} values, b) treatment of SK-BR-3 cells will unmodified Trastuzumab and c) low-expressing HER2 T-47D cells

4.3 Conclusions

In this work we aim to generate a high DAR ADC construct while preserving the core chitobiose *N*-glycan structure. We achieved this through *en bloc* chemoenzymatic remodeling to generate the triantennary glycoform, then enzymatically incorporated azide-tagged GalNAz residues using human GalT Y289L and click conjugated cytotoxic payload to generate a homogenous DAR-6 ADC construct. This work highlights the efficacy of using the mutant GalT

enzyme together with ENGase-catalyzed Fc glycan remodelimg to directly tag and label IgG glycans. Future work should explore how an intact *N*-glycan chitobiose core may effect ADC pharmacokinetics *in vivo* relative to a conjugation strategy that truncates the glycan, such as the constructs made by we reported in our 2021[129].

4.4 Materials and Methods

Materials: All chemicals, reagents, and solvents purchased from Sigma Aldrich. Humanized Herceptin monoclonal antibody was expressed in house by Margaryta Gomozkova. *Elizabethkingia meningoseptica* β-*N*-acetyl-glucosaminidase and its glycosynthase mutant (EndoF3 WT and D165A mutant) were expressed in *E. coli* BL21(DE3) by IPTG induction. GalT Y289L was expressed in house by Natasha Owitipana. Cytotoxic drug MMAE-PEG5-PAB-DBCO was synthesized by former lab member Dr. Guanghui Zong.

4.4.1 Isolation of intact triantennary *N*-glycan (TG0-GN$_2$)

A solution of fetal bovin serum fetuin (100 mg)(Sigma Aldrich) was treated with PNGase F (200 μg, 1:500 Enzyme to Substrate) at 37 °C in 10 mL of 150 mM PBS pH 7.4 for 2 days. All protein was then precipitated by 1 volume of ice cold 95% ethanol and centrifuged at 4,300 rpm for 5 minutes to pellet protein aggregates. Solution volume reduced *in vacuo* and the mixture was desalted by G-15 gel filtration. The desalted trisialylated triantenary complex type isolated by anion exchange chromatography (5 mL Capto Q XL) and desalted once more by G-15 gel filtration. The glycan was then treated with neuraminidase and galactosidase, followed by G-15 desalting and lyophilization to yield a white powder (8.3 mg, 89.2%)

4.4.2 GalNAz transfer onto free TG0-GN$_2$ acceptor substrate

A solution of TG0-GN_2 (304 µg) and UDP-GalNAz (0.64 mg, 5 eq.) was incubated with hGalT Y289L (2 µg) at 37 °C in 20 µL of 10 mM $MnCl_2$ in 50 mM MOPS pH 6.0 overnight. Reaction completion confirmed by MALDI-TOF. MALDI-TOF; calculated mass of tri-GalNAz product (TGalNAz3-GN_2): M = 2251.8 Da; found (m/z) 2274.9 $[M + Na]^+$.

4.4.3 Isolation of truncated triantennary *N*-glycan

A solution of fetal bovin serum fetuin (100 mg)(Sigma Aldrich) was treated with wild-type EndoF3 (1 mg, 1:500 Enzyme to Substrate) at 37 °C in 10 mL of 100 mM Acetate Buffer pH 4.5 for 3 days, pushing every 24 hours with enzyme. All protein was then precipitated by 1 volume of ice cold 95% ethanol and centrifuged at 4,300 rpm for 5 minutes to pellet protein aggregates. Solution volume reduced *in vacuo* and the mixture was desalted by G-15 gel filtration. The desalted trisialylated triantenary complex type isolated by anion exchange chromatography (5 mL Capto Q XL) and desalted once more by G-15 gel filtration. The glycan was then treated with neuraminidase and galactosidase, followed by G-15 desalting and lyophilization to yield TG0 as a white powder (5.3 mg, 77.6%)

4.4.4 Glycengineering of Trastuzumab to generate TG0F-Trastuzumab

Recombinant trastuzumab deglycosylation and TG0 oxazoline production were performed as previously described. A solution of GNF-Trastuzumab (1 mg) was incubated with TG0-oxazoline (0.26 mg, 30 eq.) and EndoF3 D165A (50 µg) at 30 °C in 0.5 mL of 100 mM Tris-Cl pH 7.0, monitored by LC-MS to completion. The mixture was purified by protein A chromatography and buffer exchanged into MOPS pH 6.0 to obtain the final triantienary TG0F-Herceptin glycoform (800 µg, 80%) LC-MS: calculated mass of the TG0F-Trastuzumab monomer: M = 25,433 Da; found (m/z) 25,434 (Deconvoluted)

4.4.5 GalNAz transfer onto TG0F-Trastuzumab

A solution of TG0F-Trastuzumab (800 µg) and UDP-GalNAz (217.7 µg, 100 eq per IgG) was incubated with hGalT Y289L (50 µg) at 37 °C in 0.5 mL 10 mM $MnCl_2$ in 50 mM MOPS pH 6.0 overnight, co-incubated with BgaA (50 µg) to remove monogalatosylated trastuzumab contamination. The reaction was monitored by LC-MS and purified by protein A chromatography (60 µg, 75.0%). LC-MS: calculated mass of the TGalNAz3F-Trastuzumab Fc: M = 26,165 Da, found (m/z) 26,166.

4.4.6 Click-Conjugation of drug linker payload onto TGalNAz3F-Trastuzumab for ADC generation

A solution of TGalNAz3F-Trastuzumab (600 µg) was incubated with DBCO-C4-PABC-MMAE (204 µg, 5 eq per azide site) at room temperature in 500 µL of 30% DBCO (v/v) in MilliQ water. The reaction was monitored by LC-MS and purified by protein A chromatography (462 µg, 77.0%). LC-MS: calculated mass of the TMMAE3F-Trastuzumab Fc: M = 31,271 Da, found (m/z) 31,273.

4.4.7 ADC cell killing assay with breast cancer cell lines

This assay was performed in house by Margaryta Gomozkova. T47D and SKBR3 (ATCC) cells were cultured in DMEM supplemented with 10% FBS, 50 U/ml penicillin, and 50 µg/mL streptomycin (ThermoFisher) and seeded at 200,000 cells/mL into a 96 well plate (20,000 cells/well) and grown overnight. Media was removed and replaced with fresh media containing the ADCs at concentrations ranging from 0.085-5000 ng/mL via serial threefold dilutions. Each compound concentration was assessed in triplicate wells, and cells without compound served as controls. Plates were incubated for 72 hours and cell viability was analyzed by cell counting kit-8 (Sigma). The absorbance of formazan released by viable cells was measured at 450 nm using a

spectrophotometer after incubation for 2–3 h at 37 °C and 5% CO_2. Finally, the EC_{50} values and the cell viability curve were calculated using GraphPad Prism software.

4.5 Supplementary Data

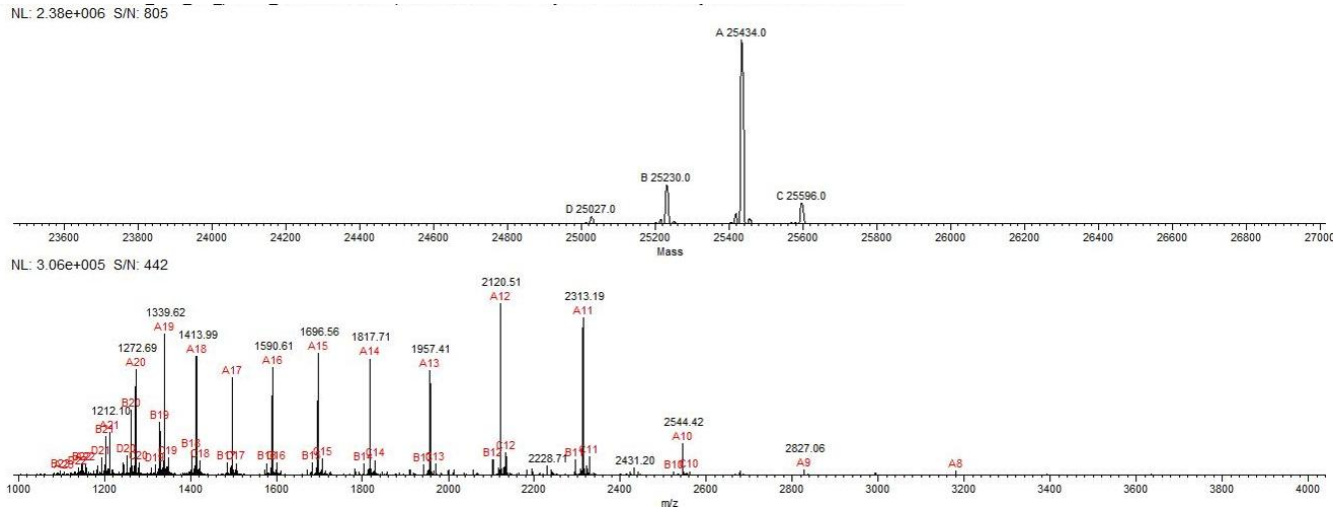

Figure 4.5. LC-ESI-MS spectrum of IdeS-treated TG0F-Trastuzumab Fc monomer.

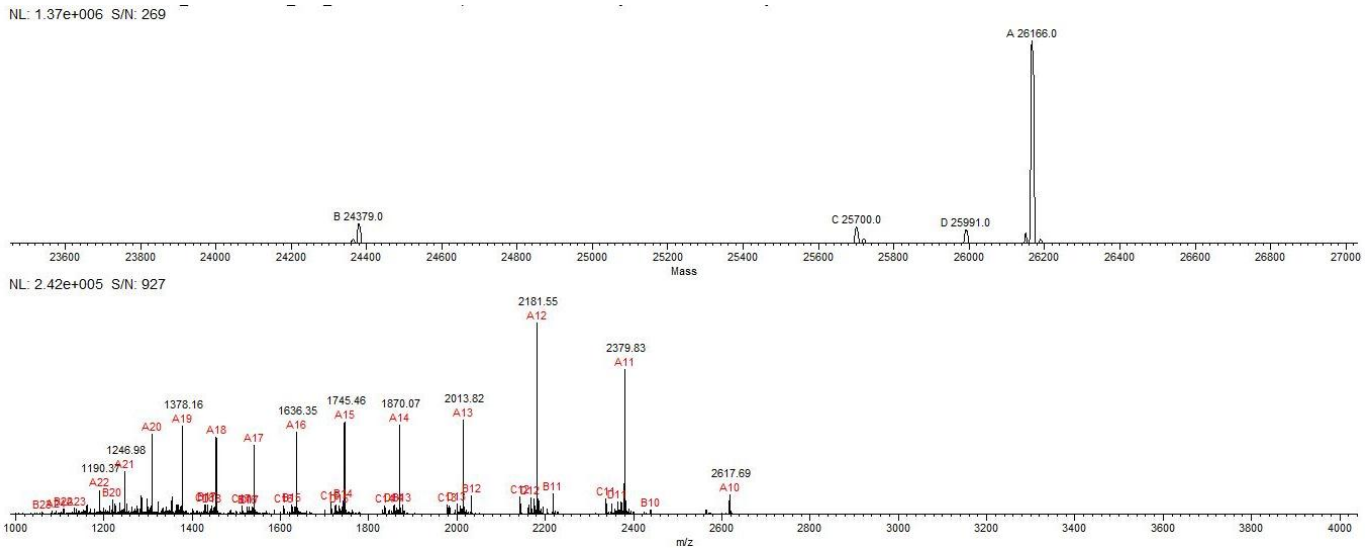

Figure 4.6. LC-ESI-MS spectrum of IdeS-treated TGalNAz3F-Trastuzumab Fc monomer.

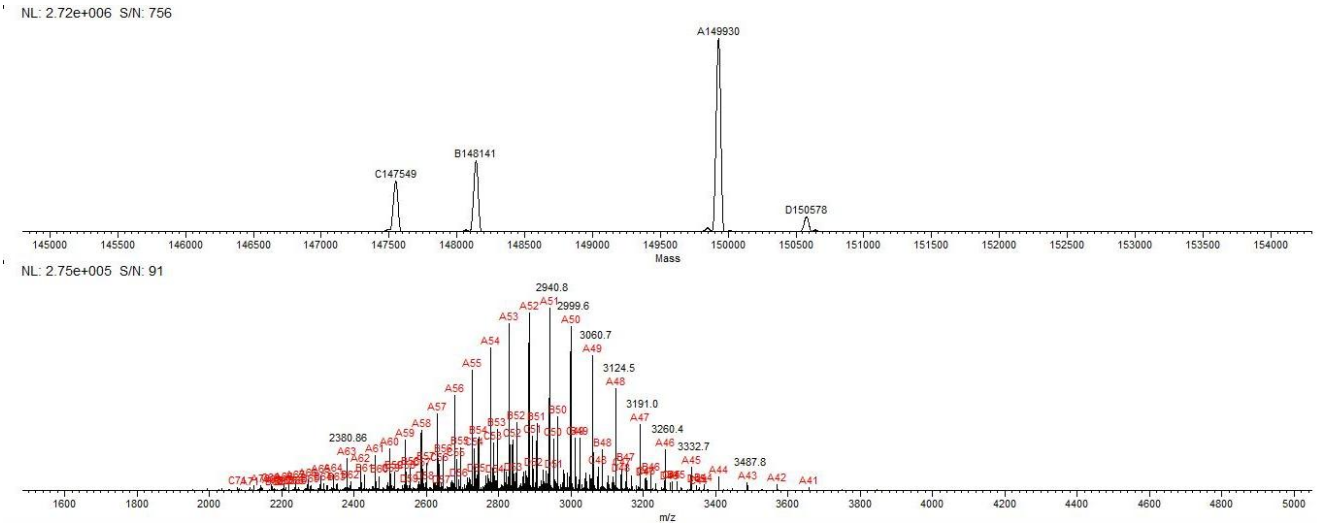

Figure 4.7. LC-ESI-MS spectrum of intact TGalNAz3F-Trastuzmab antibody.

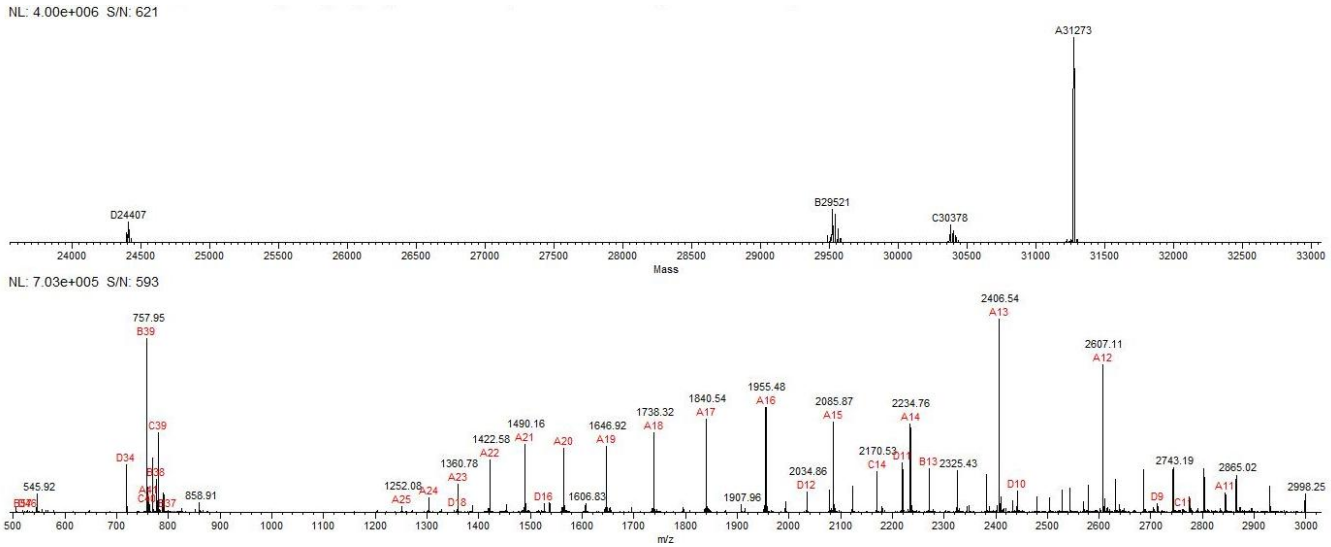

Figure 4.8. LC-ESI-MS spectrum of IdeS-treated TMMAE3F-Trastuzumab Fc monomer.

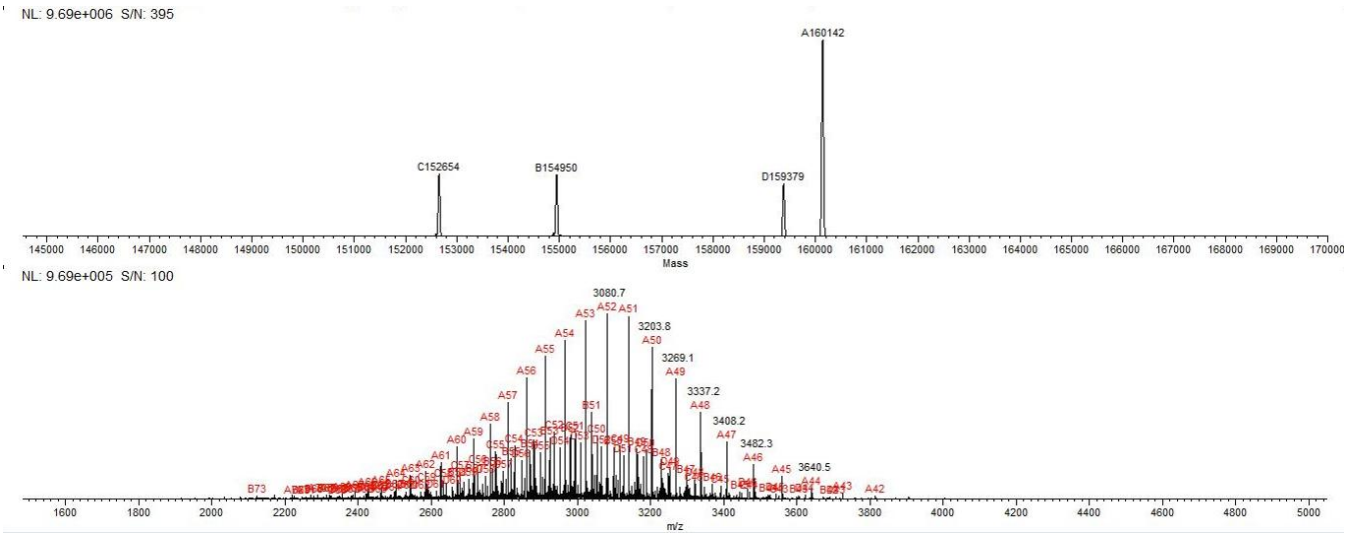

Figure 4.9. LC-ESI-MS spectrum of intact TMMAE3F-Trastuzumab antibody

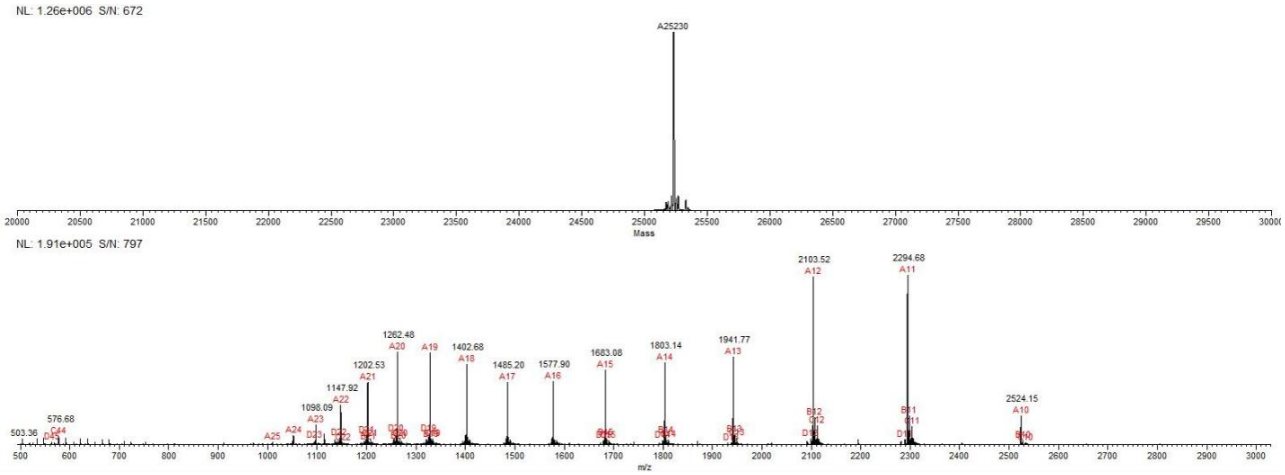

Figure 4.10. LC-ESI-MS spectrum of IdeS-treated G0F-Trastuzumab Fc monomer.

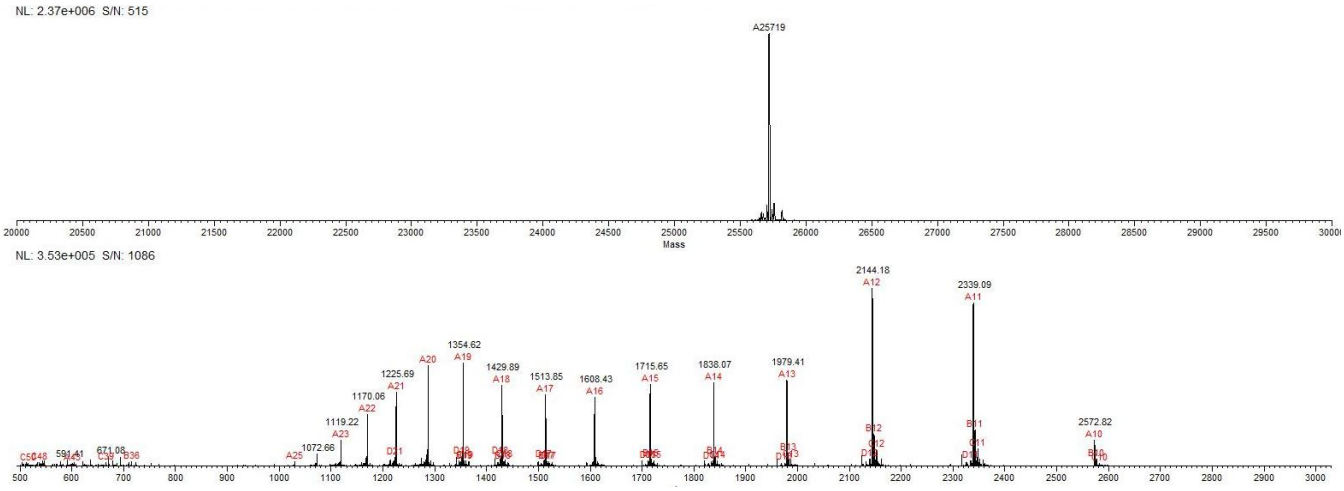

Figure 4.11. LC-ESI-MS spectrum of IdeS-treated GalNAz2F-Trastuzumab Fc monomer.

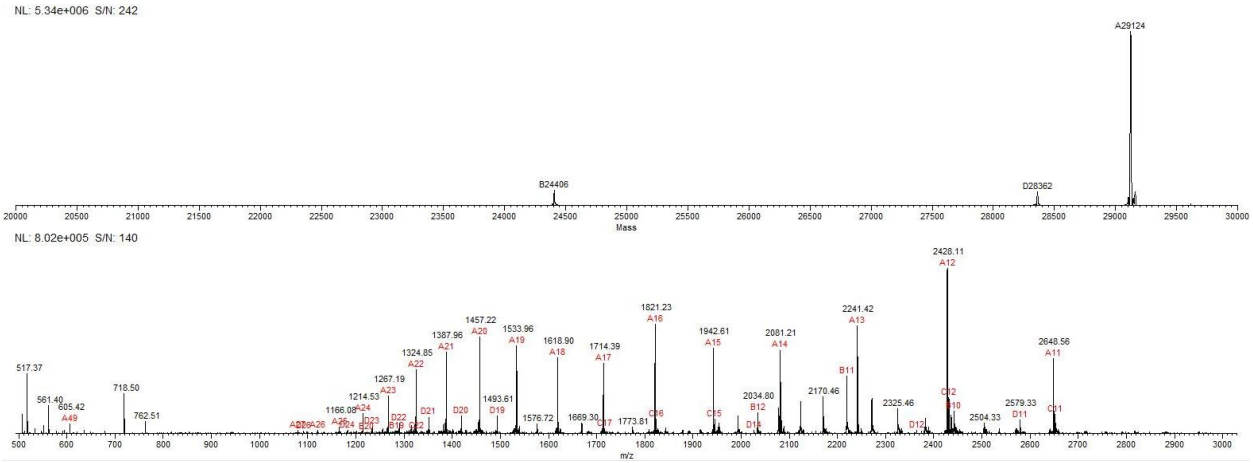

Figure 4.12. LC-ESI-MS spectrum of IdeS-treated MMAE2F-Trastuzumab Fc monomer

Chapter 5: Conclusions and Future Directions

In summary, the overarching goal of my research was to leverage various glycozymes and their unique substrates specificities to generate natural and non-natural antibody glycoforms. My work aimed to investigate and establish chemoenzymatic methodologies for antibody Fc glycoengineering. Accomplishing this required the utilization of our lab's chemoenzymatic remodeling technology, further demonstrating its versatility in both basic and applied research settings for the modification and enhancement of therapeutic antibodies.

In chapter two, we compared the activities of three STs on both free *N*-glycans and IgG Fc glycans. Not only did we characterize the efficiencies of these STs, but we also observed substrate preferences of ST of the different arms if branched glycans. We report that HcST-22 is the most efficient ST at both the sialylation of free glycan as well as intact IgG Fc that terminate with galactose residues. We also observe that the enzyme works well in a two-enzyme one-pot reaction with NmCSS generating CMP-Neu5Ac *in situ*. Pd2,6ST works well in the two-enzyme one-pot setting, consistent with previous reports[80, 81, 83], but it failed to produce the disialylated IgG Fc glycoform. The widely used hST6Gal-I has an optimal pH of 6.0, which makes this enzyme ill-suited for this one-pot system due the optimal pH of NmCSS being in the range of 7-9[108]. However, despite the high efficiency of HcST-22 to sialylated glycoproteins, it has displayed low tolerance for modifications of the donor substrate. Wakarchuk and colleagues tested various STs for the capacity to incorporate BODIPY-tagged sialic acid at either the C5 or C9 position onto glycoproteins or cell surfaces. Of the two α2,6STs (hST6Gal-I and HcST) only hST6Gal-I could transfer BODIPY-tagged onto the glycoprotein substrates as well as the cell surface. HcST had low transfer efficiency with the C5 labeled sialic acid on glycoprotein, and no transfer with the C9 modified sialic acid[130]. This finding is interesting considering hST6Gal-I

and HcST both possess GT-A fold architecture, but hST6Gal-I shows a greater tolerance for donor substrate modification.

In addition to observing the enzymatic efficiency and IgG acceptor capabilities, we also observed substrate arm preference of when using free biantennary *N*-glycan as an acceptor substrate. We used HPAEC-PAD chromatography to observe the production of each of the monosialylated isoform intermediates to determine whether the enzyme exhibited acceptor substrate preferences for one arm over another and found that while HcST-22 prefers the upper α1,6Man arm acceptor substrate, Pd2,6ST prefers the lower α1,3Man arm. Consistent with previous reports, ST6Gal-I displayed near exclusive preference for sialylating the lower α1,3Man arm first[91, 92]. Interestingly, despite ST6Gal-I and HcST-22 having similar GT-A folds, they display opposite acceptor substrate preference. This, along with the differences in donor substrate specificity, suggests that it's more than the 3D fold of the catalytic domain contributing to the discrepancy in enzyme-substrate interactions. Future studies should include STs from different GT families to illucidate structure-function relationships and aid in evaluating and predicting substrate efficiency and specificity of future STs.

In chapter 3, we report novel IVIg glycoforms to illucidate structural features of IVIg that are important for its anti-inflammatory activity. This work was in collaboration not only with various members of my lab, but also with the Anthony group at the Harvard Medical School. My part in this project was to generate the KDN-ylated IVIg glycoform (K2G2F-IVIg) and the hypersialylated glycoform ($(S2G2)_2$S2G2F-IVIg). The K2G2 glycoform would reveal if the C5 *N*-acetyl group of Neu5Ac was consequential in IVIg anti-inflammatory activity. The hypersialylated glycoform would give us insight into potential long range interactions that aid in anti-inflammatory activity. Notably, this glycoform may put significant strain on the IVIg Fc due

the significant increase in the Fc glycan size. This strain could interfere with antibody Fc receptors, disrupting anti-inflammatory activity of the IVIg construct. It is worth mentioning that both of these glycoforms may alter IVIg anti-inflammatory activity due to changes in interactions between the sialylated glycan and its receptors, but also by changing interactions of the sialylated glycan with the protein backbone residues of the IgG Fc region. Thus, while disruption of anti-inflammatory activity of either of these glycoforms would be an interesting observation, more work studies would be needed thereafter to confirm whether the effect came from interactions with other *in vivo* biological components, or from inhibition of normal IgG processes and interactions. Nevertheless, these data would be an important step to understanding the structural component responsible for interacting and initiating the anti-inflammatory response observed with treatment of sialylated IVIg.

Several receptors have been implicated in directly interacting with sialylated IVIg. SIGN-R1, as well as the human homolog DC-SIGN, has been deemed important to the anti-inflammatory activity of IVIg. However, implications of direct interactions between SIGN-R1 and sialylated IVIg have been met with contention due to SIGN-R1 having a know substrate specificity for high-mannose glycans, and binding between these two proteins cannot be observed *in vitro*[101]. Siglecs are the next potential candidates due to their immune inhibitory functions as well as their regioselectivity for ligand binding. Much work has gone into characterizing siglec substrate specificity, with some studies even characterizing molecular interactions that facilitate protein-ligand binding[104, 105]. These studies, along with the insights potentially provided by the structural derivatives of IVIg generated described in chapter 2, could help to solve the direct binding partner of Fc sialylated IVIg for anti-inflammatory functionality.

In chapter four, we describe a site-specific conjugation methodology to make a high DAR ADC while conserving the *N*-glycan chitobiose core structure. We then confirmed its activity using a cell-based cytotoxicity assay to demonstrate effective target cell killing with minimal off target killing. Additionally, our reported EC_{50} value of 7.6 ng/mL is comparable with a previously reported construct generated in our lab with the same DAR value, but did not retain the core chitobiose glycan structure[129].

The *N*-glycan chitobiose core is essential for IgG receptor binding, serum longevity, and stability of the antibody Fc tertiary structure. However, it is unclear to what extent the chitobiose core contributes to the efficacy of an ADC when the payload is conjugated to the glycosite. There are some site-specific ADC synthesis strategies that conjugate payload to the IgG Fc glycan while preserving the chitobiose core structure, but most of these strategies can only generate upwards of DAR-4 constructs. In this work, we wanted to increase the DAR value to 6 while maintaining the chitobiose core to assess the efficacy of this resulting ADC. Our results suggests that this conjugation strategy does not drastically affect the efficacy of the ADC. However, a comparison of these two drugs in terms of efficacy and pharmacokinetics *in vivo* has yet to be tests. In a living system, the construct is likely to engage with various receptors and serum components, and the presence or absence of the chitobiose core could drastically change key properties of the enzyme in the context of cancer treatment. Conversely, the conjugation of bulky, hydrophobic moieties could destabilize the antibody, inhibiting interactions with effector components.

Future studies should explore the structural stability of these ADC, as well as binding efficacy of these constructs to effector components *in vitro*. These studies should determine how retention of the core chitobiose glycan structure will affect *in vivo* drug efficacy. Modification of

the glycan, such as terminal sialylation and afucosylation, could also be tested *in vivo*. It is possible that certain glycan structures can aid in target cell killing *in vivo* by engaging the effector components to mediate CDC and ADCC in addition to delivering a cytotoxic payload to the cell. Conversely, triantennary structures may hinder activity by interacting with receptors designed to scavenge and degrade glycoproteins with certain glycan structural motifs, such as the asialoglycoprotein receptor (ASGPR), which scavenges glycoproteins with exposed galactose or GalNAc from the serum into the liver for degradation[131]. Understanding the role glycosylation can play not only in generating site-specific ADC constructs but also in aiding ADC efficacy through effector function interactions and prolonging serum half-life may help to develop much more effective drugs for cancer and disease treatments going forward.

Bibliography

1. De Haan, N.; Falck, D.; Wuhrer, M., Monitoring of immunoglobulin N- and O-glycosylation in health and disease. *Glycobiology* **2020,** *30* (4), 226-240.
2. Krištić, J.; Lauc, G., Ubiquitous Importance of Protein Glycosylation. In *Methods in Molecular Biology*, Springer New York: 2017; pp 1-12.
3. Ten Hagen, K. G., All in the family: the UDP-GalNAc:polypeptide N-acetylgalactosaminyltransferases. *Glycobiology* **2003,** *13* (1), 1R-16.
4. Gerken, T. A.; Revoredo, L.; Thome, J. J. C.; Tabak, L. A.; Vester-Christensen, M. B.; Clausen, H.; Gahlay, G. K.; Jarvis, D. L.; Johnson, R. W.; Moniz, H. A.; Moremen, K., The Lectin Domain of the Polypeptide GalNAc Transferase Family of Glycosyltransferases (ppGalNAc Ts) Acts as a Switch Directing Glycopeptide Substrate Glycosylation in an N- or C-terminal Direction, Further Controlling Mucin Type O-Glycosylation. *The Journal of Biological Chemistry* **2013,** *288* (27), 19900-19914.
5. Thompson, N.; Wakarchuk, W., O-glycosylation and its role in therapeutic proteins. *Bioscience Reports* **2022,** *42* (10).
6. Cerliani, J. P.; Blidner, A. G.; Toscano, M. A.; Croci, D. O.; Rabinovich, G. A., Translating the 'Sugar Code' into Immune and Vascular Signaling Programs. *Trends in Biochemical Sciences* **2017,** *42* (4), 255-273.
7. Roth, J., Protein N-Glycosylation along the Secretory Pathway: Relationship to Organelle Topography and Function, Protein Quality Control, and Cell Interactions. *Chemical Reviews* **2002,** *102* (2), 285-304.
8. Schwarz, F.; Aebi, M., Mechanisms and principles of N-linked protein glycosylation. *Current Opinion in Structural Biology* **2011,** *21* (5), 7.
9. Huber, R.; Deisenhofer, J.; Colman, P. M.; Matsushima, M.; Palm, W., Crystallographic structure studies of an IgG molecule and an Fc fragment. *Nature* **1976,** *264* (5585), 415-420.
10. Diebolder, C. A.; Beurskens, F. J.; De Jong, R. N.; Koning, R. I.; Strumane, K.; Lindorfer, M. A.; Voorhorst, M.; Ugurlar, D.; Rosati, S.; Heck, A. J. R.; Van De Winkel, J. G. J.; Wilson, I. A.; Koster, A. J.; Taylor, R. P.; Ollmann Saphire, E.; Burton, D. R.; Schuurman, J.; Gros, P.; Parren, P. W. H. I., Complement Is Activated by IgG Hexamers Assembled at the Cell Surface. *Science* **2014,** *343* (6176), 1260-1263.
11. Wang, T.; Liu, L.; Voglmeir, J., mAbs N-glycosylation: Implications for biotechnology and analytics. *Carbohydr Res* **2022,** *514*, 108541.
12. Ravetch, J. V.; Bolland, S., IgG Fc Receptors. *Annual Review of Immunology* **2001,** *19* (1), 275-290.
13. Radaev, S.; Motyka, S.; Fridman, W.-H.; Sautes-Fridman, C.; Sun, P. D., The Structure of a Human Type III Fcγ Receptor in Complex with Fc. *The Journal of Biological Chemistry* **2001,** *276* (19), 16469-16477.
14. Pincetic, A.; Bournazos, S.; Dilillo, D. J.; Maamary, J.; Wang, T. T.; Dahan, R.; Fiebiger, B.-M.; Ravetch, J. V., Type I and type II Fc receptors regulate innate and adaptive immunity. *Nature Immunology* **2014,** *15* (8), 707-716.
15. Bournazos, S.; DiLillo, D. J.; Ravetch, J. V., The role of Fc-FcgammaR interactions in IgG-mediated microbial neutralization. *Nature Reviews Immunology* **2015,** *212* (9), 1361-9.

16. Brückner, C.; Lehmann, C.; Dudziak, D.; Nimmerjahn, F., Sweet SIGNs: IgG glycosylation leads the way in IVIG-mediated resolution of inflammation. *International immunology* **2017,** *29* (11), 11.
17. Krapp, S.; Mimura, Y.; Jefferis, R.; Huber, R.; Sondermann, P., Structural Analysis of Human IgG-Fc Glycoforms Reveals a Correlation Between Glycosylation and Structural Integrity. *Journal of Molecular Biology* **2003,** *325* (5), 979-989.
18. Arnold, J. N.; Wormald, M. R.; Sim, R. B.; Rudd, P. M.; Dwek, R. A., The Impact of Glycosylation on the Biological Function and Structure of Human Immunoglobulins. *Annual Review of Immunology* **2007,** *25* (1), 21-50.
19. Zhang, Z.; Shah, B.; Richardson, J., Impact of Fc N-glycan sialylation on IgG structure. *mAbs* **2019,** *11* (8), 1381-1390.
20. Zheng, K.; Bantog, C.; Bayer, R., The impact of glycosylation on monoclonal antibody conformation and stability. *mAbs* **2011,** *3* (6), 568-576.
21. Ferrara, C.; Grau, S.; Jäger, C.; Sondermann, P.; Brünker, P.; Waldhauer, I.; Hennig, M.; Ruf, A.; Rufer, A. C.; Stihle, M.; Umaña, P.; Benz, J., Unique carbohydrate–carbohydrate interactions are required for high affinity binding between FcγRIII and antibodies lacking core fucose. *Proceedings of the National Academy of Sciences* **2011,** *108* (31), 12669-12674.
22. Duncan, A. R.; Winter, G., The binding site for C1q on IgG. *Nature* **1988,** *332* (6166), 738-740.
23. Peschke, B.; Keller, C. W.; Weber, P.; Quast, I.; Lunemann, J. D., Fc-Galactosylation of Human Immunoglobulin Gamma Isotypes Improves C1q Binding and Enhances Complement-Dependent Cytotoxicity. *Frontiers in Immunology* **2017,** *8*, 646.
24. Chen, X.; Shi, M.; Tong, X.; Kim, H. K.; Wang, L.-X.; Schneewind, O.; Missiakas, D., Glycosylation-dependent opsonophagocytic activity of staphylococcal protein A antibodies. *Proceedings of the National Academy of Sciences* **2020,** *117* (37), 22992-23000.
25. Quast, I.; Keller, C. W.; Maurer, M. A.; Giddens, J. P.; Tackenberg, B.; Wang, L.-X.; Münz, C.; Nimmerjahn, F.; Dalakas, M. C.; Lünemann, J. D., Sialylation of IgG Fc domain impairs complement-dependent cytotoxicity. *The Journal of Clinical Investigation* **2015,** *125* (11), 4160-4170.
26. Pereira, N. A.; Chan, K. F.; Lin, P. C.; Song, Z., The "less-is-more" in therapeutic antibodies: Afucosylated anti-cancer antibodies with enhanced antibody-dependent cellular cytotoxicity. *mAbs* **2018,** *10* (5), 693-711.
27. Kaneko, Y.; Nimmerjahn, F.; Madaio, M. P.; Ravetch, J. V., Pathology and protection in nephrotoxic nephritis is determined by selective engagement of specific Fc receptors. *Journal of Experimental Medicine* **2006,** *203* (3), 789-797.
28. Kaneko, Y.; Nimmerjahn, F.; Ravetch, J. V., Anti-inflammatory activity of immunoglobulin G resulting from Fc sialylation. *Science* **2006,** *313* (5787), 670-673.
29. Anthony, R. M.; Nimmerjahn, F.; Ashline, D. J.; Reinhold, V. N.; Paulson, J. C.; Ravetch, J. V., Recapitulation of IVIG Anti-Inflammatory Activity with a Recombinant IgG Fc. *Science* **2008,** *320* (5874), 373-376.
30. Anumula, K. R., Quantitative glycan profiling of normal human plasma derived immunoglobulin and its fragments Fab and Fc. *Journal of Immunological Methods* **2012,** *382* (1), 167-176.
31. Jefferis, R., Recombinant antibody therapeutics: the impact of glycosylation on mechanisms of action. *Trends in Pharmacological Sciences* **2009,** *30* (7), 356-362.

32. Krištić, J.; Lauc, G., The importance of IgG glycosylation—What did we learn after analyzing over 100,000 individuals. *Immunological Reviews* **2024,** *328* (1), 143-170.
33. van de Bovenkamp, F. S.; Hafkenscheid, L.; Rispens, T.; Rombouts, Y., The Emerging Importance of IgG Fab Glycosylation in Immunity. *The Journal of Immunology* **2016,** *196* (4), 1435-1441.
34. Parekh, R. B.; Dwek, R. A.; Sutton, B. J.; Fernandes, D. L.; Leung, A.; Stanworth, D.; Rademacher, T. W.; Mizuochi, T.; Taniguchi, T.; Matsuta, K.; Takeuchi, F.; Nagano, Y.; Miyamoto, T.; Kobata, A., Association of rheumatoid arthritis and primary osteoarthritis with changes in the glycosylation pattern of total serum IgG. *Nature* **1985,** *316* (6027), 452-457.
35. Bond, A.; Alavi, A.; Axford, J. S.; Bourke, B. E.; Bruckner, F. E.; Kerr, M. A.; Maxwell, J. D.; Tweed, K. J.; Weldon, M. J.; Youinou, P.; Hay, F. C., A Detailed Lectin Analysis of IgG Glycosylation, Demonstrating Disease Specific Changes in Terminal Galactose and N-acetylglucosamine. *Journal of Autoimmunity* **1997,** *10* (1), 77-85.
36. Kao, M.-R.; Ma, T.-H.; Chou, H.-Y.; Chang, S.-C.; Cheng, L.-C.; Liao, K.-S.; Shie, J.-J.; Harris, P. J.; Wong, C.-H.; Hsieh, Y. S. Y., A Robust α-L-Fucosidase from Prevotella nigrescens forGlycoengineering Therapeutic Antibodies. *ACS Chemical Biology* **2024,** *19* (7), 1515-1524.
37. Tsai, T.-I.; Li, S.-T.; Liu, C.-P.; Chen, K. Y.; Shivatare, S. S.; Lin, C.-W.; Liao, S.-F.; Lin, C.-W.; Hsu, T.-L.; Wu, Y.-T.; Tsai, M.-H.; Lai, M.-Y.; Lin, N.-H.; Wu, C.-Y.; Wong, C.-H., An Effective Bacterial Fucosidase for Glycoprotein Remodeling. *ACS Chemical Biology* **2016,** *12* (1), 63-72.
38. Shinkawa, T.; Nakamura, K.; Yamane, N.; Shoji-Hosaka, E.; Kanda, Y.; Sakurada, M.; Uchida, K.; Anazawa, H.; Satoh, M.; Yamasaki, M.; Hanai, N.; Shitara, K., The Absence of Fucose but Not the Presence of Galactose or Bisecting N-Acetylglucosamine of Human IgG1 Complex-type Oligosaccharides Shows the Critical Role of Enhancing Antibody-dependent Cellular Cytotoxicity. *The Journal of Biological Chemistry* **2003,** *278* (5), 3466-3473.
39. Guhr, T.; Bloem, J.; Derksen, N. I. L.; Wuhrer, M.; Koenderman, A. H. L.; Aalberse, R. C.; Rispens, T., Enrichment of Sialylated IgG by Lectin Fractionation Does Not Enhance the Efficacy of Immunoglobulin G in a Murine Model of Immune Thrombocytopenia. *PLoS ONE* **2011,** *6* (6), e21246.
40. Käsermann, F.; Boerema, D. J.; Rüegsegger, M.; Hofmann, A.; Wymann, S.; Zuercher, A. W.; Miescher, S., Analysis and Functional Consequences of Increased Fab-Sialylation of Intravenous Immunoglobulin (IVIG) after Lectin Fractionation. *PLoS ONE* **2012,** *7* (6), e37243.
41. Umaña, P.; Jean–Mairet, J.; Moudry, R.; Amstutz, H.; Bailey, J. E., Engineered glycoforms of an antineuroblastoma IgG1 with optimized antibody-dependent cellular cytotoxic activity. *Nature Biotechnology* **1999,** *17* (2), 176-180.
42. Davies, J.; Jiang, L.; Pan, L.-Z.; Labarre, M. J.; Anderson, D.; Reff, M., Expression of GnTIII in a recombinant anti-CD20 CHO production cell line: Expression of antibodies with altered glycoforms leads to an increase in ADCC through higher affinity for FcγRIII. *Biotechnology and Bioengineering* **2001,** *74* (4), 288-294.
43. Ferrara, C.; Brunker, P.; Suter, T.; Moser, S.; Puntener, U.; Umana, P., Modulation of therapeutic antibody effector functions by glycosylation engineering: Influence of Golgi enzyme localization domain and co-expression of heterologous β1, 4-N-acetylglucosaminyltransferase III and Golgi α-mannosidase II. *Biotechnology and Bioengineering* **2005,** *93* (5), 11.

44. Sharman, J. P.; Farber, C. M.; Mahadevan, D.; Schreeder, M. T.; Brooks, H. D.; Kolibaba, K. S.; Fanning, S.; Klein, L.; Greenwald, D. R.; Sportelli, P.; Miskin, H. P.; Weiss, M. S.; Burke, J. M., Ublituximab (TG-1101), a novel glycoengineered anti-CD20 antibody, in combination with ibrutinib is safe and highly active in patients with relapsed and/or refractory chronic lymphocytic leukaemia: results of a phase 2 trial. *British Journal of Haematology* **2017,** *176* (3), 412-420.
45. Yamane-Ohnuki, N.; Kinoshita, S.; Inoue-Urakubo, M.; Kusunoki, M.; Iida, S.; Nakano, R.; Wakitani, M.; Niwa, R.; Sakurada, M.; Uchida, K.; Shitara, K.; Satoh, M., Establishment of FUT8 knockout Chinese hamster ovary cells: An ideal host cell line for producing completely defucosylated antibodies with enhanced antibody-dependent cellular cytotoxicity. *Biotechnology and Bioengineering* **2004,** *87* (5), 614-622.
46. Imai-Nishiya, H.; Mori, K.; Inoue, M.; Wakitani, M.; Iida, S.; Shitara, K.; Satoh, M., Double knockdown of α1,6-fucosyltransferase (FUT8) and GDP-mannose 4,6-dehydratase (GMD) in antibody-producing cells: a new strategy for generating fully non-fucosylated therapeutic antibodies with enhanced ADCC. *BMC Biotechnology* **2007,** *7* (1), 84.
47. Lund, J.; Takahashi, N.; Pound, J. D.; Goodall, M.; Jefferis, R., Multiple interactions of IgG with its core oligosaccharide can modulate recognition by complement and human Fc gamma receptor I and influence the synthesis of its oligosaccharide chains. *The Journal of Immunology* **1996,** *157* (11), 4963-4969.
48. Raymond, C.; Robotham, A.; Spearman, M.; Butler, M.; Kelly, J.; Durocher, Y., Production of α2,6-sialylated IgG1 in CHO cells. *mAbs* **2015,** *7* (3), 571-583.
49. Ahmed, A. A.; Giddens, J.; Pincetic, A.; Lomino, J. V.; Ravetch, J. V.; Wang, L.-X.; Bjorkman, P. J., Structural Characterization of Anti-Inflammatory Immunoglobulin G Fc Proteins. *Journal of Molecular Biology* **2014,** *426* (18), 3166-3179.
50. Washburn, N.; Schwab, I.; Ortiz, D.; Bhatnagar, N.; Lansing, J. C.; Medeiros, A.; Tyler, S.; Mekala, D.; Cochran, E.; Sarvaiya, H.; Garofalo, K.; Meccariello, R.; Meador, J. W.; Rutitzky, L.; Schultes, B. C.; Ling, L.; Avery, W.; Nimmerjahn, F.; Manning, A. M.; Kaundinya, G. V.; Bosques, C. J., Controlled tetra-Fc sialylation of IVIg results in a drug candidate with consistent enhanced anti-inflammatory activity. *Proceedings of the National Academy of Sciences* **2015,** *112* (11), E1297-E1306.
51. Schuster, M.; Umana, P.; Ferrara, C.; Brünker, P.; Gerdes, C.; Waxenecker, G.; Wiederkum, S.; Schwager, C.; Loibner, H.; Himmler, G.; Mudde, G. C., Improved effector functions of a therapeutic monoclonal Lewis Y-specific antibody by glycoform engineering. *Cancer Research* **2005,** *65* (17), 8.
52. Wang, M.; Wang, Y.; Liu, K.; Dou, X.; Liu, Z.; Zhang, L.; Ye, X.-S., Engineering a bacterial sialyltransferase for di-sialylation of a therapeutic antibody. *Organic & biomolecular chemistry* **2020,** *18* (15), 2886-2892.
53. Davies, G.; Henrissat, B., Structures and mechanisms of glycosyl hydrolases. *Structure* **1995,** *3* (9), 853-9.
54. Yamamoto, K.; Kadowaki, S.; Watanabe, J.; Kumagai, H., Transglycosylation activity of Mucor hiemalis endo-beta-N-acetyl-glucosaminidase which transfers complex oligosaccharides to the N-acetylglucosamine moieties of peptides. *Biochemical and Biophysical Research Communications* **1994,** *203* (1), 244-52.
55. Umekawa, M.; Huang, W.; Li, B.; Fujita, K.; Ashida, H.; Wang, L. X.; Yamamoto, K., Mutants of Mucor hiemalis endo-beta-N-acetylglucosaminidase show enhanced

transglycosylation and glycosynthase-like activities. *Journal of Biological Chemistry* **2008,** *283* (8), 4469-79.
56. Huang, W.; Li, C.; Li, B.; Umekawa, M.; Yamamoto, K.; Zhang, X.; Wang, L.-X., Glycosynthases Enable a Highly Efficient Chemoenzymatic Synthesis of N-Glycoproteins Carrying Intact Natural N-Glycans. *Journal of the American Chemical Society* **2009,** *131* (6), 2214-2223.
57. Umekawa, M.; Li, C.; Higashiyama, T.; Huang, W.; Ashida, H.; Yamamoto, K.; Wang, L.-X., Efficient Glycosynthase Mutant Derived from Mucor hiemalis Endo-β-N-acetylglucosaminidase Capable of Transferring Oligosaccharide from Both Sugar Oxazoline and Natural N-Glycan. *The Journal of Biological Chemistry* **2010,** *285* (1), 511-521.
58. Huang, W.; Li, J.; Wang, L. X., Unusual Transglycosylation Activity of Flavobacterium meningosepticum Endoglycosidases Enables Convergent Chemoenzymatic Synthesis of Core Fucosylated Complex N-Glycopeptides. *ChemBioChem* **2011,** *12* (6), 932-941.
59. Fan, S.-Q.; Huang, W.; Wang, L.-X., Remarkable Transglycosylation Activity of Glycosynthase Mutants of Endo-D, an Endo-β-N-acetylglucosaminidase from Streptococcus pneumoniae. *The Journal of Biological Chemistry* **2012,** *287* (14), 11272-11281.
60. Trastoy, B.; Du, J. J.; Li, C.; García-Alija, M.; Klontz, E. H.; Roberts, B. R.; Donahue, T. C.; Wang, L.-X.; Sundberg, E. J.; Guerin, M. E., GH18 endo-β-N-acetylglucosaminidases use distinct mechanisms to process hybrid-type N-linked glycans. *The Journal of Biological Chemistry* **2021,** *297* (2), 101011.
61. Wei, Y.; Li, C.; Huang, W.; Li, B.; Strome, S.; Wang, L.-X., Glycoengineering of Human IgG1-Fc through Combined Yeast Expression and in Vitro Chemoenzymatic Glycosylation. *Biochemistry* **2008,** *47* (39), 10294-10304.
62. Collin, M., EndoS, a novel secreted protein from Streptococcus pyogenes with endoglycosidase activity on human IgG. *The EMBO Journal* **2001,** *20* (12), 3046-3055.
63. Goodfellow, J. J.; Baruah, K.; Yamamoto, K.; Bonomelli, C.; Krishna, B.; Harvey, D. J.; Crispin, M.; Scanlan, C. N.; Davis, B. G., An endoglycosidase with alternative glycan specificity allows broadened glycoprotein remodelling. *Journal of American Chemical Society* **2012,** *134* (19), 8030-3.
64. Huang, W.; Giddens, J.; Fan, S.-Q.; Toonstra, C.; Wang, L.-X., Chemoenzymatic Glycoengineering of Intact IgG Antibodies for Gain of Functions. *Journal of the American Chemical Society* **2012,** *134* (29), 12308-12318.
65. Giddens, J. P.; Lomino, J. V.; Amin, M. N.; Wang, L.-X., Endo-F3 Glycosynthase Mutants Enable Chemoenzymatic Synthesis of Core-fucosylated Triantennary Complex Type Glycopeptides and Glycoproteins. *The Journal of Biological Chemistry* **2016,** *291* (17), 9356-9370.
66. Li, T.; Tong, X.; Yang, Q.; Giddens, J. P.; Wang, L.-X., Glycosynthase Mutants of Endoglycosidase S2 Show Potent Transglycosylation Activity and Remarkably Relaxed Substrate Specificity for Antibody Glycosylation Remodeling. *The Journal of Biological Chemistry* **2016,** *291* (32), 16508-16518.
67. Li, T.; Dilillo, D. J.; Bournazos, S.; Giddens, J. P.; Ravetch, J. V.; Wang, L.-X., Modulating IgG effector function by Fc glycan engineering. *Proceedings of the National Academy of Sciences* **2017,** *114* (13), 3485-3490.
68. Giddens, J. P.; Lomino, J. V.; Dilillo, D. J.; Ravetch, J. V.; Wang, L.-X., Site-selective chemoenzymatic glycoengineering of Fab and Fc glycans of a therapeutic antibody. *Proceedings of the National Academy of Sciences* **2018,** *115* (47), 12023-12027.

69. Wang, L.-X.; Tong, X.; Li, C.; Giddens, J. P.; Li, T., Glycoengineering of Antibodies for Modulating Functions. *Annual Review of Biochemistry* **2019,** *88* (1), 433-459.
70. Paulson, J. C.; Colley, K. J., Glycosyltransferases. Structure, localization, and control of cell type-specific glycosylation. *Journal of Biological Chemistry* **1989,** *264* (30), 17615-8.
71. Audry, M.; Jeanneau, C.; Imberty, A.; Harduin-Lepers, A.; Delannoy, P.; Breton, C., Current trends in the structure-activity relationships of sialyltransferases. *Glycobiology* **2011,** *21* (6), 716-726.
72. Kuhn, B.; Benz, J.; Greif, M.; Engel, A. M.; Sobek, H.; Rudolph, M. G., The structure of human alpha-2,6-sialyltransferase reveals the binding mode of complex glycans. *Acta Crystallographica Section D Biological Crystallography* **2013,** *69* (Pt 9), 1826-38.
73. Lairson, L. L.; Henrissat, B.; Davies, G. J.; Withers, S. G., Glycosyltransferases: structures, functions, and mechanisms. *Annual Review Biochemistry* **2008,** *77*, 521-55.
74. Jeanneau, C.; Chazalet, V.; Auge, C.; Soumpasis, D. M.; Harduin-Lepers, A.; Delannoy, P.; Imberty, A.; Breton, C., Structure-function analysis of the human sialyltransferase ST3Gal I: role of n-glycosylation and a novel conserved sialylmotif. *The Journal of Biological Chemistry* **2004,** *279* (14), 13461-8.
75. Schworer, R.; Schmidt, R. R., Efficient sialyltransferase inhibitors based on glycosides of N-acetylglucosamine. *Journal of American Chemical Society* **2002,** *124* (8), 1632-7.
76. Guo, J.; Li, W.; Xue, W.; Ye, X. S., Transition State-Based Sialyltransferase Inhibitors: Mimicking Oxocarbenium Ion by Simple Amide. *Journal of Medicinal Chemistry* **2017,** *60* (5), 2135-2141.
77. Li, X.; Fang, T.; Boons, G. J., Preparation of Well-Defined Antibody–Drug Conjugates through Glycan Remodeling and Strain-Promoted Azide–Alkyne Cycloadditions. *Angewandte Chemie* **2014,** *126* (28), 7307-7310.
78. Shade, K. C.; Conroy, M. E.; Washburn, N.; Kitaoka, M.; Huynh, D. J.; Laprise, E.; Patil, S. U.; Shreffler, W. G.; Anthony, R. M., Sialylation of immunoglobulin E is a determinant of allergic pathogenicity. *Nature* **2020,** *582* (7811), 265-270.
79. Yamamoto, T.; Nakashizuka, M.; Terada, I., Cloning and expression of a marine bacterial beta-galactoside alpha2,6-sialyltransferase gene from Photobacterium damsela JT0160. *Journal of Biochemistry* **1998,** *123* (1), 94-100.
80. Yu, H.; Huang, S.; Chokhawala, H.; Sun, M.; Zheng, H.; Chen, X., Highly Efficient Chemoenzymatic Synthesis of Naturally Occurring and Non-Natural α-2,6-Linked Sialosides: AP. damsela α-2,6-Sialyltransferase with Extremely Flexible Donor–Substrate Specificity. *Angewandte Chemie International Edition* **2006,** *45* (24), 3938-3944.
81. Yu, H.; Chen, X., Aldolase-Catalyzed Synthesis of B-D-Galp-(1-9)- D-KDN: A NovelAcceptor for Sialyltransferases. *ACS Organic Letters* **2006,** *8* (11), 2393-2396.
82. Huynh, N.; Li, Y.; Yu, H.; Huang, S.; Lau, K.; Chen, X.; Fisher, A. J., Crystal structures of sialyltransferase from Photobacterium damselae. *FEBS Letters* **2014,** *588* (24), 4720-4729.
83. Yu, H.; Chokhawala, H. A.; Huang, S.; Chen, X., One-pot three-enzyme chemoenzymatic approach to the synthesis of sialosides containing natural and non-natural functionalities. *Nature Protocols* **2006,** *1* (5), 2485-92.
84. Kajihara, Y.; Akai, S.; Nakagawa, T.; Sato, R.; Ebata, T.; Kodama, H.; Sato, K., Enzymatic synthesis of Kdn oligosaccharides by a bacterial alpha-(2-->6)-sialyltransferase. *Carbohydrate Research* **1999,** *315* (1-2), 137-41.

85. Teo, C. F.; Hwang, T. S.; Chen, P. H.; Hung, C. H.; Gao, H. S.; Chang, L. S.; Lin, C. H., Synthesis of Sialyl TN Glycopeptides – Enzymatic Sialylation by α2,6-Sialyltransferase from Photobacterium damsela. *Advanced Synthesis & Catalysis* **2005,** *347* (7-8), 967-972.
86. Gilbert, M.; Brisson, J. R.; Karwaski, M. F.; Michniewicz, J.; Cunningham, A. M.; Wu, Y.; Young, N. M.; Wakarchuk, W. W., Biosynthesis of ganglioside mimics in Campylobacter jejuni OH4384. Identification of the glycosyltransferase genes, enzymatic synthesis of model compounds, and characterization of nanomole amounts by 600-mhz (1)h and (13)c NMR analysis. *The Journal of Biological Chemistry* **2000,** *275* (6), 3896-906.
87. Gilbert, M.; Karwaski, M. F.; Bernatchez, S.; Young, N. M.; Taboada, E.; Michniewicz, J.; Cunningham, A. M.; Wakarchuk, W. W., The genetic bases for the variation in the lipo-oligosaccharide of the mucosal pathogen, Campylobacter jejuni. Biosynthesis of sialylated ganglioside mimics in the core oligosaccharide. *The Journal of Biological Chemistry* **2002,** *277* (1), 327-37.
88. Chiu, C. P. C.; Watts, A. G.; Lairson, L. L.; Gilbert, M.; Lim, D.; Wakarchuk, W. W.; Withers, S. G.; Strynadka, N. C. J., Structural analysis of the sialyltransferase CstII from Campylobacter jejuni in complex with a substrate analog. *Nature Structural & Molecular Biology* **2004,** *11* (2), 163-170.
89. Schur, M. J.; Lameignere, E.; Strynadka, N. C.; Wakarchuk, W. W., Characterization of α2,3- and α2,6-sialyltransferases from Helicobacter acinonychis. *Glycobiology* **2012,** *22* (7), 997-1006.
90. Janesch, B.; Saxena, H.; Sim, L.; Wakarchuk, W. W., Comparison of α2,6-sialyltransferases for sialylation of therapeutic proteins. *Glycobiology* **2019,** *29* (10), 735-747.
91. Barb, A. W.; Brady, E. K.; Prestegard, J. H., Branch-specific sialylation of IgG-Fc glycans by ST6Gal-I. *Biochemistry* **2009,** *48* (41), 3.
92. Joziasse, D. H.; Schiphorst, W. E.; van den Eijnden, D. H.; van Kuik, J. A.; van Halbeek, H.; Vliegenthart, J. F., Branch specificity of bovine colostrum CMP-sialic acid: N-acetyllactosaminide alpha 2----6-sialyltransferase. Interaction with biantennary oligosaccharides and glycopeptides of N-glycosylproteins. *The Journal of Biological Chemistry* **1985,** *260* (2), 6.
93. Noguchi, M.; Tanaka, T.; Gyakushi, H.; Kobayashi, A.; Shoda, S.-I., Efficient Synthesis of Sugar Oxazolines from Unprotected N-Acetyl-2-amino Sugars by Using Chloroformamidinium Reagent in Water. *Journal of Organic Chemistry* **2009,** *74* (5), 2210-2212.
94. Schwab, I.; Nimmerjahn, F., Intravenous immunoglobulin therapy: how does IgG modulate the immune system? *Nature Reviews Immunology* **2013,** *13* (3), 176-189.
95. Anthony, R. M.; Kobayashi, T.; Wermeling, F.; Ravetch, J. V., Intravenous gammaglobulin suppresses inflammation through a novel TH2 pathway. *Nature* **2011,** *475* (7354), 110-113.
96. Hematianlarki, M.; Nimmerjahn, F., Immunomodulatory and anti-inflammatory properties of immunoglobulin G antibodies. *Immunological Reviews* **2024**.
97. Anthony, R. M.; Ravetch, J. V., A Novel Role for the IgG Fc Glycan: The Anti-inflammatory Activity of Sialylated IgG Fcs. *Journal of Clinical Immunology* **2010,** *30* (S1), 9-14.
98. Samuelsson, A.; Towers, T. L.; Ravetch, J. V., Anti-inflammatory Activity of IVIG Mediated Through the Inhibitory Fc Receptor. *Science* **2001,** *291* (5503), 484-486.

99. Bruhns, P.; Samuelsson, A.; Pollard, J. W.; Ravetch, J. V., Colony-Stimulating Factor-1-Dependent Macrophages Are Responsible for IVIG Protection in Antibody-Induced Autoimmune Disease. *Immunity* **2003,** *18* (4), 573-581.
100. Schwab, I.; Mihai, S.; Seeling, M.; Kasperkiewicz, M.; Ludwig, R. J.; Nimmerjahn, F., Broad requirement for terminal sialic acid residues and FcγRIIB for the preventive and therapeutic activity of intravenous immunoglobulins in vivo. *European Journal of Immunology* **2014,** *44* (5), 1444-1453.
101. Anthony, R. M.; Wermeling, F.; Karlsson, M. C. I.; Ravetch, J. V., Identification of a receptor required for the anti-inflammatory activity of IVIG. *Proceedings of the National Academy of Sciences* **2008,** *105* (50), 19571-19578.
102. Campbell, I. K.; Miescher, S.; Branch, D. R.; Mott, P. J.; Lazarus, A. H.; Han, D.; Maraskovsky, E.; Zuercher, A. W.; Neschadim, A.; Leontyev, D.; McKenzie, B. S.; Käsermann, F., Therapeutic effect of IVIG on inflammatory arthritis in mice is dependent on the Fc portion and independent of sialylation or basophils. *The Journal of immunology* **2014,** *192* (11), 8.
103. Schauer, R., Sialic acids as regulators of molecular and cellular interactions. *Current Opinion in Structural Biology* **2009,** *19* (5), 507-514.
104. Kelm, S.; Brossmer, R.; Isecke, R.; Gross, H.-J.; Strenge, K.; Schauer, R., Functional groups of sialic acids involved in binding to siglecs (sialoadhesins) deduced from interactions with synthetic analogues. *European Journal of Biochemistry* **1998,** *255* (3), 663-672.
105. Crocker, P. R.; Paulson, J. C.; Varki, A., Siglecs and their roles in the immune system. *Nature Reviews Immunology* **2007,** *7* (4), 255-266.
106. von Gunten, S.; Bochner, B. S., Basic and Clinical Immunology of Siglecs. *Annals of the New York Academy of Sciences* **2008,** *1143* (1), 61-82.
107. Tjon, A. S.; van Gent, R.; Geijtenbeek, T. B.; Kwekkeboom, J., Differences in Anti-Inflammatory Actions of Intravenous Immunoglobulin between Mice and Men: More than Meets the Eye. *Frontiers in Immunology* **2015,** *6*, 197.
108. Yu, H.; Yu, H.; Karpel, R.; Chen, X., Chemoenzymatic synthesis of CMP-sialic acid derivatives by a one-pot two-enzyme system: comparison of substrate flexibility of three microbial CMP-sialic acid synthetases. *Bioorganic and Medicinal Chemistry* **2004,** *12* (24), 6427-35.
109. Toonstra, C.; Wu, L.; Li, C.; Wang, D.; Wang, L. X., Top-Down Chemoenzymatic Approach to Synthesizing Diverse High-Mannose N-Glycans and Related Neoglycoproteins for Carbohydrate Microarray Analysis. *Bioconjugate Chemistry* **2018,** *29* (6), 1911-1921.
110. Strebhardt, K.; Ullrich, A., Paul Ehrlich's magic bullet concept: 100 years of progress. *Nature Reviews Cancer* **2008,** *8* (6), 473-480.
111. Mathe, G.; Tran Ba, L. O.; Bernard, J., Effect on mouse leukemia 1210 of a combination by diazo-reaction of amethopterin and gamma-globulins from hamsters inoculated with such leukemia by heterografts. *Comptes Rendus Hebdomadaires des Seances de l Academie des Sciences* **1958,** *246* (10), 1626-8.
112. Hafeez, U.; Parakh, S.; Gan, H. K.; Scott, A. M., Antibody-Drug Conjugates for Cancer Therapy. *Molecules* **2020,** *25* (20).
113. Gao, Y.; Xia, Y.; Chen, Y.; Zhou, S.; Fang, Y.; Yu, J.; Zhang, L.; Sun, L., Key considerations based on pharmacokinetic/pharmacodynamic in the design of antibody-drug conjugates. *Frontiers in Oncology* **2024,** *14*, 1459368.

114. Tsuchikama, K.; An, Z., Antibody-drug conjugates: recent advances in conjugation and linker chemistries. *Protein Cell* **2018,** *9* (1), 33-46.
115. Uadia, P.; Blair, A. H.; Ghose, T., Tumor and tissue distribution of a methotrexate-anti-EL4 immunoglobulin conjugate in EL4 lymphoma-bearing mice. *Cancer Research* **1984,** *44* (10), 4263-6.
116. Shen, W. C.; Ballou, B.; Ryser, H. J.; Hakala, T. R., Targeting, internalization, and cytotoxicity of methotrexate-monoclonal anti-stage-specific embryonic antigen-1 antibody conjugates in cultured F-9 teratocarcinoma cells. *Cancer Research* **1986,** *46* (8), 3912-6.
117. Chari, R. V., Targeted cancer therapy: conferring specificity to cytotoxic drugs. *Accounts of Chemical Research* **2008,** *41* (1), 98-107.
118. Hamblett, K. J.; Senter, P. D.; Chace, D. F.; Sun, M. M.; Lenox, J.; Cerveny, C. G.; Kissler, K. M.; Bernhardt, S. X.; Kopcha, A. K.; Zabinski, R. F.; Meyer, D. L.; Francisco, J. A., Effects of drug loading on the antitumor activity of a monoclonal antibody drug conjugate. *Clinical Cancer Research* **2004,** *10* (20), 7063-70.
119. Junutula, J. R.; Bhakta, S.; Raab, H.; Ervin, K. E.; Eigenbrot, C.; Vandlen, R.; Scheller, R. H.; Lowman, H. B., Rapid identification of reactive cysteine residues for site-specific labeling of antibody-Fabs. *Journal of Immunological Methods* **2008,** *332* (1-2), 41-52.
120. Junutula, J. R.; Raab, H.; Clark, S.; Bhakta, S.; Leipold, D. D.; Weir, S.; Chen, Y.; Simpson, M.; Tsai, S. P.; Dennis, M. S.; Lu, Y.; Meng, Y. G.; Ng, C.; Yang, J.; Lee, C. C.; Duenas, E.; Gorrell, J.; Katta, V.; Kim, A.; McDorman, K.; Flagella, K.; Venook, R.; Ross, S.; Spencer, S. D.; Lee Wong, W.; Lowman, H. B.; Vandlen, R.; Sliwkowski, M. X.; Scheller, R. H.; Polakis, P.; Mallet, W., Site-specific conjugation of a cytotoxic drug to an antibody improves the therapeutic index. *Nature Biotechnology* **2008,** *26* (8), 925-32.
121. Axup, J. Y.; Bajjuri, K. M.; Ritland, M.; Hutchins, B. M.; Kim, C. H.; Kazane, S. A.; Halder, R.; Forsyth, J. S.; Santidrian, A. F.; Stafin, K.; Lu, Y.; Tran, H.; Seller, A. J.; Biroc, S. L.; Szydlik, A.; Pinkstaff, J. K.; Tian, F.; Sinha, S. C.; Felding-Habermann, B.; Smider, V. V.; Schultz, P. G., Synthesis of site-specific antibody-drug conjugates using unnatural amino acids. *Proceedings of the National Academy of Sciences* **2012,** *109* (40), 16101-6.
122. Tian, F.; Lu, Y.; Manibusan, A.; Sellers, A.; Tran, H.; Sun, Y.; Phuong, T.; Barnett, R.; Hehli, B.; Song, F.; DeGuzman, M. J.; Ensari, S.; Pinkstaff, J. K.; Sullivan, L. M.; Biroc, S. L.; Cho, H.; Schultz, P. G.; DiJoseph, J.; Dougher, M.; Ma, D.; Dushin, R.; Leal, M.; Tchistiakova, L.; Feyfant, E.; Gerber, H. P.; Sapra, P., A general approach to site-specific antibody drug conjugates. *Proceedings of the National Academy of Sciences* **2014,** *111* (5), 1766-71.
123. Laguzza, B. C.; Nichols, C. L.; Briggs, S. L.; Cullinan, G. J.; Johnson, D. A.; Starling, J. J.; Baker, A. L.; Bumol, T. F.; Corvalan, J. R., New antitumor monoclonal antibody-vinca conjugates LY203725 and related compounds: design, preparation, and representative in vivo activity. *Journal of Medicinal Chemistry* **1989,** *32* (3), 548-55.
124. Zhou, Q.; Stefano, J. E.; Manning, C.; Kyazike, J.; Chen, B.; Gianolio, D. A.; Park, A.; Busch, M.; Bird, J.; Zheng, X.; Simonds-Mannes, H.; Kim, J.; Gregory, R. C.; Miller, R. J.; Brondyk, W. H.; Dhal, P. K.; Pan, C. Q., Site-specific antibody-drug conjugation through glycoengineering. *Bioconjugate Chemistry* **2014,** *25* (3), 510-20.
125. Ramakrishnan, B.; Qasba, P. K., Structure-based Design of β1,4-Galactosyltransferase I (β4Gal-T1) with Equally Efficient N-Acetylgalactosaminyltransferase Activity. *The Journal of Biological Chemistry* **2002,** *277* (23), 20833-20839.

126. Zeglis, B. M.; Davis, C. B.; Aggeler, R.; Kang, H. C.; Chen, A.; Agnew, B. J.; Lewis, J. S., Enzyme-Mediated Methodology for the Site-Specific Radiolabeling of Antibodies Based on Catalyst-Free Click Chemistry. *Bioconjugate Chemistry* **2013,** *24* (6), 1057-1067.
127. Van Geel, R.; Wijdeven, M. A.; Heesbeen, R.; Verkade, J. M. M.; Wasiel, A. A.; Van Berkel, S. S.; Van Delft, F. L., Chemoenzymatic Conjugation of Toxic Payloads to the Globally Conserved N-Glycan of Native mAbs Provides Homogeneous and Highly Efficacious Antibody–Drug Conjugates. *Bioconjugate Chemistry* **2015,** *26* (11), 2233-2242.
128. Ou, C.; Li, C.; Zhang, R.; Yang, Q.; Zong, G.; Dai, Y.; Francis, R. L.; Bournazos, S.; Ravetch, J. V.; Wang, L.-X., One-Pot Conversion of Free Sialoglycans to Functionalized Glycan Oxazolines and Efficient Synthesis of Homogeneous Antibody–Drug Conjugates through Site-Specific Chemoenzymatic Glycan Remodeling. *Bioconjugate Chemistry* **2021,** *32* (8), 1888-1897.
129. Zhang, X.; Ou, C.; Liu, H.; Prabhu, S. K.; Li, C.; Yang, Q.; Wang, L.-X., General and Robust Chemoenzymatic Method for Glycan-Mediated Site-Specific Labeling and Conjugation of Antibodies: Facile Synthesis of Homogeneous Antibody–Drug Conjugates. *ACS Chemical Biology* **2021,** *16* (11), 2502-2514.
130. Abukar, T.; Rahmani, S.; Thompson, N. K.; Antonescu, C. N.; Wakarchuk, W. W., Development of BODIPY labelled sialic acids as sialyltransferase substrates for direct detection of terminal galactose on N- and O-linked glycans. *Carbohydrate Research* **2021,** *500*, 1-7.
131. D'Souza, A. A.; Devarajan, P. V., Asialoglycoprotein receptor mediated hepatocyte targeting - strategies and applications. *Journal of Controlled Release* **2015,** *203*, 126-39.